ISSN 2461-4254

EUREKA: PHYSICS AND ENGINEERING

- Chemical Engineering
- Chemistry
- Computer Science
- Earth and Planetary Sciences
- Energy
- Engineering
- Materials Science
- Mathematics
- Physics and Astronomy

Volume 4(11)
2017

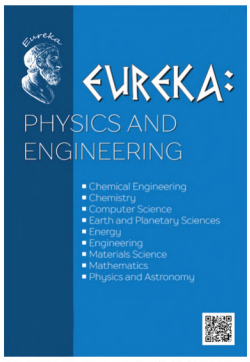

SCIENTIFIC JOURNAL

EUREKA: Physics and Engineering – scientific journal whose main aim is to publish materials allowed to see ***new discoveries at the intersection of sciences.***

- Chemical Engineering
- Chemistry
- Computer Science
- Earth and Planetary Sciences
- Energy
- Engineering
- Material Science
- Mathematics
- Physics and Astronomy
- Technology Transfer

EUREKA: **Physics and Engineering**
publishes
4 types of materials:
– review article,
– progress reports,
– original Research Article
– reports on research projects

PUBLISHER OÜ «Scientific Route»
European Union
Editorial office
«EUREKA: Physical Sciences and Engineering»
Narva mnt 7-634, Tallinn, Eesti
Harju maakond, 10117
Tel. + 372 602-7570
e-mail: info@eu-jr.eu
Website: http://eu-jr.eu

EDITORIAL BOARD

CONTENT

RESEARCH OF MINERAL ADSORBENTS APPLICATION FOR WATER-ALCOHOL SOLUTIONS PURIFICATION IN TECHNOLOGY OF ALCOHOLIC BEVERAGES

Lolita Marynchenko
Department of Bioinformatic
National Technical University of Ukraine "Igor Sikorsky Kyiv Polytechnic Institute"
37 Peremohy ave., Kyiv, Ukraine, 03056
lolitamar@ukr.net

Viktor Marynchenko
Department of Biotechnology of fermentation and wine making
National University of Food Technologies
68 Volodymyrska str., Kyiv, Ukraine, 01601
marinchenko37@ukr.net

Mariana Hyvel
PJSC "Ukrainian Tachnology Company"
69 Alisher Navoi ave., Kyiv, Ukraine, 02125
givelm@ukr.net

Abstract

The possibility of using natural mineral adsorbents – clinoptilolite and schungite – in the adsorption purification of water-alcohol solutions of different concentrations was studied using the example of impurities of ethanol of acetaldehyde and ethyl acetate. The feasibility of studying the above-mentioned minerals for the adsorption of simple organic substances is justified. The best concentration of a water-alcohol solution for adsorption of acetaldehyde 80–85 % vol., ethyl acetate-40 % vol., is experimentally established. The rational duration of phase contact for adsorption of acetaldehyde is from 10 to 20 minutes, for adsorption of ethyl acetate – 5 minutes.

An explanation for the dependence of the sorption efficiency on the ethanol content in a water-alcohol solution is proposed based on the known dependencies of the rectification factor on the ethanol concentration. The larger the rectification factor, the less the hydrogen bond of this impurity with ethanol and the easier it is to sorb it from ethanol by mineral adsorbents. The practical and economic feasibility of using the mineral adsorbent clinoptilolite of Ukrainian origin in the preparation of alcoholic beverages instead of imported active coal is shown. It is determined that to purify water-alcohol solutions from aldehydes, which most worsen the taste of alcoholic beverages, it is more expedient to use clinoptilolite as an adsorbent. It is shown that the use of clinoptilolite for the preparation of vodkas from non-standard rectified alcohol will improve the tasting indicators of the final product.

Keywords: adsorption, volatile alcohol impurities, quality of ethyl alcohol, zeolites, clinoptilolite, schungite.

DOI: 10.21303/2461-4262.2017.00397

1. Introduction

One of the key quality problems of alcoholic beverages is the minimum amount of volatile ethanol impurities obtained by fermentation of starch or sugar-containing raw materials and released during the process of distillation. The main among such impurities are aldehydes, higher alcohols, organic acids and esters, methanol. Some impurities can be removed by passing a water-alcohol solution through a column of activated carbon.

However, this technology of vodka preparation has a number of drawbacks, above all, the price of active coal imported to Ukraine from Russia. It is also flammability, the possibility of catalytic oxidation and esterification reactions, i. e. the formation of new impurities and inefficiency, for example, in the sorption of esters.

Therefore, the search for new effective adsorbents for purification from volatile impurities of ethanol is an urgent task both from a scientific and practical point of view. Dispersion of zeolites allows to consider natural clay minerals as potentially possible adsorbents and for purification of water-alcohol solutions. This assumption is due to reports on the effectiveness of using different

types of zeolites for the sorption of small-sized simple chemicals. For example, is the separation of carbon dioxide from flue gases [1], water from natural methane or biogas [2, 3], separation of complex mixtures (methane, carbon dioxide, hydrogen sulfide, water vapor) [3, 4]. In addition, the efficiency of wastewater or wine purification from heavy metals and nitrates is shown [5–7].

Thus, the study of the possibility of using zeolites to purify water-alcohol solutions from ethanol-related volatile impurities is the goal of this research.

2. Materials and Methods

Zeolites in structure are a complex tetrahedral structure in which the main silicon or aluminum atom is bound by four oxygen atoms. Within the chains of such structures, adsorption voids are formed, which can be filled with water or other small substances, which causes the use of zeolites as adsorbents. To do this, before use, the zeolites are dried by removing water. However, the possibility of adsorption is due not so much to the size of the pores as to the size of the input windows, which depends on the crystal lattice, the number of oxygen atoms, and the spatial orientation. Thus, it is the critical size of the molecules that is decisive for the absorption of a particular substance. In addition, active anionic centers are located on the surface of the aluminosilicate skeleton of these structures, the excess charge of which is compensated by the cations of sodium, potassium, calcium, and magnesium. The presence of charge is an additional factor of adsorption and/or ion-exchange capacity [8].

Reserves of natural mineral adsorbents such as bentonite, hydromica, montmorilonite, palygorskite, saponite, clinoptilolite, etc., in Ukraine estimate more than 1 billion tons [9]. Zeolites of the Sokirnitsa deposit can be used for the purification of sewage, in animal husbandry, poultry farming, fish farming, and plant growing [10, 11]. This, as well as the absence of extraneous odors and flavors, which could spoil the organoleptic characteristics of food raw materials, products or water, allows to consider these minerals for use in the food industry.

One of the most common minerals of soils and bottom sediments - clinoptilolite – found in Asia, South Africa, Australia, North and South America. In Europe, clinoptilolite is common in Hungary, Italy, Romania, Slovakia, Slovenia, Turkey, Ukraine and the West of Russia [12]. The ion-exchange capacity of clinoptilolite is due to the high surface charge, the crystal-chemical formula of which $(Na,K)_6[Al_6Si_{30}O_{72}]_{20}H_2O$ (per unit cell) and $|(Na,K)_{0,17}(H_2O)_{0,56}|[Al_{0,17}Si_{0,83}O_2]$ (normalized to $[(Al,Si)O_2]$) [13]. Despite the possible partial replacement of sodium ions by potassium, magnesium or sodium ions, which depends on the geology of the occurrence of ores, the inequality (Na+K)>(Ca+Mg) is characteristic for clinoptilolite. The thermal stability of the Ukrainian zeolite at the Sokirnitsa deposit (850 °C) is sufficient for the possibility of using clinoptilolite for technological purposes – there have been no significant changes in its structure. Exceeding the ratio of silicon to aluminum for the structure is insignificant – 3.84–4.13. At the same time, a decrease in this ratio leads to a change in the size and shape of the unit cell, the parameters of which are normally within the limits of, nm: 1.77:1.80:0.74. Stretching in one direction and compression in the other leads to a change in the configuration of the channels, which take the form of an ellipsoid. The normal size of the input windows of crystal lattices is about 0.35 nm [14].

Schungite rocks are found in Karelia (Russia) and Bulgaria. The structural basis of the carbon part of this natural mineral is the globule-fullerene-like formations of 10 to 30 nm in size [15]. The fullerene shell (closed or composed of fragments) consists of smoothly curved packets of carbon layers that form a nanoscale pore. Globules differ in form and size, which depends, in the main, on the number of carbon atoms (from tens to hundreds). The thickness of the spherical shell of a fullerene molecule consisting of 60 carbon atoms is ~0.1 nm, the molecular radius is 0.357 nm. The average distance between layers of more ordered carbon is 0.34 nm on the surface of microcrystals, in layers of a more complex structure this size varies from 0.2 to 0.5 nm.

Mineral components are represented by finely dispersed crystals, nanocrystals and layered inclusions. The main mineral part of the schungite is represented by magnesium silicates of the type: $3MgO{\times}4SiO_2{\times}6H_2O$ (hydrated talc) and $3MgO{\times}2SiO_2{\times}6H_2O$ (hydrated serpentine). There is also free α-SiO_2 (quartz), α-Fe_2O_3 (hematite), TiO_2 (rutile), $8MgO{\times}\ 4SiO_2{\times}Mg(F,OH)$ (clinohumite), α-Al_2O_3 (corundum) and α-CrO_3 (eskolaite) [15].

2. 1. Experimental procedures

To establish a certain fractional composition of the zeolite, sieves with different hole diameters were used, which were a set of five sieves with holes 1, 2, 3, 4 and 5 mm in diameter. Adsorbents were poured into the upper sieve, which was covered with a lid, shaken violently and the minerals were sieved to different fractions. A fraction of 2–3 mm was used for the studies.

Before use, the dispersed minerals were weighed and dried in СЭШ-1 drying box (manufactured in the USSR) at a temperature of 120 °C for 12 hours. Such parameters were chosen to ensure that water is removed from the adsorbent pores. The dried bunks with adsorbent weights were held in the desiccator for 30 min before cooling to room temperature, and then adsorbers were filled with adsorbents or stored in closed vessels.

Each fraction was stored separately in a glass vessel sealed with a ground glass stopper.

To carry out the research, a laboratory unit was created by the authors (**Fig. 1**), which is an adsorption column 3 filled with an adsorbent 4 laid on a piece of cotton with a height of not more than 1 cm. Above, the adsorbent is also covered with a piece of cotton wool to the level of the drain tube. In the lower part of the adsorption column, water-alcohol solutions of different concentrations were fed from the pressure collector 1. The different contact times of the water-alcohol solution with the adsorbent were provided by a different solution delivery rate of 3 to 35 ml/min, which was regulated by the valve 2. The test samples were taken to a collecting receptacle (measuring cylinder) 5 fixed by a clip 6 on a support 7 from the top of the adsorption column. The studies were carried out at room temperature, that is, 20–22 °C. The first 150 ml of a water-alcohol solution leaving the adsorption column was poured and only after that a sample was taken.

Parameters of the adsorption column: column height H=0.45 m; the internal diameter of the column is d_{in}=0.024 m. Then the volume of the column is:

$$V = \frac{\pi \cdot d_{in}^{\ 2}}{4} \cdot H, \tag{1}$$

$$V = \frac{3,14 \cdot 0,024^2}{4} \cdot 0,45 = 0,203 \cdot 10^{-3}\,\text{m}^3 = 203\ \text{ml}.$$

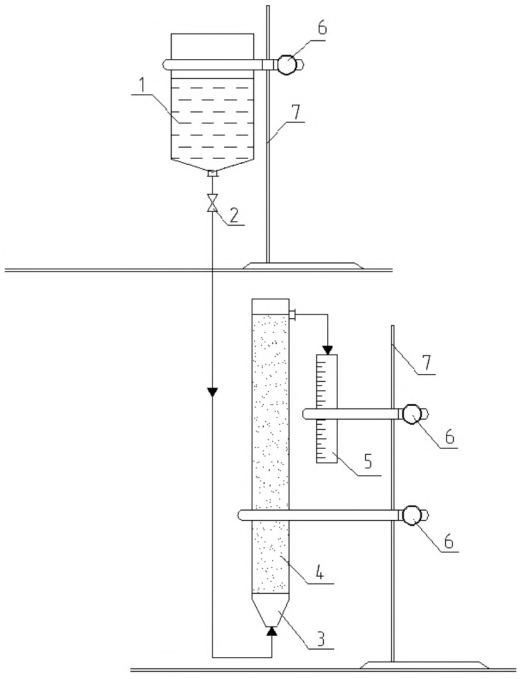

Fig. 1. Laboratory unit for purification of water-alcohol solutions: 1 – pressure collector; 2 – control valve; 3 – adsorption column; 4 – adsorption material; 5 – measuring cylinder; 6 – clip; 7 – support

To prepare water-alcohol solutions of different concentrations, alcoholimetric tables were used, taking into account the temperature and contraction corrections that occurred when the alcohol or aqueous alcohol solutions were diluted [16]. To quickly determine the concentration of water-alcohol solutions, areometer-alcoholometers were used, which were immersed in a vertical cylinder filled with alcohol with an ethyl rectified concentration of 96.8 % vol., and a water-alcohol mixture with concentrations of 40, 50 and 80 % vol. To determine the correction for temperature, mercury laboratory thermometers were used [17].

The concentration of impurities of aldehydes and esters by the example of acetaldehyde and ethyl acetate in control and test samples was determined by gas chromatography on a gas chromatograph "Crystal 2000" (Chromatec, Russia) [18]. As control, ethyl alcohol was rectified with a concentration of 96.8 % vol., and water-alcohol solutions diluted to a concentration of 40, 50 and 80 % vol., which were not subjected to adsorption purification in a laboratory plant.

The average arithmetic value of the components of two parallel measurements for the concentration of the microcomponent in the control and test samples was accepted, the permissible difference between which did not exceed the norm of the operational control of convergence r_n at P=0.95 %, n=2 (r_n – operative control of convergence, P – confidence coefficient, N – the number of parallel measurements). For ethyl acetate and acetaldehyde at their mass concentration in recalculation on anhydrous alcohol, mg/dm^3, from 0.5 to 10.0 – r_n=15 %; from 10.0 to 50.0 – r_n=10 %. The results that exceeded these values, which are given in the normative document [19] for the determination of the content of microcomponents by the gas chromatographic method, were discarded.

The study was conducted with non-standard ethyl alcohol (non-compliance with the normative document on the indices of the concentration of aldehydes and esters). According to the normative document [20], the mass concentration of aldehydes in terms of acetic aldehyde in anhydrous alcohol should not exceed 4 mg/dm^3, the mass concentration of esters, calculated per acetic-ethyl ester in anhydrous alcohol, should not exceed 5 mg/dm^3 for an alcohol of the grade "Higher purification".

Adsorption of aldehydes was investigated using acetaldehyde as an example, the content of which is usually 90 % or more of the total aldehyde in rectified ethyl alcohol. The adsorption of the esters was determined by the example of ethyl acetate as the main component of the esters. The results were calculated in mg/dm^3 of anhydrous alcohol.

3. Results

The dynamics of acetaldehyde adsorption by clinoptilolite from water-alcohol solutions of different concentrations showed the same trend. With an increase in the duration of phase contact to 5–10 min, the concentration of this impurity in the outgoing solution decreased, but then began to increase again. Thus, the sorption process must be carried out fairly quickly, since an increase in the duration of the contact seems to cause either desorption of acetaldehyde or the oxidation of ethanol.

However, acetaldehyde sorption was different for different concentrations of water-alcohol solutions: the best results were noted for a concentration of 80 % vol.; the acetaldehyde concentration decreased by almost 63 % (from 4.47 to 1.67 mg/dm^3). To concentrate the water-alcohol solution 50 % vol., the lowest value was fixed at the level of 2.3 mg/dm^3, for a concentration of 96.8 % vol., – 2.58 mg/dm^3, for a concentration of 40 % vol., – 3.08 mg/dm^3.

Thus, it is least expedient to carry out purification from a water-alcohol solution with a concentration of 40 % vol. However, for all concentrations, it has been shown that it is possible to improve the acetaldehyde concentration to a standard value.

In the study of the dynamics of the aldehydes adsorption process by schungite on acetaldehyde, depending on the concentration of water-alcohol solutions and the duration of phase contact, the quality of the samples did not meet the requirements of the standard for the concentration of aldehydes [20] – 8.28 mg/dm^3. The sorption of acetaldehyde by schungite occurred most intensively

during the first 5–10 minutes. But a further increase in the transmission time of the water-alcohol solution did not cause such an obvious process of increasing the concentration of acetaldehyde, as with sorption by clinoptilolite. The most effective acetaldehyde was adsorbed by schungite also from a water-alcohol solution with a concentration of 80 % vol., – up to 6.37 mg/dm^3 or more than 25 %. It should be noted that up to duration of contact of 20 min, the scatter of data on the content of acetaldehyde after sorption for concentrations of 80, 50 and 96.8 % vol., was within the error of experience.

In the next series of studies, the content of ethyl acetate was analyzed, the concentration of which among esters is highest in rectified ethyl alcohol and alcoholic beverages.

Analysis of the sorption of ethyl acetate by clinoptilolite shows a completely different distribution of the results for different concentrations of water-alcohol solutions. The results showed that the concentration of 40 % vol., is preferable (decrease from 3.4 to 0.6 mg/dm^3), and an increase in the concentration of ethanol in the purified solution impaired the efficiency of the process. It is possible that the optimal duration of phase contact may be time, even less than 5 minutes. However, it was technically impossible to provide such conditions at such column height. And with increasing contact time up to 60 minutes, the concentration of ethyl acetate almost reached the value in the control sample, which may indicate the presence of catalytic reactions.

The results of sorption of ethyl acetate by schungite have a wider spread of indices for different concentrations of water-alcohol solutions, but the efficiency of sorption has repeated the tendency of sorption by clinoptilolite. Increase the dilution of the water-alcohol solution to a concentration of 40 % vol., gave the best results – the content of ethyl acetate after 5 minutes of the process decreased by almost 5 times. Thus, it can be state that it is possible to achieve the normative indices of the concentration of ethyl acetate by a schungite adsorption in a water-alcoholic solution of 40 % vol.

To calculate the economic efficiency of the use of zeolites for purification of aqueous-alcoholic solutions, the initial data was taken: the working month is 24 days, the one-change operation mode, and the productivity is 20,000 decalitres (dkl) per month. Then the daily capacity of the adsorption unit is:

$$G = \frac{20000}{24} = 833,3 \text{ (dkl/day)}$$

and the adsorber capacity per change

$$G_1 = \frac{833,3}{8} = 104,2 \text{ (dkl/change).}$$

The adsorber volume at d= 0,7 m, h=4 m is:

$$V = \frac{\pi D^2}{4} h = \frac{3,14 \cdot 0,7^2}{4} \cdot 4 = 1,54 \text{ (m}^3\text{).}$$

If we assume that for purification of 3 dkl of sorting prior to ensuring the normative indices, it is necessary to have 0.4 kg of zeolites, then the flow will be:

$$m = \frac{104,2 \cdot 0,4}{3} = 13,9 \text{ (kg/day).}$$

When the adsorber is filled to 80 % (taking into account the breakthrough), the volume of the adsorbent will be:

$$V_{ads} = 1,54 \cdot 0,8 = 1,2 \text{ (m}^3\text{).}$$

For a bulk adsorbent mass of 1100 kg/m^3, the mass of the zeolite in the adsorber:

$$m_{ads} = 1100 \times 1,2 = 1320 \text{ (kg)}.$$

The number of changes of the adsorber before regeneration of the adsorbent will be:

$$\tau_{sch} = \frac{m_{ads}}{m} = \frac{1320}{13,9} = 95.$$

Annual consumption of zeolite:

$$1320 \text{ g} \rightarrow 95 \text{ changes};$$

$$m_c \rightarrow 288 \text{ changes};$$

$$m_{sch} = \frac{1320 \cdot 288}{95} = 4000(\text{kg}) \approx 4(\text{t}).$$

Annual cost of the adsorbent:

$$B = 1500 \cdot 4 = 6000 \text{ (UAH)},$$

where 1500 UAH – the cost of 1 ton of zeolite [21].

At a consumption of active coal per year about 4.2 tons

$$m_{coal} = \frac{350 \cdot 240000}{20000} = 4200(\text{kg}) \approx 4,2(\text{t}),$$

where 350 – the mass of active coal necessary for purification of 20,000 dkl; 240000 – annual plant productivity, dkl, at a cost of active coal 35000 UAH [22] the annual cost will be 147 thousand UAH.

Thus, the economic efficiency of using zeolites instead of active coal will be about 140 thousand UAH or more than 5 thousand USD. To reduce the consumption of zeolites can also be the use of regeneration, since natural zeolites are wear-resistant.

It is also known about the use of natural zeolites for extraction of ethanol from dilute ethanol-water solutions [23] and dehydration of bioethanol [24, 25]. The possibility of sorption of primary alcohols C1-C4 [26, 27], as well as isoamylol, isobutanol, isopropanol, [27] is also shown. The conclusion in [26] is that the stability of adsorbed alcohols is controlled by van der Waals dispersion interactions and steric zeolite limitations, which destabilize the local formation of hydrogen bonds.

4. Conclusions

Analysis of the research results on the possibility of using mineral adsorbents (clinoptilolite and schungite) for purification of water-alcohol solutions from impurities shows the practical and economic feasibility of using natural zeolites.

The best concentration of a water-alcohol solution for adsorption of acetaldehyde is 80–85 % vol.; ethyl acetate is 40 % vol. This is explained by the lowest energy of hydrogen bonds with ethanol, indirectly determined from the dependence of the rectification factor on the ethanol content of the solution.

The rational duration of phase contact for adsorption of acetaldehyde is from 10 to 20 minutes, for adsorption of ethyl acetate – 5 minutes.

To purify water-alcohol solutions from aldehydes, which most worsen the organoleptic characteristics of alcoholic beverages, it is more appropriate to use clinoptilolite. It can also allow to achieve the normative parameters of vodka made from non-standard rectified alcohol.

A problematic issue of using clinoptilolite can be its spraying and the ingress of small particles into the product. And although manufacturers guarantee the safety of this adsorbent for a person (such as active coal), an additional filter must be provided. This will help preserve the marketable condition of the product.

References

[1] Xiao, P., Zhang, J., Webley, P., Li, G., Singh, R., Todd, R. (2008). Capture of CO_2 from flue gas streams with zeolite 13X by vacuum-pressure swing adsorption. Adsorption, 14 (4-5), 575–582. doi: 10.1007/s10450-008-9128-7

[2] Li, Y., Yi, H., Tang, X., Li, F., Yuan, Q. (2013). Adsorption separation of CO_2/CH_4 gas mixture on the commercial zeolites at atmospheric pressure. Chemical Engineering Journal, 229, 50–56. doi: 10.1016/j.cej.2013.05.101

[3] Farag, H. A. A., Ezzat, M. M., Amer, H., Nashed, A. W. (2011). Natural gas dehydration by desiccant materials. Alexandria Engineering Journal, 50 (4), 431–439. doi: 10.1016/j.aej.2011.01.020

[4] Lively, R. P., Chance, R. R., Kelley, B. T., Deckman, H. W., Drese, J. H., Jones, C. W., Koros, W. J. (2009). Hollow Fiber Adsorbents for CO2Removal from Flue Gas. Industrial & Engineering Chemistry Research, 48 (15), 7314–7324. doi: 10.1021/ie9005244

[5] Bezdieniezhnykh, L. Ya., Aleksieieva, T. M. (2009). Mozhlyvosti adsorbtsiinoho ochyshchennia stichnykh vod vid ioniv vazhkykh metaliv. Ekolohichna bezpeka, 2 (6), 54–57.

[6] Nechytailo, L. Ya., Ersteniuk, H. M. (2015). Efektyvnist vykorystannia pryrodnoho sorbentu dlia ochyshchennia pytnoi vody vid nitrat-yoniv. Naukovi zapysky TNPU. Seriya:Khimiya, 22, 24–28.

[7] Luchian, C. E., Colibaba, C., Niculaua, M., Codreanu, M., Cotea, V. V. (2015). Innovative materials in winemaking. BIO Web of Conferences, 5, 02023. doi: 10.1051/bioconf/20150502023

[8] Melnyk, V. M., Melnyk, V. P., Mank, V. V. et. al. (2002). Pat. No. 51497 UA. Sposib deghidratatsiyi etylovogho spyrtu. MPK A7 C07C7/13. No. 2002042978; declareted: 12.04.2002; published: 15.11.2002, Bul. No. 11.

[9] Mineral'ni resursy Ukrayiny (2014). Kyiv: Derzhavne naukovo-vyrobnyche pidpryyemstvo «Derzhavnyy informatsiynyy heolohichnyy fond Ukrayiny», 270.

[10] Tekhnicheskaya dokumentaciya. Zakarpatskiy ceolitovyi zavod. Available at: http://www.dpzzz.com/ru/docs.htm

[11] Shushkov, D. A., Kotova, O. B., Naumko, I. M. (2011). Svoystva i primenenie klinoptilolitovyih tufov Zakarpatya i analtsimsoderzhaschih porod Timana. Zapiski Ukrayinskogo mineralogichnogo tovaristva, 8, 226–229.

[12] Ambrozova, P., Kynicky, J., Urubek, T., Nguyen, V. (2017). Synthesis and Modification of Clinoptilolite. Molecules, 22 (7), 1107. doi: 10.3390/molecules22071107

[13] Bakakyn, V. V., Seriotkyn, Yu. V. (2009). Unificirovannye formul'nye i ob»emnye harakteristiki v sravnitel'noy kristallohimii prirodnyh ceolitov. Zhurnal strukturnoi khymii, 50 (7), 123–130.

[14] Hrechanovskaia, E. E. (2010). Metrika elementarnoi yacheiky i otnoshenye Si/Al v tseolytakh riada heilandyt-klynoptylolyt Sokyrnytskoho mestorozhdenyia (Zakarpate, Ukrayna). Mineralohichnyi zhurnal, 32 (4), 12–22.

[15] Ignatov, I., Mosin, O. V. (2014). The structure and composition of carbonaceous fullerene containing mineral shungite and microporous crystalline aluminosilicate mineral zeolite. Mathematical model of interaction of shungite and zeolite with water molecules. Advances in Physics Theories and Applications, 28, 10–21.

[16] Yanchevskyi, V. K., Oliynychuk, S. T., Kravchuk, Z. D. et. al. (2002). Tablicy spirtometricheskie. Kyiv: UkrNYYspyrtbyoprod, 592.

[17] Instrukciya po tekhnologhicheskomu i mikrobyologhicheskomu kontrolyu spirtovogho proizvodstva (2008). Moscow: VNIIPBT, 399.

[18] Carev, N. Y., Carev, V. Y., Katrakov, Y. B. (2000). Praktycheskaya gazovaya khromatoghrafiya. Barnaul: AGhU, 156.

[19] DSTU 4222:2003. Natsional'nyi standart Ukrayiny. Horilky, spyrt etylovyi ta vodno-spyrtovi rozchyny. Hazokhromatohrafichnyi metod vyznachannya vmistu mikrokomponentiv (2004). Kyiv: Derzhspozhyvstandart Ukrayiny, 12.

[20] DSTU 4221:2003. Spyrt etylovyi rektyfikovanyi. Tekhnichni umovy (2004). Kyiv: Derzhspozhyvstandart Ukrayiny, 10.

[21] Tseolit. Available at: https://sokirnitskij-tseoltovij-zavod.prom.ua/g6619229-tseolt

[22] Aktivirovannyi ugol (marka BAU-A, BAU-MF, DAK, OU-A). Available at: http://snabhim.com.ua/vodoochistka/aktivirovannyj-ugol-bau-a.html?gclid=CjwKEAjwqcHLBRCq5uHTpLL12FISJAD6Pg-DIDGKtUzxLGaueJyUVFM-58u-Xr-c-xE2-msM7QO8J-xoC8Mjw_wcB

[23] Zhang, K., Lively, R. P., Noel, J. D., Dose, M. E., McCool, B. A., Chance, R. R., Koros, W. J. (2012). Adsorption of Water and Ethanol in MFI-Type Zeolites. Langmuir, 28 (23), 8664–8673. doi: 10.1021/la301122h

[24] Kontar, O. Ya., Valievakhin, H. M., Haleiev, E. R., Dokhov, O. I. (2014). Pat. No. 105707 UA. Sposib otrymannia spyrtu etylovoho znevodnenoho. MPK A7 C07C7/13. No. a201300030; declareted: 02.01.2013; published: 10.02.2014, Bul. No. 11.

[25] Onuki, S., Koziel, J. A., (Hans) van Leeuwen, J., Jenks, W. S., Grewell, D., Cai, L. (2008). Ethanol production, purification, and analysis techniques: a review. 2008 Providence, Rhode Island. doi: 10.13031/2013.25186

[26] Nguyen, C. M., Reyniers, M.-F., Marin, G. B. (2010). Theoretical study of the adsorption of C1–C4 primary alcohols in H-ZSM-5. Physical Chemistry Chemical Physics, 12 (32), 9481–9493. doi: 10.1039/c000503g

[27] Marynchenko, V. P., Marynchenko, L. V., Fil, O. V. (2014). Ochyshchennia vodno-spyrtovykh rozchyniv vid vyshchykh spyrtiv mineralnymy adsorbentamy. Naukovi pratsi NUKhT, 20 (5), 214–219.

STUDYING OF THE STRUCTURE OF Al_2O_3–SiO_2–CaO–P_2O_5 SYSTEM AND ITS SIGNIFICANCE IN THE TECHNOLOGY OF REFRACTORIES

Yulia Kharybina
Department technology of ceramics, refractories, glass and enamels
National Technical University «Kharkiv Polytechnic Institute»
2 Kirpicheva str., Kharkiv, Ukraine, 61002
hyvbyv86@gmail.com

Yaroslav Pitak
Department technology of ceramics, refractories, glass and enamels
National Technical University «Kharkiv Polytechnic Institute»
2 Kirpicheva str., Kharkiv, Ukraine, 61002

Abstract

The paper shows that presence of such phases as mullite, corundum is required in order to obtain high quality refractories that are able to work effectively under the conditions of the simultaneous effects of corrosive environments, high temperatures and pressure, sudden changes in temperature. The structures of Al_2O_3–SiO_2–CaO–P_2O_5 system are examined in the materials in which the formation of defined phases is probably. Based on data it is carried out partitioning of the system on the elementary tetrahedrons. The data on the lengths of tie lines, volumes, the asymmetry degree and the eutectic temperature of elementary tetrahedrons are given. The geometric-topological characteristic of the phases of this system are presented. The choice of oxides compositions areas for the production of refractories is justified based on the obtained results.

Keywords: geometric-topological characteristics, mullite, corundum, phase, refractories, elementary tetrahedrons, system.

DOI: 10.21303/2461-4262.2017.00367

1. Introduction

Systems comprising refractory oxides, and compounds as well as phosphates of the composition are of great interest for the study of the kinetics and mechanism for determining the hardening of phosphate tangles composed refractory like at normal temperature or under heating. It is important because the processes of hardening and the products of formation occur in different ways [1–4]. One of such system is the Al_2O_3–SiO_2–CaO–P_2O_5 system. This system has practical value in the technology of refractory non-metallic materials. Especially it is necessary in considering the life of refractories in thermal units of construction industry [5–7]. The first version of the partition of this system into elementary tetrahedral is given [5].

The aim of research is determination of the geometric-topological characteristics of the phases of the system, taking into account new data on the coexistence of phases and structure of the system.

According to the classification [1], Al_2O_3–SiO_2–CaO–P_2O_5 system is the system of high complexity (43 elementary tetrahedrons, 32 compounds). Absence of the thermodynamic data about this system will not allow to clarify the processes of phase formation that occur in the material at high temperatures, as well as to solve important problems associated with the scientifically grounded choice of compositions and development of rational technological methods. The study of this system will be continued due to its great value for the construction and metallurgical areas. Also it is necessary to be studied by the authors in a form such as described in [8–10].

2. Materials and Methods

The geometric-topological characteristics of phase of the system consist of: number of the tetrahedrons where this phase is in, number of phases with which coexist, the volume of existence (ΣV_i, the total volume of all elementary tetrahedrons where this phase is in), probability of existence (ω).

The calculating formula of probability existence of phases in this concentration tetrahedron is presented (1):

$$\omega_i = \frac{\sum V_i}{n \times V_0}, \quad (1)$$

where $\sum V_i$ – total volume of elementary tetrahedrons in which there is this phase, V_0 – the volume of concentration tetrahedron, n – the number of components in the system, in this case n = 4.

The relative volume of the elementary tetrahedron is calculated using the determinant by the formula (2):

$$V_i = \begin{vmatrix} X_1 & Y_1 & Z_1 & 1 \\ X_2 & Y_2 & Z_2 & 1 \\ X_3 & Y_3 & Z_3 & 1 \\ X_4 & Y_4 & Z_4 & 1 \end{vmatrix}, \quad (2)$$

where X_i, Y_i, Z_i – content of oxides Al_2O_3, SiO_2, CaO, P_2O_5 in the compounds constituting the elementary tetrahedron.

The degrees of asymmetry of elementary tetrahedrons are estimated as the ratio of the maximum (L_{max}) to a minimum edge length (L_{min}) by the formula (3):

$$K = \frac{L_{max}}{L_{min}}. \quad (3)$$

The conode length of elementary tetrahedrons is calculated using the barycentric coordinates and elements of Euclidean geometry by the formula (4):

$$\begin{aligned} L^2 = &(x_2 - x_1)^2 + (y_2 - y_1)^2 + (z_2 - z_1)^2 + \\ &+ (T_2 - T_1)^2 + (x_2 - x_1)(y_2 - y_1) + (x_2 - x_1)(z_2 - z_1) + \\ &+ (x_2 - x_1)(T_2 - T_1) + (y_2 - y_1)(z_2 - z_1) + \\ &+ (y_2 - y_1)(T_2 - T_1) + (z_2 - z_1)(T_2 - T_1), \end{aligned} \quad (4)$$

where x_1, y_1, z_1, x_2, y_2, z_2 – the coordinates (component concentration) of coexisting vapor phase.

To illustrate the relationship of elementary tetrahedrons of system it is necessary to use the method of topological graphs, as described in [11]. The number of edges (R) is calculated according to Euler's formula (5):

$$R = \frac{Z_1 + 2Z_2 + 3Z_3 + 4Z_4}{2}. \quad (5)$$

Taking into account that the eutectic temperature of the liquid curves for all components of the system are equal, the calculation of the temperature and eutectic composition for the four-systems are produced by the decision of the system of equations (6) given in [11]:

$$\begin{cases} T_i = \dfrac{T_{пл.i}}{1 - \dfrac{\ln(X_i)}{N_i}} = T_2 = T_{пл.2} \Big/ \left(1 - \dfrac{\ln(X_2)}{N_2}\right), \\ T_2 = \dfrac{T_{пл.2}}{1 - \dfrac{\ln(X_2)}{N_2}} = T_3 = T_{пл.3} \Big/ \left(1 - \dfrac{\ln(X_3)}{N_3}\right), \\ T_3 = \dfrac{T_{пл.3}}{1 - \dfrac{\ln(X_3)}{N_3}} = T_4 = T_{пл.4} \Big/ \left(1 - \dfrac{\ln(X_4)}{N_4}\right), \\ X_1 + X_2 + X_3 + X_4 = 1. \end{cases} \quad (6)$$

Calculation of geometric-topological characteristics of the phases of the system is carried out using programs developed at the department of technology of ceramics, refractories, glass and enamels of NTU "KPI".

3. Research results of the Al_2O_3–SiO_2–CaO–P_2O_5 system

To analyze the probability of formation reactions of the crystalline phases, the calculation of the free Gibbs energy are made from the equations given by [12, 13].

It is established the possibility of the occurrence of conjugate reactions by considering the structure of the Al_2O_3–SiO_2–CaO–P_2O_5 system:

1) $AP+3C_3P+2S \rightarrow 3C_2P+C_3APS_2$;
2) $AP+A_3S_2+C_3P \rightarrow C_3APS_2+A_3P$;
3) $S+C_3P+CAS_2 \rightarrow C_3APS_2+CS$;
4) $2C_3P+3CS+C_2AS \rightarrow CAS_2+2C_5SP$;
5) $C_3P+CA+C_2AS \rightarrow CA_2+C_5SP$;
6) $A_3S_2+C_3P \rightarrow C_3APS_2+2A$.

The temperature dependence of the free Gibbs energy for which is determined (**Fig. 1**).

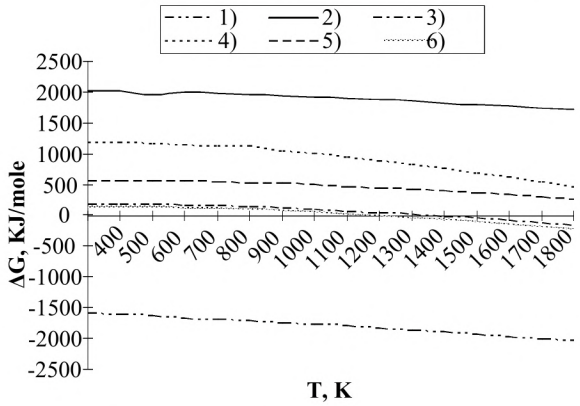

Fig. 1. The dependence $\Delta G_T = f(T)$ for the reactions in the system: 1 – reaction 1; 2 – reaction 2; 3 – reaction 3; 4 – reaction 4; 5 – reaction 5; 6 – reaction 6

Thermodynamic analysis of the reactions in Al_2O_3 – SiO_2 – CaO – P_2O_5 system (accepted conventions of Al_2O_3–A, SiO_2–S, CaO–C, P_2O_5–P) has allowed to establish the following co-existing phases of the pair (conodes taking place in three-dimensional space): C_3P–CAS_2; C_3APS_2–C_3P; C_3APS_2–C_2P; S–C_3APS_2; A_3S_2–C_3APS_2; A_3P–C_3APS_2; A_3S_2–C_3P; C_3APS_2–CS; C_3APS_2–CAS_2; AP–C_3APS_2; C_3P–C_2AS; CAS_2–C_5SP; C_5SP–CA; C_5SP–C_2AS; C_7S_2P–CA; C_7S_2P–C_2AS; C_7S_2P–$C_{12}A_7$; C_7S_2P – C_3A; C_5SP – $C_{12}A_7$; C_3A – C_5SP.

32 phases, 4 oxides constituting the system, 23 according to the number of binary oxides of simple compounds, 4 ternary compounds, 1 four-component are taken in determining the structure of the system. The system is partitioned on 45 elementary tetrahedrons in the subsolidus. The characteristics (data volume V_i, the temperature T_i of occurrence and degree of asymmetry of the melt) are shown in **Table 1.**

It is evident (from **Table 1** data) that the minimum temperature of the melt in the appearance of Al_2O_3–SiO_2–CaO–P_2O_5 system is equal to 854 K, and corresponding composition is located in elementary tetrahedron No. 7 (AP–CP–S_5P_3–S). The maximum temperature is equal to 1781 K (C_7S_2P–C_2S–C_3A–C_3S) at which the solid phase still persists in the system.

The tetrahedrons AP–A_3S_2–S–C_3APS_2 (V_i=133,95 ‰, T_i=1552 K), A–A_3S_2–C_3P–A_3P (V_i= =49,22 ‰, T_i=1742 K), C_3APS_2–A_3S_2–S–CAS_2(V_i=39,27 ‰, T_i=1573 K) are the most technologically considering the volume of the elementary tetrahedron, the degree of asymmetry and minimal occurrence of melt temperature of the composition. The compositions of elementary tetrahedrons including mullite, corundum are the most appropriate for the technology of refractory materials (**Table 1**, tetrahedron number 15).

Table 1

Elementary tetrahedrons of Al_2O_3–SiO_2–CaO–P_2O_5 system

#	Elementary tetrahedrons	The degree of asymmetry	T_i, K	V_i, ‰
1	2	3	4	5
1	AP_3–CP_2–SP–P	1,8	858	9,64
2	AP_3–C_2P_3–SP–CP_2	5,99	1020	2,54
3	AP_3–CP–SP–C_2P_3	3,87	1017	4,36
4	AP_3–CP–SP–A_2P_3	2,38	no data	11,16
5	AP–CP–SP–A_2P_3	4,01	no data	8,02
6	AP–CP–SP–S_5P_3	1,90	855	39,37
7	AP–CP–S_5P_3–S	2,42	854	45,01
8	AP–CP–C_7P_5–S	12,23	1208	30,95
9	AP–C_7P_5–C_2P–S	10,33	1251	36,13
10	AP–C_3P–C_2P–C_3APS_2	4,87	1512	9,64
11	AP–C_3APS_2–C_2P–S	2,83	1469	74,99
12	AP–A_3S_2–A_3P–C_3APS_2	2,78	1589	23,95
13	AP–A_3S_2–S–C_3APS_2	1,85	1552	133,95
14	AP–A_3S_2–C_3P–A_3P	2,78	1669	41,09
15	A–A_3S_2–C_3P–A_3P	2,88	1742	49,22
16	C_3APS_2–S–C_3P–CS	2,93	1526	43,13
17	C_3APS_2–A_3S_2–C_3P–CAS_2	2,64	1611	10,15
18	C_3APS_2–A_3S_2–S–CAS_2	2,56	1573	39,27
19	C_3P–A_3S_2–A–CAS_2	3,07	1759	26,49
20	C_3P–CA_6–A–CAS_2	10,32	1761	16,85
21	C_3P–CA_6–C_2AS–CAS_2	3,78	1721	53,28
22	C_3P–CS–C_2AS–CAS_2	2,71	1620	35,92
23	S–CAS_2–C_3APS_2–CS	2,62	1523	43,33
24	C_3P–CA_6–CA_2–C_2AS	6,01	1778	13,39
25	C_3P–CA_2–CA–C_2AS	4,91	1691	14,21
26	C_3P–C_5SP–CA–C_2AS	3,89	1703	7,61
27	C_7S_2P–C_5SP–CA–C_2AS	7,59	1721	3,65
28	C_3P–C_5SP–CS–C_2AS	3,85	1661	10,39
29	C_7S_2P – C_5SP – CS – C_2AS	5,17	1676	4,87
30	C_7S_2P–CA–C_2S–C_2AS	2,85	1717	10,15
31	C_7S_2P–C_3S_2–CS–C_2AS	3,41	1591	8,22
32	C_7S_2P–C_2S–C_3S_2–C_2AS	4,91	1674	5,58
33	C_7S_2P–C_2S–CA–$C_{12}A_7$	4,30	1652	10,05
34	C_7S_2P–C_2S–$C_{12}A_7$–C_3A	3,30	1654	10,55
35	C_7S_2P–C_2S–C_3A–C_3S	4,23	1781	7,10
36	C_7S_2P–C_5SP–CA–$C_{12}A_7$	7,59	1654	3,55
37	C_7S_2P–C_3A–$C_{12}A_7$–C_5SP	6,17	1665	3,75
38	C_7S_2P–C_3A–C_4P–C_3S	2,15	1748	10,05
39	C_7S_2P–C_3A–C_4P–C_5SP	5,44	1747	1,62
40	C_5SP–C_3A–C_4P–C_3P	6,05	1729	3,35
41	C_5SP–C_3A–C_3P–$C_{12}A_7$	4,45	1652	8,02
42	C_5SP–C_3P–$C_{12}A_7$–CA	4,84	1651	7,51
43	C–C_3S–C_3A–C_4P	1,48	1707	39,07
44	C_3P–S–C_2P–C_3APS_2	8,59	1487	19,69
45	C_3P–CAS_2–C_3APS_2–CS	2,03	1568	9,18
	The total volume		1000	

The tie lines rearrangement in the ternary subsystem Al_2O_3–SiO_2–CaO–P_2O_5 is shown in **Fig. 2**.

The geometric-topological characteristics of phases of the system are presented (**Table 2**) [14–17].

Table 2

Geometric-typological characteristics of phases of Al_2O_3–SiO_2–CaO–P_2O_5 system

No.	Phase	Number of the tetrahedrons where this phase is in	Number of phases with which coexist	The volume of existence, $\sum V_i$, ‰	Probability of the existence, ω_i
1	C	1	3	39,05	0,00976
2	A	3	5	92,54	0,0231
3	S	9	10	466,28	0,116
4	P	1	3	9,65	0,00241
5	C_3A	8	8	83,48	0,0208
6	$C_{12}A_7$	6	6	43,42	0,0109
7	CA	6	7	49,20	0,0123
8	CA_2	2	4	27,58	0,00690
9	CA_6	3	5	83,49	0,0208
10	C_3S	3	5	56,20	0,0141
11	C_2S	5	7	43,42	0,0109
12	C_3S_2	2	4	13,79	0,00345
13	CS	7	8	154,98	0,0387
14	C_4P	4	6	54,07	0,0135
15	C_3P	18	17	378,97	0,0948
16	C_2P	4	5	140,40	0,0351
17	C_7P_5	2	4	67,06	0,0168
18	CP	6	8	138,82	0,0347
19	C_2P_3	2	4	6,89	0,00173
20	CP_2	2	4	12,18	0,00305
21	A_3S_2	7	7	323,99	0,0810
22	A_3P	3	5	114,21	0,0286
23	AP	10	11	442,94	0,111
24	A_2P_3	2	4	19,18	0,00480
25	AP_3	4	6	27,69	0,00692
26	S_5P_3	2	4	84,35	0,0211
27	SP	6	8	75,05	0,0188
28	C_2AS	11	10	167,20	0,0418
29	CAS_2	8	8	243,38	0,0608
30	C_7S_2P	12	10	79,12	0,0198
31	C_5SP	10	8	54,30	0,0136
32	C_3APS_2	10	8	407,12	0,102
33	The total volume	179	212	4000,0	1,0000
	Maximum	18	17	466,28	0,116
	Minimum	1	3	6,89	0,00173

C_3P, AP, C_5SP, C_2AS, S phases (respectively – No. 15, 23, 31, 28, 3) have the largest number of coexisting phases (**Table 2**). C_3P phase presents in 18 elementary tetrahedron and has a maxi-

mum amount of existence – 424,6 ‰. Significant volumes of existence in this system have a phase: S (481,5), AP (414,2), C_3APS_2 (396,0), A_3S (287,5).

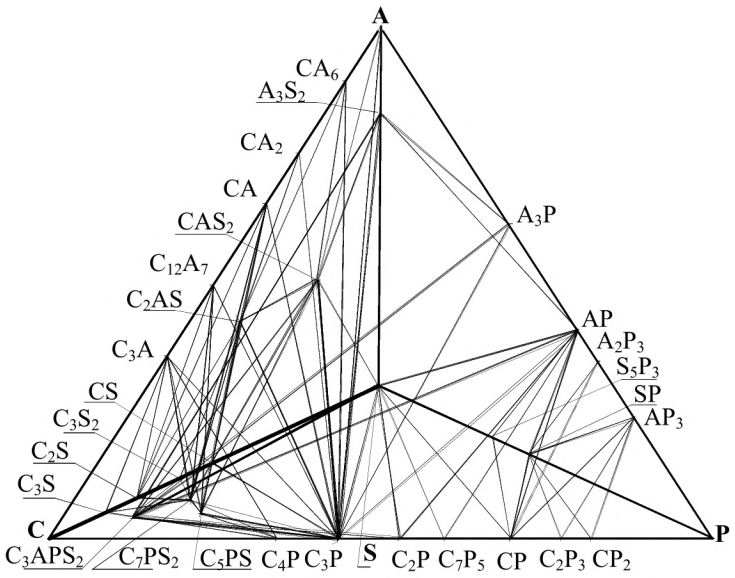

Fig. 2. The state of elementary tetrahedrons of Al_2O_3–SiO_2–CaO–P_2O_5 system in the concentration tetrahedron

4. Discussing of research results

Comparative analysis of the data is revealed the most technological range of compositions for the production of refractory products. They are located in the immediate vicinity to the edges of elementary tetrahedrons AP–A_3S_2–S–C_3APS_2; A–A_3S_2–C_3P–A_3P; C_3APS_2–A_3S_2–S–CAS_2.

To the basis of the structure of the system data it is of interest to modeling changes the phase structure in the compositions of mullite refractory – slag in the future. It will allow coming nearly to explain the reasons for the destruction of refractories in service when the ratio of the components and their interaction temperature are changing [18].

5. Conclusions

The geometric-topological characteristics of the phases of Al_2O_3–SiO_2–CaO–P_2O_5 system are defined; there are identified the elementary volume, the degree of asymmetry and the eutectic temperature of the elementary tetrahedrons.

The results of studies on the structure of the four-component system (Al_2O_3–SiO_2–CaO–P_2O_5) serve as a theoretical basis for further developments in the field of new technology of refractory non-metallic materials.

References

[1] Launch, J., Buhr, A. (1999). Synthetic alumina raw materials – key elements for refrectories innovations. Progressing of the Unified International Conference on Refrectories, Unitecr – 99. Berlin, 348–355.

[2] Ma, W., Brown, P. W. (2004). Mechanisms of Reaction of Hydratable Aluminas. Journal of the American Ceramic Society, 82 (2), 453–456. doi: 10.1111/j.1551-2916.1999.tb20085.x

[3] Keush, D., Lutiy, R., Guria, I. (2015). Strengthening core mixtures with phosphoric acid and metal salts. Foundry Production, 7, 27–29.

[4] Schacht, C. (Ed.) (2004). Refractories Handbook. CRS Press, New York. doi: 10.1201/9780203026328

[5] Berezhnoy, A. (1988). Multi-alkaline oxide systems. Kyiv: Naukova Dumka, 200.

[6] Berezhnoy, A. (1970). Multicomponent oxide system. Kyiv: Naukova Dumka, 544.

[7] Berezhnoy, A., Pitak, Ya., Ponomarenko, A., Sobol, N. (1992). The physico-chemical system of refractory, non-metal and silicate materials. Kyiv: UMK VO, 172.

[8] Krebs, R. (1999). Modern solution of refractory problems with unshaped refractories. Proceeding of the Unified International Conference on Refrectories, Unitecr – 99. Berlin, 1–5.

[9] Bondar, I., Malyshikov, A. (1992). Phosphates elements of the fourth group. Sankr-Peterburg: Science, 112.

[10] Kopeikin, V., Klementeva, V. Krasniy, B. (1986). Refractory solutions on phosphate binders. Moscow: Metallurgy, 102.

[11] Rischenko, M., Fedorenko, O., Pitak, Ya. (2013). Chemical technology of refractory non-metal and silicate materials in the examples and problems. Part II. Physical and chemical systems, phase equilibrium, thermodynamics, resource and energy saving technology TNSM. Kharkiv: NTU «KPI», 326.

[12] Kharybina, Yu. (2016). Thermodynamic analysis of reactions in the system Al_2O_3–SiO_2–CaO–P_2O_5. Technology Audit and Production Reserves, 5 (3 (31)), 7–11. doi: 10.15587/2312-8372.2016.80422

[13] Kharybina, Yu., Pitak, Ya. (2016). Research coexistence of phases in the system Al_2O_3 – SiO_2 – CaO – P_2O_5. Modern trends in production and silicate materials. Lviv: Rastr – 7, 52–54.

[14] Pitak, Ya., Shabanova, G., Nagorny, A. (1995). Geometric-topological characteristics of CaO – Al_2O_3 – SiO_2 – P_2O_5 system using computers. Information technology: science, technology, education, health. Kharkiv, Miskolc: KhSPU, 58.

[15] Pitak, Y. N., Nagornyi, A. O., Shabanova, G. N. (1997). Subsolidus structure of the CaO−Al_2O_3−SiO_2−P_2O_5 system. Refractories and Industrial Ceramics, 38 (9-10), 351–353. doi: 10.1007/bf02767890

[16] Pitak, Ya., Taranenkova, V. (2004). Application of topological graphs for studying the quaternary oxide systems. Geometric Topology: Infinite – Dimensional Topology, Absolute Extensors, Applications. Lviv: Ivan Franko National University, 49–50.

[17] Nagorny, A., Shabanova, G., Pitak, Ya. (1997). Using of Mechanic-chemical Method the Phosphates Containing Binders Obtaining for. 13th International Conference on Building Materials. «13.ibausil». Weimar, 2, 445–450.

[18] Keush, D., Lutiy, R. (2015). Thermodynamics of processes of binding components in mixtures for foundry cores. Special Metals: yesterday, today and tomorrow. Kyiv, 543–548.

USING OF THE WAVE TECHNOLOGIES IN INTENSIFICATION PROCESSES OF HEAT AND MASS TRANSFER

Oleg Burdo
Department of processes, equipment and energy management
Odessa National Academy of Food Technologies
112 Kanatna str., Odessa, Ukraine, 65039

Valentyna Bandura
Department of processes and equipment processing and food production
named after Prof. P. S. Bernik
Vinnytsia National Agrarian University
3 Solniachna str., Vinnitsa, Ukraine, 21008
bandura_3@ukr.net

Aleksandr Zykov
Department of processes, equipment and energy management
Odessa National Academy of Food Technologies
112 Kanatna str., Odessa, Ukraine, 65039

Igor Zozulyak
Department of processes and equipment processing and food production
named after Prof. P. S. Bernik
Vinnytsia National Agrarian University
3 Solniachna str., Vinnitsa, Ukraine, 21008

Julia Levtrinskaya
Department of processes, equipment and energy management
Odessa National Academy of Food Technologies
112 Kanatna str., Odessa, Ukraine, 65039

Elena Marenchenko
Department of processes, equipment and energy management
Odessa National Academy of Food Technologies
112 Kanatna str., Odessa, Ukraine, 65039

Abstract

The advantages of wave technologies in comparison with traditional thermal technologies are considered. The aim of research is using of innovative wave technologies to intensify the processes of heat and mass transfer in the processes of dehydration and extraction, while reducing energy costs. A classification of the mechanisms of intensification of heat and mass transfer processes is proposed. Technical methods for intensifying heat and mass transfer during the processing of plant raw materials using technologies for targeted delivery of energy are developed. Samples of equipment are presented that implement technologies of directed energy action and innovative products obtained at these facilities. The results of experimental studies of drying in the microwave and infrared fields are shown.

Keywords: wave technologies, targeted energy delivery, microwave technologies, mass transfer intensification, extraction, dehydration, innovative food concentrates.

DOI: 10.21303/2461-4262.2017.00399

1. Introduction

The scarcity of resources, especially energy, is one of the key problems of our time. Even in prosperous countries, there is a shortage of energy resources [1]. Because of the shortage of energy

carriers, there is a problem of food shortages, since the food industry is one of the most energy-intensive industries in developed countries [2].

In the production of food products, significant energy losses arise in the processes of concentrating the raw materials: drying, dehydration, thickening, etc. [3]. The methods of heat treatment products for the subsequent transfer of water into steam are the most common. With this approach, the influence of high temperatures on the product is unavoidable, which has a bad effect on quality and leads to energy losses. For the production of food concentrates, fruit and vegetable raw materials containing a large number of vitamin complexes, organic acids, natural pigments and other valuable substances are dehydrated [4]. Products of animal origin contain a large number of proteins required by the body [5]. The effect of high temperatures destroys most of these components, and the nutritional value of the product is significantly reduced. A similar situation occurs in the extraction processes, where high temperatures make it possible to intensify diffusion processes [6].

Traditional thermal technologies, despite their availability and prevalence in food production, have significant shortcomings, which can't be reconciled. High-temperature equipment, in the overwhelming majority, does not comply with the norms of environmental safety, energy-consuming and, to a considerable extent, worsens the quality of the finished product [7].

It is necessary to search for alternative approaches to the organization of dehydration and extraction processes using innovative solutions aimed at increasing energy efficiency and reducing the high-temperature impact on the product and increasing the environmental friendliness of production [8].

2. Materials and Methods

The scientific and technical method proposed in the work is the organization of the effect on the boundary layers in the processes of heat and mass transfer by means of external inertial fields. Such fields are created by special generators, and the technology of their application is called wave. Wave technologies (WT) are technologies of directed mechanical or selective electromagnetic action on elements of raw materials and biological objects. It is possible to organize a directed influence on both nanoscale objects, micro- and nanoscale structures of food raw materials [8].

Both in the first and in the second cases, the task of the selective energy effect is to control the fields, to add directions of the force effects of weak fields, to reduce the size of the diffusion boundary layer, to organize the flow from the micro- and nanocapillary structure, to form the composition of these flows, the direction of the force impacts on the shells of the cellular structure of microbiological objects, etc. [9, 10].

For food systems, reducing the amount of consumed energy will not only increase the energy efficiency of the process and reduce the cost of the product, but also reduce the level of thermal effects on the product. This will lead to the preservation of thermolabile and biologically active components of food raw materials. For example, food products and culinary products obtained by WT will fully meet the requirements of functional nutrition.

The task is finding the effective principles, approaches for local actions aimed at intensive, low-energy operations with food raw materials, and even with individual nanosize elements of this raw material. One of the ways in this direction is WT. The basis of WT is innovative mechanisms of organization of mass transfer processes (**Fig. 1**). The means of intensification are electromagnetic (EMF) and mechanical vibrational fields, which are generated by external sources. This makes it possible to influence the hydrodynamic situation, to control the formation of the hydrodynamic, thermal and diffusion boundary layers. As a result, it becomes possible to substantially intensify mass transfer processes.

There are new opportunities, due to the action of specific mechanisms, combined moving forces. The authors of the study [9] put forward two hypotheses about the reserves of energy efficiency of food technologies. According to the first, the combined effect of the wave vibrational field and the heat flux should contribute to thinning the diffusion boundary layer. This can contribute to the intensification of dehydration and drying processes. According to the second hypothesis, the use, when extracting and dehydrating raw materials, of targeted delivery of electromagnetic energy directly to polar liquid molecules in capillaries will allow initiating a powerful, specific hydro-

dynamic flow. As a result, the intensity of mass transfer will increase significantly due to a sharp decrease in internal diffusion resistance, energy costs and duration of the process will decrease.

The justification of the formulated hypotheses in mathematical modeling is based on phenomenological principles. The methodological novelty of the work is the representation of a complex hydrodynamic and diffusion flux in the form of an effective mass-transfer coefficient. New numbers of similarity are derived on the basis of the "dimensionality analysis" method, which are called "wave similarity numbers". The classical similarity numbers are modified and the Reynolds, Peclet and Stanton wave numbers are obtained. These numbers take into account the specificity of the action of electromagnetic and vibrational fields.

Experimental studies have used the techniques generally accepted for heat and mass transfer [1]. Particular dependences of the influence of regime and constructive parameters on the intensity of mass transfer have been established [10]. The obtained bases of the experimental data are generalized in the form of criterial equations [11].

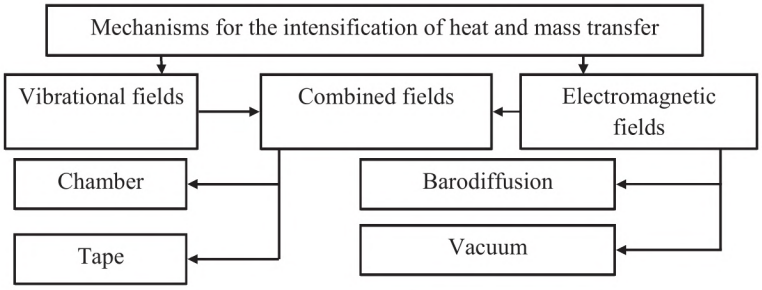

Fig. 1. Classification of the mechanisms of intensification of heat and mass transfer processes in food processing technologies

3. Experimental procedures

Based on the principles of targeted energy delivery, dehydration and extraction devices have been developed that use electromagnetic energy generators or combined effects on the product.

Tape microwave device (patent of Ukraine No. 28889) is designed for drying thermolabile raw materials and uses the above principles. The speed of the tape drive and the load capacity are regulated in a wide range (0.007...0.025 m/s). The power of the emitters has a step-by-step control in the range 30...100 % of the nominal power of the magnetron. Stand testing of the device determined its high technical characteristics. Tape dryer has successive zones of microwave and infrared exposure to the product. Power control is the pulse modulation. Appearance of the device is shown in **Fig. 2, *a***. Samples of dried fruits and vegetables were obtained using a tape dryer. The product well preserves color, aroma and taste. The obtained samples are shown in **Fig. 2, *b*.**

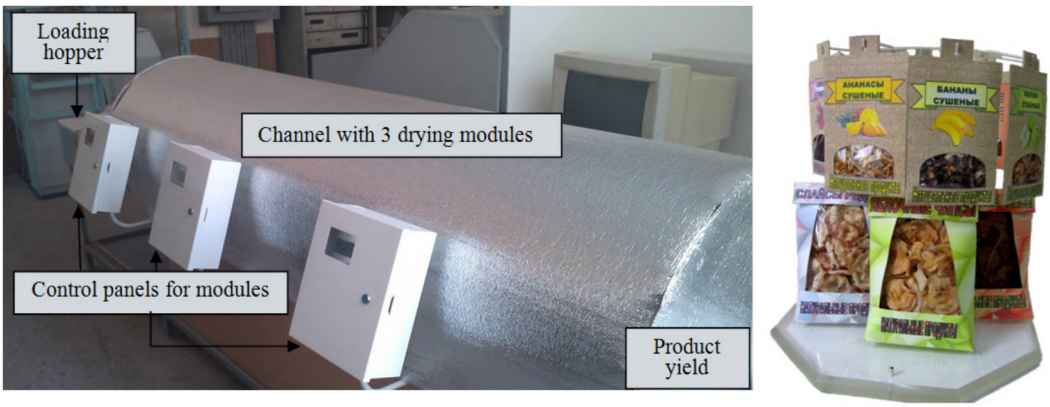

a *b*

Fig. 2. Appearance of tape dryer with combined energy supply and samples of finished products

The developed microwave drier (**Fig. 2**) differs and high intensity of mass transfer. Experimental data obtained during soybean drying (**Fig. 3**) showed that when the tape load is m=3,96 kg/m^2, the normative value of the final moisture content is reached in 35–40 minutes.

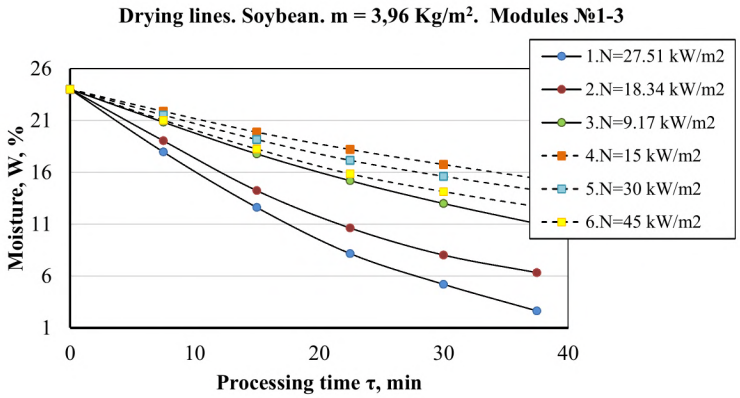

Fig. 3. Soybean drying lines in a tape microwave dryer

On the drying line (**Fig. 3**), the influence of the type of supplied energy and the specific power on the dehydration process is clearly observed. The use of three infrared emitters (IR-dotted lines) twice as much dries the soybeans to the required humidity level of 9 %. It has been experimentally established that microwave energy generators (straight lines) with different number of modules contribute to the removal of moisture almost equally, and for drying soybeans up to 9 % it will take three times longer than using IR energy generators.

The process of moisture removal passed with a high intensity (**Fig. 4**).

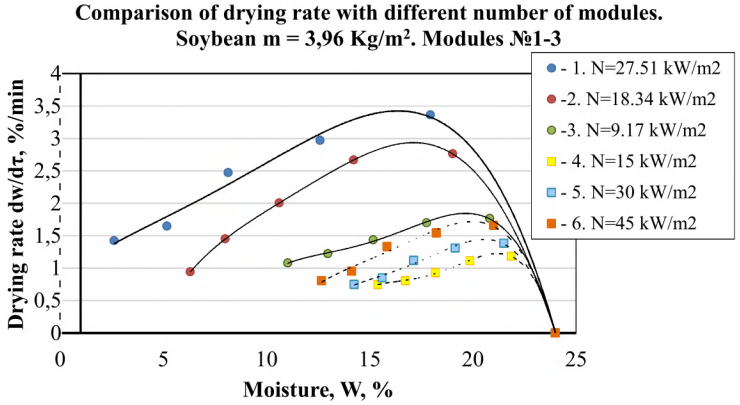

Fig. 4. Soybean drying rate lines with combined energy input

With an increase in the number of modules (**Fig. 4**), there are minor changes in the rate of soybean drying with the use of a microwave energy generator and quite significant changes in drying rate with the use of infrared emitters.

To obtain plant extracts of high concentration, a microwave countercurrent device, protected by patent of Ukraine No. 87503, has been developed. In the microwave extractor, a counterflow movement of the extractant and solid phase takes place, which makes it possible to intensify the process. The design characteristics of the extractor are given in **Table 1**, the external appearance – in **Fig. 5**. A concentrate of coffee extract with a solids content of 55 % was obtained in the extractor. With traditional extraction methods, the concentration of solids in the extract does not exceed 18...20 % [8].

It is planned to introduce such extractors into production. Due to the fact that the extraction is carried out at atmospheric pressure − the design is simplified considerably, weight and size parameters of the equipment are reduced. Extraction is carried out at temperatures not higher than

100 °C, which has a favorable effect on product quality. Microwave extractors are used to produce a concentrate of coffee extract, hips extracts, medicinal herbs (stevia, tarragon, etc.).

Table 1

Microwave extractor design characteristics

Power consumption, kW	Working volume, dm^3	Magnetrons (0,9 kW), pcs.	Overall dimensions (l/w/h), m	Productivity by raw material, kg/h
≤7,3 kW	180	5	0,52/0,68/2,05	≤ 24

Fig. 5. Microwave extractor

4. Results

Drying in the microwave and infrared field allows to obtain a high quality product, due to the absence of high temperatures. When using wave generators, the rate of drying is significantly increased.

The use of wave technologies in the extraction process allows obtaining high-quality concentrates that retain useful properties due to the absence of high temperatures. The coffee concentrate obtained in the microwave extractor received a positive evaluation, which was noted in a number of acts of degustation.

The study of wave technologies and the principles of targeted energy delivery make it possible to create equipment with high efficiency indicators of mass transfer processes. The study of approaches to mathematical modeling of wave technologies will allow creating more efficient equipment, moving from a laboratory installation to an operating industrial model.

The use of wave technologies in the production of food products allows to reduce the temperature of the process, which gives a positive energy effect and allows to maintain the quality of the product.

5. Discussion of research results

As a result of the studies with electromagnetic energy sources, the following facts are established:

– energy costs for removing moisture from raw materials are less than that of traditional drying equipment by 20...50 %;

– when extracted in the electromagnetic field of the microwave range, the output of the target components from raw materials is 4...8 % more than in traditional devices;

– when extracting in a microwave field in an extract, in addition to soluble components, insoluble substances also appear.

These facts confirm the hypotheses put forward by the authors about the possibility of targeted delivery of energy to individual elements of food raw materials. So, when drying, electromagnetic energy interacts with water molecules, dissipation of electromagnetic energy into heat occurs. As a result, a barodiffusion flow of a mixture of steam and moisture emerges from the capillaries of the raw material. It is a combination of diffusion and hydrodynamic flows. The more raw material (water) out in the form of a liquid phase, the lower the energy costs for dehydration.

When extracting, the barodiffusion flux from the volume of raw materials is carried out due to inertial forces and those substances that are absent in traditional extractive technologies. This explains the fact that the samples of the product obtained in the microwave extractor differ significantly for the better from the analogs.

At the same time, the full realization of the capabilities of devices that use the principles of directed energy action depends on a deep understanding of the complex and interrelated processes of interaction of electromagnetic fields and the structure of the product.

Studies aimed at an in-depth study of the effect of electromagnetic and vibration fields on dehydration and extraction processes are necessary for the effective development of equipment that implements innovative principles of directed energy action.

6. Conclusions

It is established that directed local energy action on nanoscale elements of food raw materials will allow developing innovative approaches to the organization of food technologies. Impulse actions are powerful means of initiating the appearance of nanokinetics. Combination of pulsed electromagnetic and vibrational fields allows significantly intensify the processes of heat and mass in the electromagnetic field.

The developed approaches to the mathematical description and evaluation of the influence of the field intensity on the intensity of mass exchange processes allow to find the principles of optimization of technological and design parameters, to formulate a methodology for designing innovative equipment.

Devices created with the use of wave technologies are protected by patents, it is planned to introduce microwave extractors and dryers in the food concentrates industry. Equipment created using the principles of targeted delivery of energy is distinguished by a reduced thermal effect, which positively affects the quality of food products and reduces energy costs. At the same time, the lack of practice of using such equipment in enterprises forms a barrier for the practical application of such equipment. It is necessary to determine the reliability reserves of such devices, to develop standard series for dryers and extractors, and to conduct additional production tests.

References

[1] Weibbach, D., Ruprecht, G., Huke, A., Czerski, K., Gottlieb, S., Hussein, A. (2013). Energy intensities, EROIs (energy returned on invested), and energy payback times of electricity generating power plants. Energy, 52, 210–221. doi: 10.1016/j.energy.2013.01.029

[2] Gromadzki, G., Konol, W. (2008). Energy game: Ukraine, Moldova and Belarus between the EU and Russia. Energy Security in Central and Eastern Europe. Prague, 19.

[3] Aloqbi, A., Omar, U., Yousr, M., Grace, M., Lila, M. A., Howell, N. (2016). Antioxidant Activity of Pomegranate Juice and Punicalagin. Natural Science, 8 (6), 235–246. doi: 10.4236/ns.2016.86028

[4] Sorour, M. A. (2015). Optimization of Multiple Effect Evaporators Designed for Fruit Juice Concentrate. American Journal of Energy Engineering, 3 (2), 6. doi: 10.11648/j.ajee.s.2015030201.12

[5] Azoev, G. L., Degterev, D. A., Degtereva, E. A., Zobov, A. M.; Azoeva, G. L. (2011). Ryinok nano: ot nanotehnologiy-k nanoproduktam. Moscow: BYNOM, 320.

[6] Potapov, V. A., Yakushenko, E. N. (2013). Povyshenie energoeffektivnosti sushki vinogradnyih vyizhimok v massoobmennom module s konduktivnyim podvodom teplotyi. Naukovi pratsi Odeskoyi natsionalnoyi akademiyi harchovih tehnologiy, 43 (2), 179–184.

[7] Bernic, M., Raducan, M., Ciobanu, E. (2013). Drying Kinetics of Sunflower Seeds using Pulsed UHF Energy Intake. TEM Journal, 2 (4), 305–308.

[8] Burdo, O., Terziev, S., Levtrinskaya, Y. (2015). Energetika ekoindustrii pischevyih kontsentratov. Problemyi regionalnoy energetiki [Problemele energetici regionale], 3 (29), 112–118.

[9] Burdo, O. G. (2013). Pischevyie nanoenergotehnologii. Kherson: GRIN D.S., 294.

[10] Burdo, O. G., Terziev, S. G., Bandura, V. N. (2015). Printsipy napravlennogo energeticheskogo deystviya v pischevyih nanotehnologiyah. Problemyi regionalnoy energetiki, 1 (27), 79–85.

[11] Burdo, O. G., Zykov, A. V., Terziev, S. G., Ruzhitskaya, N. V. (2016). The Nanotechnological Innovation in Food Industry. International Journal of Engineering Research and Applications, 6 (3), 144–150.

ANALYSIS OF THE ENERGY POTENTIAL OF SOLAR LIGHT OF THE WESTERN REGION OF UKRAINE WITH THE ACCOUNT OF CLIMATIC CONDITIONS

Vladimir Andreychuk
Department of Lighting Engineering and Electrical Engineering
Ternopil Ivan Puluj National Technical University
46 Mikulinetska str., Ternopil, Ukraine, 46005
Andriychukv@rambler.ru

Yaroslav Filyuk
Department of Lighting Engineering and Electrical Engineering
Ternopil Ivan Puluj National Technical University
46 Mikulinetska str., Ternopil, Ukraine, 46005
filuk.slavik.91@gmail.com

Abstract

An experimental facility for measuring and recording the flux density of solar radiation is designed and installed. An electrical circuit is developed and a pyranometer model is developed to measure the level of solar radiation, and it is graduated with a Soler Power Meter DT-1307 solar radiation flux meter. The time distribution of the flux density of solar energy is analyzed and the surface energy density of solar radiation is calculated for Ternopil. The influence of climatic conditions on the energy of solar radiation is determined. Analytical dependencies are obtained on the basis of comparison of the measured values of the flux density of solar radiation and the cloud cover taken from meteorological services. The energy potential of solar radiation during 2012–2015 in the western region of Ukraine is calculated, as well as the average monthly and average annual energy density of solar radiation. It is determined that the annual average density of the solar energy flux is 1045.9 kW·h/m^2, and its deviation does not exceed 5 %. It is shown that the most favorable months for the use of solar energy are from March to September of each year.

Keywords: solar energy flux density, energy potential, cloudiness degree, pyranometer, microcontroller.

DOI: 10.21303/2461-4262.2017.00398

1. Introduction

A characteristic feature of modern energy systems is the movement towards the development of clean energy based on non-traditional and renewable energy sources. One of the most promising areas is solar energy. In Ukraine, there are quite favorable conditions for the use of solar energy. When studying the energy potential of solar radiation, it is necessary to take into account not only the coordinates of the terrain, but also climatic conditions. At present, there is the data of weather services for regional and district centers for the whole territory of Ukraine. They are represented by temperature, cloudiness, wind speed, cloud height, atmospheric pressure of the region [1]. Among them there is no data on the flux of solar radiation. There is the task to establish a connection between the meteorological conditions of the terrain and the flow of solar energy.

The aim of research is measuring the energy potential of solar radiation, taking into account the climatic conditions of the Ternopil region. Establishment of a connection between meteorological data and the density of energy flux of solar radiation, which will allow to determine the energy potential of the western region of Ukraine.

Formulation of the problem. Development of a technique and manufacturing of an experimental facility for measuring the energy potential of solar radiation and recording it in real time. Calculation of the energy flux density of solar radiation during the day and establishing its dependence on the degree of cloudiness.

2. Materials and methods

When analyzing the intensity of solar radiation, it is assumed that the total monthly solar energy falling on a horizontal surface, although changing annually, but their average value does

not change [2, 3]. In [4, 5], the monthly and annual values of the total solar energy falling on the horizontal surface are obtained, calculated using the calculation method, taking into account the duration of sunlight and mean cloudiness. The results of calculations of the total, direct and scattered flux of solar radiation on a horizontal surface for Ternopil are presented in [6], but it does not have data from experimental studies that take into account the specific climatic conditions of a given territory.

There are theoretical and semiempirical models created on the correlation of the flux density of solar energy with the cloudiness and transparency of the atmosphere and the transmission characteristics of various parts of the solar spectrum [7, 8]. In [9], probabilistic characteristics and laws of the distribution of the solar potential are calculated for the territory of the Kirovograd region. The paper [10] shows the mean values of solar energy for each month from 2012 to 2015 in Odessa, but they are not typical for the northern and western regions of Ukraine.

3. Experiment for measuring and recording of solar radiation

According to the intensity of solar radiation, four zones are allocated in Ukraine: the first (1350 kW·h/m^2 per year) and the second (1250 kW·h/m^2 per year), which are in the south of Ukraine and occupy more than half of its territory; the third one (1150 kW·h/m^2 per year), which occupies the regions of the western region and the fourth zone (1000 kW·h/m^2 per year), which is located in the northern and central regions of Ukraine and is least favorable for the use of solar energy [11, 12]. To analyze the energy potential of solar radiation in the western region, the territory of the Ternopil region was taken with the center in the city of Ternopil. For this purpose, an experimental facility was developed for measuring the flux density of solar radiation, the block diagram of which is shown in **Fig. 1**.

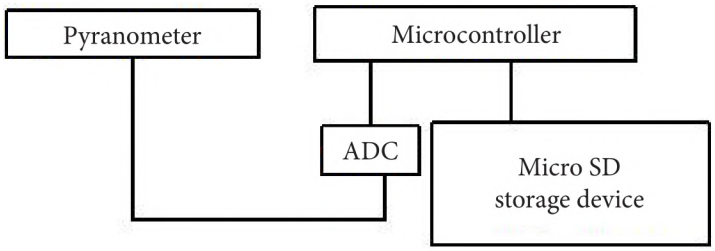

Fig. 1. Block diagram of experimental facility

The facility includes: pyranometer, which measures the flux density of solar radiation; Microcontroller Atmega 32A (ATMEL, China), which processes and records received data from an analog-to-digital converter (ADC); Micro SD storage device (Kingston, China). This facility allows to measure and record the flow of solar radiation in real time at intervals of 1 min to the drive as a separate file during the day.

The pyranometer consists of: photodetector made of single-crystal silicon; current-to-voltage conversion unit and signal amplifying unit. The photodetector operated in short-circuit mode and was graduated with a Soler Power Meter DT-1307 (CEM, China). Measurements were performed at an angle of inclination of the photodetector surface to the horizon $\alpha=49^o$, which is optimal for the latitude of the given territory [6]. The results were processed using the Matlab software environment, averaging the data by the least squares method.

All researches were carried out on the basis of the Faculty of Applied Information Technologies and Electrical Engineering of Ternopil Ivan Puluj National Technical University, Mikulinetska str. 46, geographical coordinates – 49,53^o north latitude and 25.6^o east longitude. The facility was located on the upper terrace of Building #7, did not create artificial shading and allowed to obtain the most objective measurement results. Appearance of the experimental facility is shown in **Fig. 2**.

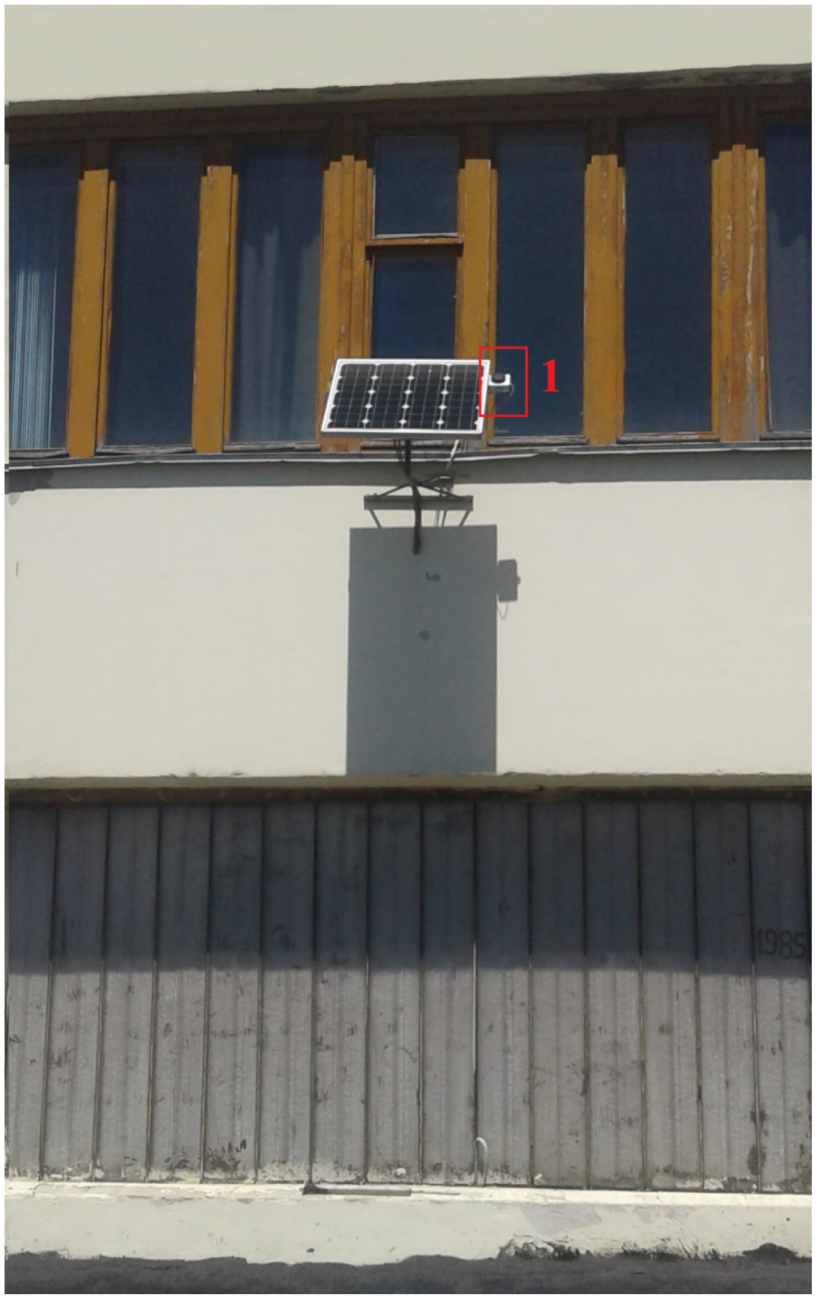

Fig. 2. Appearance of experimental facility: 1 – pyranometer

4. Research results of the energy potential of the western region of Ukraine

The results of measurements of the flux density of solar radiation were averaged overnight during each month of 2016 and recorded in the created database. This also included data on the cloudiness degree taken from the weather service website [1]. Clouds were represented in points from 0 (clear) to 10 (cloudy). **Fig. 3** shows the distribution of the radiation flux density for the solar, cloudy and mostly cloudy period of August 2016. The energy density of solar radiation during the day was calculated from the dependences obtained: E=6.9 kW·h/m^2 for solar; E=3,7 kW·h/m^2 for cloudy; E=2,2 kW·h/m^2 – a mostly cloudy day. Similar calculations were made for other months.

To find the connection between the solar energy flow and the climatic conditions of the terrain, a comparison was made of the results of measurements of the flux density of solar energy to cloud data, which were taken from the weather service website. The deviation of the results of comparing the averaged values of the measured flux of solar energy and the degree of cloudiness

for a three-hour interval and an interval of one day did not exceed 5 %. This allowed to use the average daily values of these parameters for further calculations. The mean cloudiness and mean flux density of solar radiation were calculated from the average of their arithmetic mean.

Fig. 4 shows the dependence of the energy density of solar radiation per day of average cloudiness for August 2016.

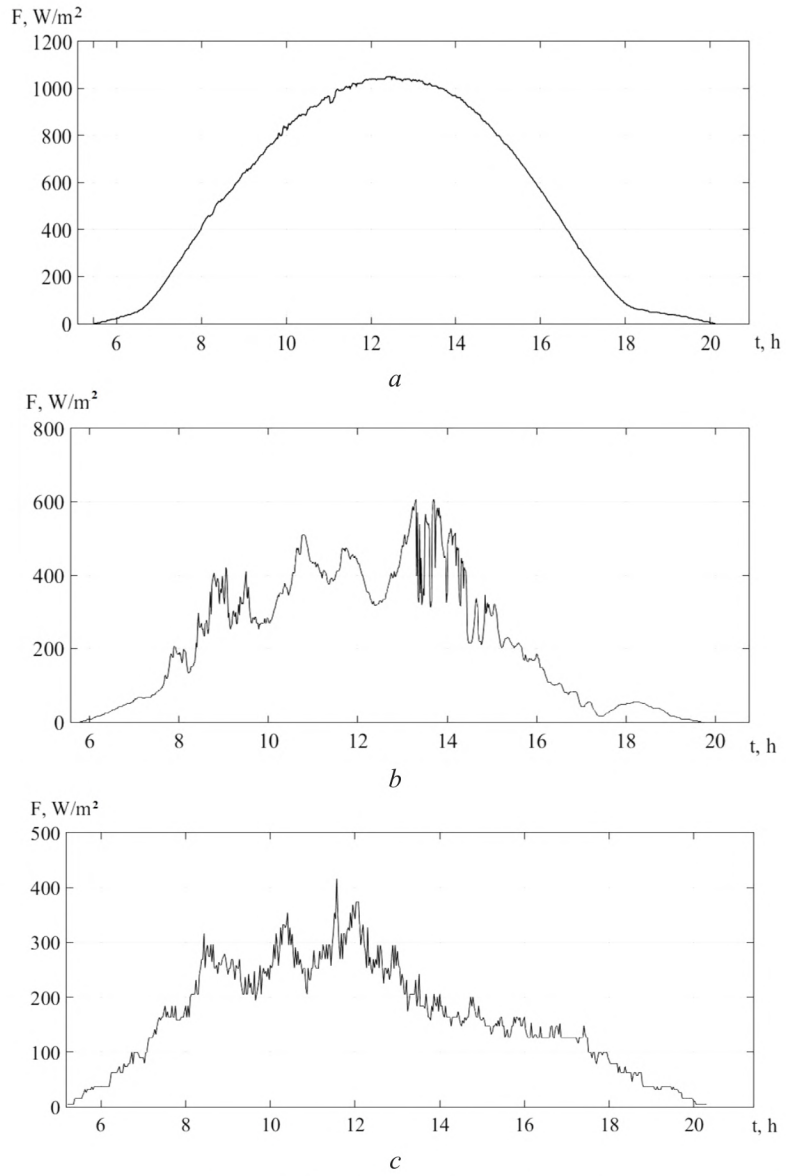

Fig. 3. The graph of the change in the flux density of solar radiation during the day of August 2016, *a* – solar; *b* – cloudy; *c* – mostly cloudy day

The graph is constructed using a least-squares averaging. As a result, a linear dependence is obtained, described by the equation:

$$E_{av}=-0{,}67\cdot N+7{,}19, \quad (1)$$

where E – solar energy kW·h/m^2, during one day; N – cloudiness.

Given that the duration of sunshine during the day and the angle of the sun's inclination to the horizon change throughout the year, the same measurements were made for each month of 016.

Their results are given in **Table 1**. Microsoft Excel 2010 software was used for calculations and data processing.

Algorithm of calculations: creation of an array of cloud data and data of measurements of the solar energy flow; data averaging; plotting the dependences of the solar energy E(N) on cloudiness; an analytical expression for the dependence E(N); calculation of the average daily and total energy of solar radiation during the month and year.

Table 1 shows the values of the total energy of solar radiation E during the month, the average daily values for each month of the E_{av}, as well as the analytical dependences of the average daily flux of solar energy on the average cloudiness E_{av}=f(N).

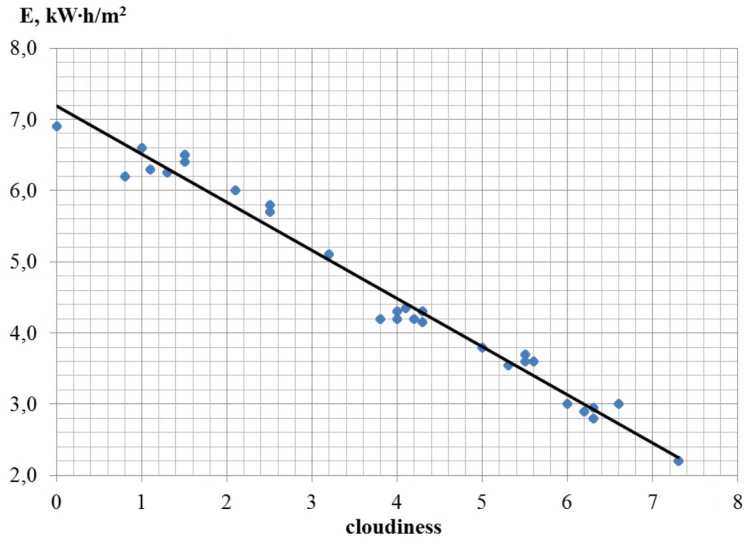

Fig. 4. Graph of the dependence of the energy density of solar radiation per day on cloudiness

Table 1

The monthly and average daily energy of solar radiation and the analytical dependences of the average daily flux density of solar energy from the mean cloudiness

Month	E, kW·h/m²	E_{av}, kW·h/m²	E_{av}=f(N)
January	45	1,4	E_{av}=–0,386×N+4,0385
February	65	2,2	E_{av}=–0,3871×N+4,7581
March	82,4	2,6	E_{av}=–0,5095×N+5,814
April	105,2	3,5	E_{av}=–0,5334×N+6,455
May	134,7	4,3	E_{av} =–0,5467×N+6,2689
June	136,7	4,5	E_{av}=–0,5575×N+7,0102
July	144	4,6	E_{av} =–0,5575×N+7,0102
August	141,3	4,5	E_{av} =–0,677×N+7,1902
September	100,7	3,3	E_{av} =–0,6072×N+5,9676
October	48,7	1,6	E_{av} =–0,4736×N+4,567
November	38,3	1,3	E_{av} =–0,4×N+4,195
December	35,4	1,1	E_{av} =–0,32×N+3,263

Based on the obtained analytical dependencies and weather data, the mean monthly energy density of solar radiation for 2012–2015 is calculated, the data are presented in **Table 2**. The total

annual and average daily energy of solar radiation are also calculated. The total annual energy for a given period ranges between 994.4–1077.7 kW·h/m^2.

Table 2

The energy density of solar radiation for 2012–2016 years

Month	2016	2015	2014	2013	2012	Average value
	E, kW·h/m^2	E, kW·h/m^2	E, kW·h/m^2	E, kW·h/m^2	E, kW·h/m^2	E, kW·h/m^2
January	45	44	39,3	45	55	45,7
February	65	71,3	68,9	58,6	76,5	68,1
March	82,4	98,9	98,5	81,3	102,2	92,7
April	105,2	112,9	100,9	119,5	108,2	109,4
May	134,7	113,9	101,5	107,8	110	113,6
June	136,7	133,6	118,9	123,3	123,3	127,2
July	144	133,3	121,7	129,7	138,1	133,4
August	141,3	136,7	123,1	129,9	125,3	131,3
September	100,7	75,3	102,6	66,9	94,6	88
October	48,7	56,2	72,3	51,8	51,3	56,1
November	38,3	47,3	45,5	42,1	38,5	42,3
December	35,4	48	32,9	38,5	36,6	38,3
Total annual energy	1077,7	1071,7	1026,3	994,4	1059,7	1045,9
Daily average value	2,94	2,93	2,81	2,72	2,9	2,9

On the basis of these data, the average annual energy of solar radiation in the western region of Ukraine is determined, which is 1045.9 kW·h/m^2. The graph of the change in the flux density of solar energy during 2012–2016 years is shown in **Fig. 5**. As can be seen from the graph, the most favorable months for the use of solar energy is from March to September each year. On the basis of the obtained data, a graph of the change in the average annual value of the flux density of solar energy is constructed, which is shown in **Fig. 6**.

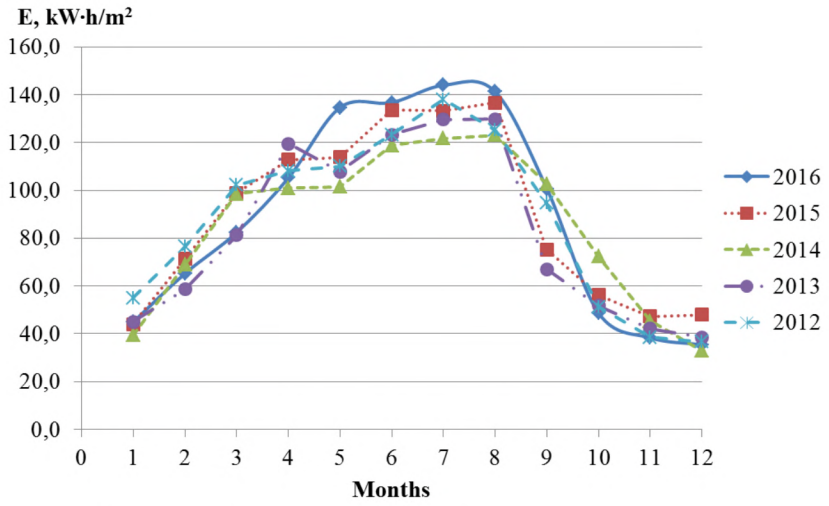

Fig. 5. Graph of changes in the energy density of solar radiation for each month in 2012–2016

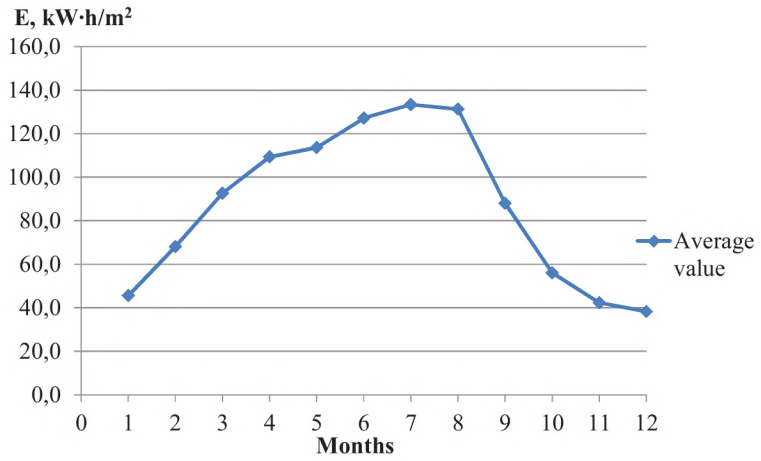

Fig. 6. Graph of the change in the average annual value of the solar energy density of the western region

Fig. 7 shows the histogram of the total annual energy of solar radiation for 2012–2016 and its average value.

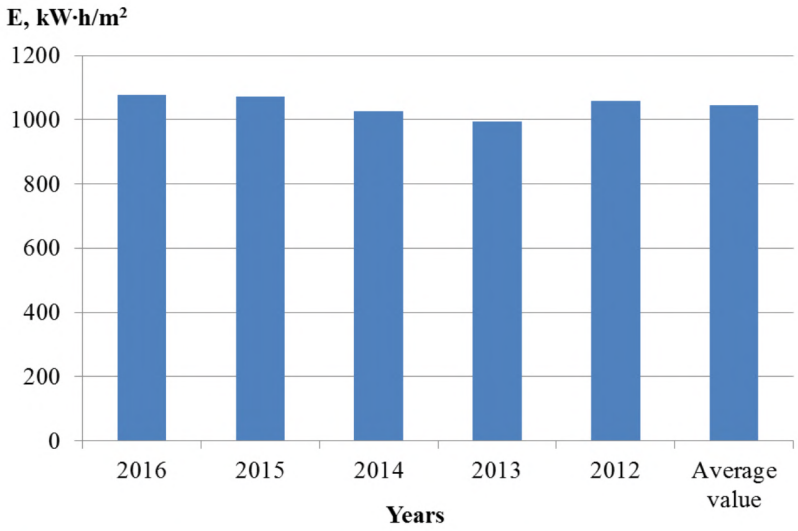

Fig. 7. Histogram of total annual energy of solar radiation for 2012–2016 and its average value

From **Fig. 7** it is shown that the deviation from the average annual value of the energy density of solar radiation does not exceed ±51,5 kW·h/m², which is 5 %. Therefore, for the technical and economic calculation of solar energy systems in the western region, it is advisable to use the average annual density of solar energy 1045.9 kW·h/m².

5. Conclusions

1. On the basis of a comparison of the measured values of the flux density of solar radiation and the cloud cover taken from meteorological services, a monthly analytical dependence of the mean daily flux density of solar radiation on the degree of cloudiness E(N) is established. This will allow, based on the cloud data of meteorological services of other regions, to calculate the flux of solar radiation and estimate their solar energy potential.

2. The calculation of the solar energy potential during 2012–2016 of the western region of Ukraine is carried out. It is determined that the average annual density of the solar energy flux is 1045.9 kW·h/m², and its deviation does not exceed 5 %. This will allow the calculation of technical and economic parameters for the design of the solar energy system in the western region of Ukraine.

References

[1] Meteopost (2017). Available at: http://meteopost.com/weather/archive/

[2] Vozniak, O. T., Yaniv, M. Ye. (2010). Enerhetychnyi potentsial soniachnoi enerhetyky ta perspektyvy yoho vykorystannia v ukraini. Visnyk Natsionalnoho universytetu "Lvivska politekhnika". Seriia: Teoriia i praktyka budivnytstva: zbirnyk naukovykh prats, 664, 7–10.

[3] Kozyrskyi, V. V., Martyniuk, L. V. (2012). Intensyvnist soniachnoho vyprominiuvannia, spriamovanoho na pokhylu poverkhniu. Naukovyi visnyk Natsionalnoho universytetu bioresursiv i pryrodokorystuvannia Ukrainy. Seriia: Tekhnika ta enerhetyka APK, 174 (1), 112–119.

[4] Fylenko, V. V. (2015). Do pytannia vyznachennia diisnykh helioenerhetychnykh resursiv. Problemy mashinostroeniya, 18 (1), 67–72.

[5] Zhelykh, V. M., Omelchuk, O. V., Shapoval, S. P., Venhryn, I. I. (2015). Enerhetychnyi potentsial soniachnoi radiatsii na terytorii Ukrainy. Visnyk Natsionalnoho universytetu "Lvivska politekhnika". Seriia: Teoriia i praktyka budivnytstva: zbirnyk naukovykh prats, 823, 117–121.

[6] Koval, V. P., Ivasechko, R. R., Kozak, K. M. (2015). Enerhetychna efektyvnist system pozytsionuvannia ploskykh soniachnykh panelei. Energosberezhenie. Energetika. Energoaudit, 3, 2–10.

[7] Look, D. C. (1975). Short method for the analytical determination of atmospheric model parameters. Solar Energy, 17 (4), 265–267. doi: 10.1016/0038-092x(75)90009-2

[8] Morrison, C. A., Feber, E. A. (1976). Development and use of solar insolation data in northern tatitube for south facing surfaces. Solar Energy, 17, 116–120.

[9] Holyk, O. P., Zhesan, R. V. (2009). Analiz danykh meteorolohichnykh sposterezhen za intensyvnistiu soniachnoi radiatsii v Kirovohradskomu rehioni z metoiu stvorennia systemy avtomatychnoho keruvannia avtonomnym enerhopostachanniam na osnovi soniachno-vitrovykh ustanovok. Zbirnyk naukovykh prats Kirovohradskoho natsionalnoho tekhnichnoho universytetu. Tekhnika v silskohospodarskomu vyrobnytstvi, haluzeve mashynobuduvannia, avtomatyzatsiia, 22, 164–172.

[10] Kravchenko, V. P., Kravchenko, Ye. V., Bodnar, I. V. (2016). Instrumentalne vyznachennia insoliatsii v raioni m. Odesy. Enerhetyka:ekonomika, tekhnolohii, ekolohiia, 1, 20–27.

[11] SOLARGIS (2017). Available at: http://solargis.com/products/maps-and-gis-data/free/download/ukraine

[12] Pivnyak H.H., Shkrabets F.P. (2013). Alternatyvna enerhetyka v Ukraini. Dnipropetrovsk: Natsionalnyi hirnychyi universytet, 109.

RESEARCH ON MAXIMIZING CRITICAL AND REDUCING INITIAL HEAT FLUX DENSITIES TO ELIMINATE ANY FILM BOILING AND MINIMIZE DISTORTION DURING QUENCHING

Nikolai Kobasko
Intensive Technologies Ltd
68/1 Peremohy ave., Kyiv, Ukraine, 03113
nkobasko@gmail.com

Anatolii Moskalenko
Thermo-Acoustical Diagnostic of Heat Transfer Processes
Institute of Engineering Thermophysics of NASU
2A Zhelyabova str., Kyiv, Ukraine, 03057
an.moskalenko@gmail.com

Petro Lohvynenko
Department of Polymers Modification
Institute of Macromolecular Chemistry of NASU
48 Kharkivske road, Kyiv, Ukraine, 02160
petmol@ukr.net

Volodymyr Dobryvechir
Intensive Technologies Ltd
68/1 Peremohy ave., Kyiv, Ukraine, 03113
dobrivecher@yahoo.com

Abstract

In the paper the results of testing three types of FUCHS oils: Thermisol QH 120, Thermisol QH 10 and Thermisol QB 46 are discussed. The main attention is paid to critical heat flux densities evaluation because they create a basis for optimizing cooling intensity of any liquid quenchant. In the paper is underlined that any film boiling during quenching is undesirable since it is a reason for big distortion and non-uniform surface harness. It is shown that intensive quenching decreases distortion of steel parts during quenching. To eliminate film boiling during quenching in mineral oils, optimal temperature of oil should be chosen which maximize the first critical heat flux density and special additives should be used to decrease initial heat flux by creating surface micro-coating. Along with the evaluation of heat transfer coefficients, critical heat flux densities inherent to liquid quenchant must be measured first to optimize quenching processes. International DATABASE on cooling characteristics of liquid quenchants must include critical heat flux densities, initial heat flux densities, and heat transfer coefficients allowing optimizing and governing quenching processes.

Keywords: critical heat flux, initial heat flux, optimization, database, distortion, calculations, cooling intensity, mineral oils.

DOI: 10.21303/2461-4262.2017.00366

1. Introduction

In the paper a main attention is paid to critical and initial heat flux densities which should be included in DATABASE which is currently developing by international team in the frame of International Federation for Heat Treatment and Surface Engineering (IFHTSE). It is shown that critical heat flux densities are the main parameters in the first step of evaluating cooling capacity the different kinds of quenchants. Depending on a ratio between initial and the first critical heat flux, it could be four possible heat-transfer modes on their hot metal surface [1, 2]. At the first type of heat-transfer mode full film boiling and nucleate boiling are present simultaneously on the probe surface. The rewetting front accompanying the transition from full film boiling, which occurs during the cooling process, typically moves axially along the metal surface during cooling. At the

second type of heat-transfer mode initially, film boiling occurs over the entire hot metal surface. At a certain point in time, nucleate boiling instantaneously replaces film boiling. When boiling ceases, convection heat transfer occurs [1, 2]. At the third type of heat-transfer mode some localized areas of the probe surface are covered by a vapor blanket, whereas at the same time other areas experience nucleate boiling. At fourth type of heat-transfer mode the film boiling and nucleate boiling periodically replace each other during quenching [1, 2]. For each type of nucleate boiling process its own specific boundary condition are used to solve correctly direct and inverse heat conductivity problems. It means that it is impossible to solve mentioned above direct and inverse problem without knowing the type of heat transfer mode. Authors of current work in their investigations used additional tools like noise control system and high speed video recording to be sure that type of film boiling was chosen correctly. In the paper the second type of heat transfer mode is considered since it was observed during testing of Inconel 600 probe in three types of oils: Thermisol QH 120, Thermisol QH 10 and Thermisol QB 46 delivered by IFHTSE for Robin Round testing with the aim of designing Liquid Quenchant Database. These oils differ from each other by their viscosity and are widely use in practice. Taking into account that for each mineral oil exists optimal bath temperature where the first critical heat flux density has maximum value (**Fig. 1**). It was decided to make testing for three types of oils within the wide diapason of temperatures: 30 °C, 50 °C, 70 °C, 90 °C and 110 °C.

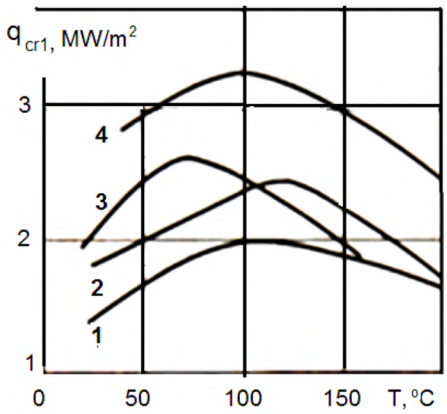

Fig. 1. The first critical heat flux density q_{crl} versus temperature of mineral oils:
1 – MZM-120; 2 – MS; 3 – Effectol; 4 – MZM-16 [3]

As seen from **Fig. 1**, there is an optimal temperature for mineral oils where the first critical heat flux density reaches maximum value. That is why, it is important for practical use investigate three types of FUCHS oils at elevated temperatures.

2. Simplified procedure for evaluating critical heat flux densities

For evaluating critical heat flux densities, developed film boiling during quenching should take place. For this purpose standard probe made of high thermal conductivity material, for example silver, should be used. Standard Inconel 600 probe also can provide information on critical heat flux densities if film boiling during quenching is clearly seen [4, 5]. Measuring transition temperature from film boiling to nucleate boiling and evaluating heat transfer coefficient at this temperature, it is possible to calculate the second critical heat flux density q_{cr2}. The first critical heat flux density is evaluated then from the well known correlation $q_{cr2}/q_{crl}=0.2$ [6–8]. Heat transfer coefficients (HTC) are evaluated by solving inverse problem [9]. For evaluating HTC, author of the paper used regular thermal condition theory [10] which provides good results of calculation for any Biot number Bi with the accuracy about ±3 %. Below, the main equation of regular thermal condition theory are considered and examples of calculating critical heat flux density is provided. To make such calculations, cooling curves and cooling rates should be available (**Fig. 2, 3**).

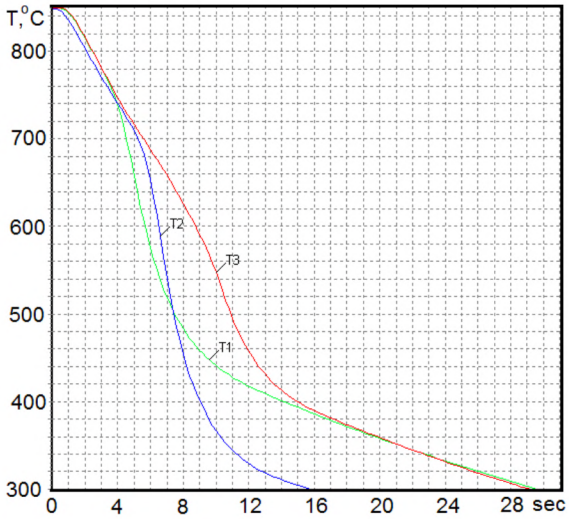

Fig. 2. Cooling curves for different types of oils at 50 °C:
1 – Thermisol QH 120; 2 – Thermisol QH 10; 3 – Thermisol QB 46

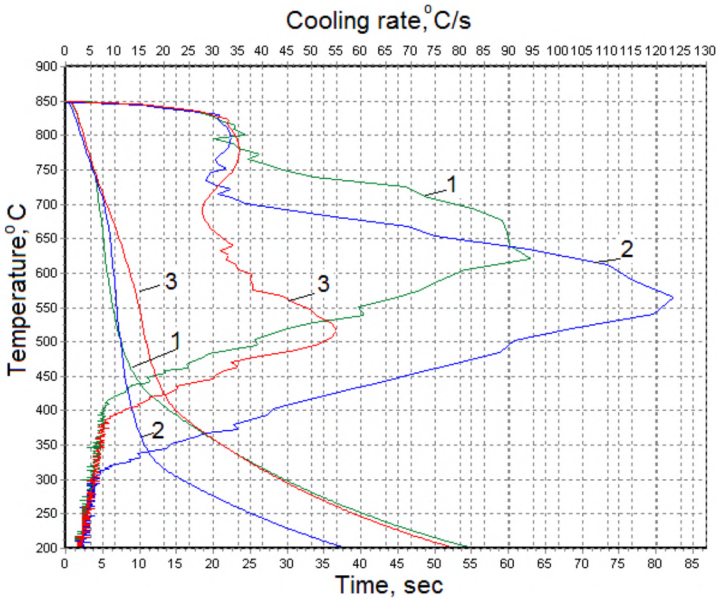

Fig. 3. Cooling rate for different types of oils at 50°C:
1 – Thermisol QH 120; 2 – Thermisol QH 10; 3 – Thermisol QB 46

Kondratjev number Kn, according to regular thermal condition, is evaluated as [6, 10]:

$$Kn = \frac{vK}{a\left(T - T_m\right)}. \qquad (1)$$

Generalized Biot number is evaluated from universal correlation

$$Kn = \psi Bi_V \quad or \quad Kn = \frac{Bi_V}{\sqrt{Bi_V^{\,2} + 1.437 Bi_V} + 1} \qquad (2)$$

and then heat transfer coefficient is evaluated as:

$$\alpha = \frac{\lambda Bi_V R}{2K}. \quad (3)$$

The second critical heat flux density is calculated from the equation

$$q_{cr2} = \alpha_F \left(T_{tr} - T_m\right). \quad (4)$$

Taking into account that $q_{cr2}/q_{cr1}=0.2$, it easy to calculate approximately the first critical heat flux density using Eq. (5) [11]:

$$q_{cr1} = 5\alpha_F \left(T_{tr} - T_m\right). \quad (5)$$

Let's calculate critical heat flux densities from data provided in **Fig. 2**. Minimum cooling rate for oil Thermisol QH 10 is 29 °C/s at core temperature 740 °C. Thermal conductivity and thermal diffusivity at this temperature are: 26 W/mK and 5.65×10^{-6} m²/s. According to (1), Kn is calculated as

$$Kn = \frac{29\ ^\circ C/s \times 6.75\times10^{-6}\ m^2}{5.65\times10^{-6}\ m^2/s\left(740\ ^\circ C - 50\ ^\circ C\right)} = 0.05.$$

Generalized Biot number according to Eq. (2) is 0.055. It means that

$$\alpha_F = \frac{29\ W/mK \times 0.055 \times 0.00625\ m}{2\times6.75\times10^{-6}\ m^2} = 738\ W/m^2K;$$

$$q_{cr2} = 738\ W/m^2K \times \left(740\ ^\circ C - 50\ ^\circ C\right) = 509220\ W/m^2;$$

$$q_{cr1} = 5\times738\ W/m^2K \times \left(740\ ^\circ C - 50\ ^\circ C\right) = 2.55\ MW/m^2.$$

As seen from **Fig. 1**, the first critical heat flux density for Thermisol QH 10 is equal to Effectol oil (curve 3).

3. Effect of oil temperature on its cooling characteristics

Temperature of Thermisol oil QH 120 affects considerably its cooling characteristics as shown in **Fig. 4.** Along with increasing critical heat flux densities, temperature increases heat transfer coefficients providing more uniform and more accelerated cooling of steel parts. To proof this statement, below maximal HTCs are calculated using (1)–(5):

At temperature 30 °C

$$Kn = \frac{76\ ^\circ C/s \times 6.75\times10^{-6}\ m^2}{5.4\ m^2/s\left(612\ ^\circ C - 30\ ^\circ C\right)} = 0.16 \text{ and } Bi_V = 0.18.$$

HTC in this case is equal to

$$\alpha = \frac{23.7\ W/mK \times 0.18 \times 0.00625\ m}{2\times6.75\times10^{-6}\ m^2} = 1975\ W/m^2K.$$

At temperature 110 °C

$$Kn = \frac{112.5\ ^\circ C/s \times 6.75\times10^{-6}\ m^2}{5.45\ m^2/s\left(648\ ^\circ C - 110\ ^\circ C\right)} = 0.26 \text{ and } Bi_V = 0.325.$$

In this case HTC is equal to

$$\alpha = \frac{24.8\ \mathrm{W/mK} \times 0.325 \times 0.00625\ \mathrm{m}}{2 \times 6.75 \times 10^{-6}\ \mathrm{m^2}} = 3730\ \mathrm{W/m^2K}.$$

Increasing is 1.88 times.

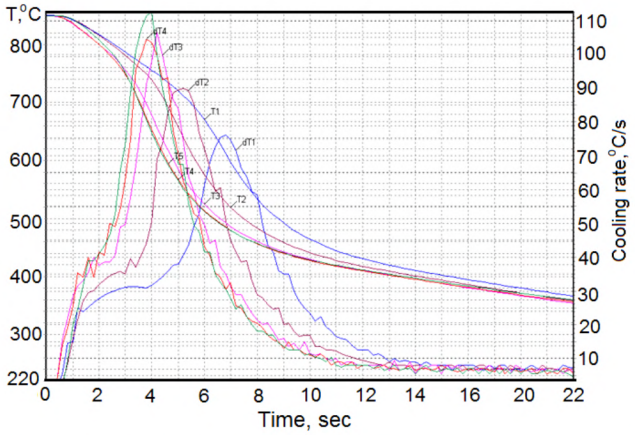

Fig. 4. Cooling curves and cooling rates depending on temperature of Thermisol QH 120 oil: 1 – 30 °C; 2 – 50 °C; 3 – 70 °C; 4 – 90 °C; 5 – 110 °C

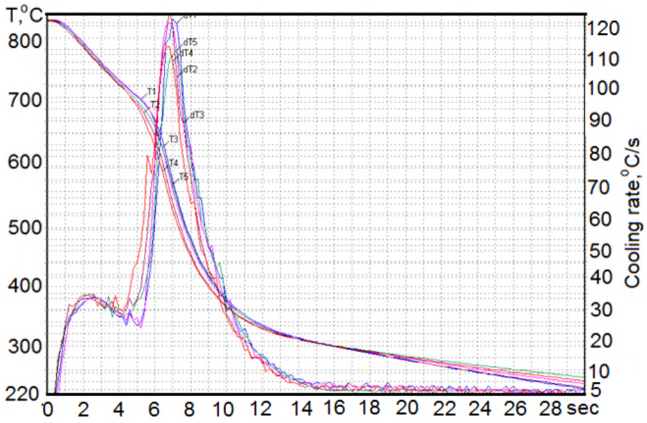

Fig. 5. Cooling curves and cooling rates depending on temperature of Thermisol QH 10 oil: 1 – 30 °C; 2 – 50 °C; 3 – 70 °C; 4 – 90 °C; 5 – 110 °C

The Thermisol QH 120 is high quality oil with a low level of evaporation and can work at elevated temperature as a quenchant reducing significantly distortion. In contrast to Thermisol QH 120 oil, Thermisol QH 10 oil doesn't react significantly on its temperature changing (**Fig. 5**). With increase temperature critical heat flux densities and HTCs increase insignificantly. For example, at temperature 30 °C

$$\mathrm{Kn} = \frac{121\ ^\circ\mathrm{C/s} \times 6.75 \times 10^{-6}\ \mathrm{m^2}}{5.35\ \mathrm{m^2/s}\left(579\ ^\circ\mathrm{C} - 30\ ^\circ\mathrm{C}\right)} = 0.278 \text{ and } \mathrm{Bi_V} = 0.36.$$

HTC in this case is equal to

$$\alpha = \frac{237\ \mathrm{W/mK} \times 0.36 \times 0.00625\ \mathrm{m}}{2 \times 6.75 \times 10^{-6}\ \mathrm{m^2}} = 3830\ \mathrm{W/m^2K}.$$

At temperature 110 °C

$$\mathrm{Kn} = \frac{111.2\ ^\circ\mathrm{C/s} \times 6.75 \times 10^{-6}\ \mathrm{m}^2}{5.2\ \mathrm{m}^2/\mathrm{s}\left(549\ ^\circ\mathrm{C} - 110\ ^\circ\mathrm{C}\right)} = 0.329 \text{ and } \mathrm{Bi_V} = 0.442.$$

In this case HTC is equal to

$$\alpha = \frac{22.7\ \mathrm{W/mK} \times 0.442 \times 0.00625\ \mathrm{m}}{2 \times 6.75 \times 10^{-6}\ \mathrm{m}^2} = 4645\ \mathrm{W/m^2K}\ .$$

Increasing is 1.2 times.

Experiments and calculations show that Thermal QH 10 oil is stable and insignificantly changes with changing its temperature. Manufacturer FUCHS is recommended this oil for forgings directly from the forge heat, quenching of wrought materials, screws and springs [12].

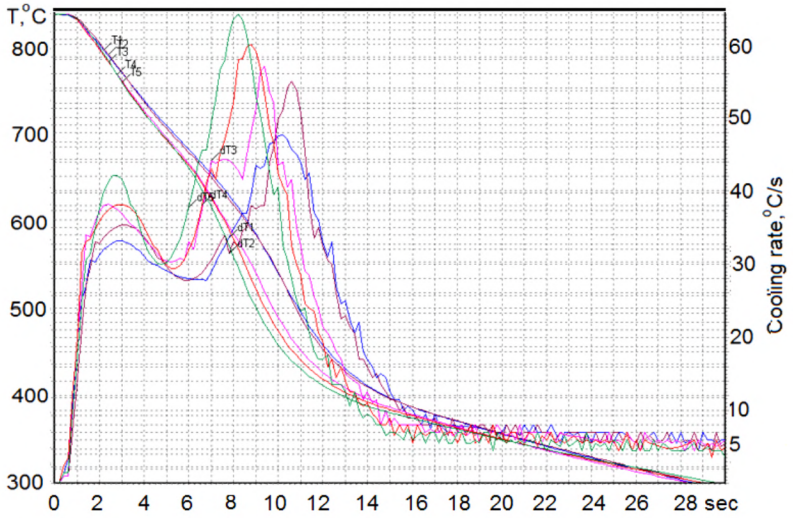

Fig. 6. Cooling curves and cooling rates depending on temperature of Thermisol QB 46 oil: 1 – 30 °C; 2 – 50 °C; 3 – 70 °C; 4 – 90 °C; 5 – 110 °C

At temperature 30 °C

$$\mathrm{Kn} = \frac{47.6\ ^\circ\mathrm{C/s} \times 6.75 \times 10^{-6}\mathrm{m}^2}{5.17\ \mathrm{m}^2/\mathrm{s}\left(537\ ^\circ\mathrm{C} - 30\ ^\circ\mathrm{C}\right)} = 0.123 \text{ and } \mathrm{Bi_V} = 0.14.$$

HTC in this case is equal to

$$\alpha = \frac{22.5\ \mathrm{W/mK} \times 0.14 \times 0.00625\ \mathrm{m}}{2 \times 6.75 \times 10^{-6}\mathrm{m}^2} = 1460\ \mathrm{W/m^2K}.$$

At temperature 110 °C

$$\mathrm{Kn} = \frac{64.1\ ^\circ\mathrm{C/s} \times 6.75 \times 10^{-6}\ \mathrm{m}^2}{5.2\ \mathrm{m}^2/\mathrm{s}\left(553\ ^\circ\mathrm{C} - 110\ ^\circ\mathrm{C}\right)} = 0.188 \text{ and } \mathrm{Bi_V} = 0.22.$$

In this case HTC is equal to

$$\alpha = \frac{22.7\ \mathrm{W/mK} \times 0.22 \times 0.00625\ \mathrm{m}}{2 \times 6.75 \times 10^{-6}\ \mathrm{m}^2} = 2310\ \mathrm{W/m^2K}.$$

Increasing is 1.58 times.

Thermisol QB 46 oil (**Fig. 6**) provides uniform cooling and is thermal stable. It displays good resistance to ageing and do not evaporate excessively [12].

Thus, increasing temperature of oil increases the first critical heat flux density and HTC that in many cases eliminates undesirable film boiling. Also, special additives creating micro-insulating layer on the surface of steel parts are used to decrease initial heat flux density and by this way eliminate film boiling (**Fig. 7**) [13, 14].

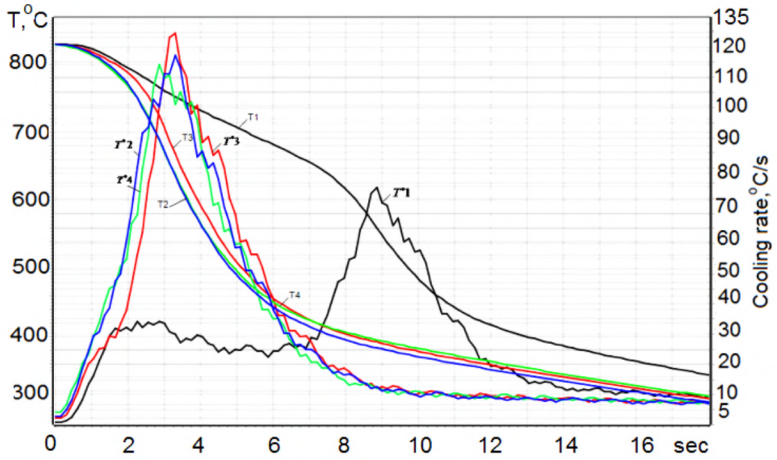

Fig. 7. Temperature T and cooling rate T^* at the center of Inconel 600 probe 10 mm in diameter and 30 mm long versus time when quenching in oil I-20 A at 50 °C: 1 – no additives at all; 2–7 % of PIB 950; 3–5 % of PIB 1300; 4–4 % of PIB 2400 [13, 14]

As seen from **Fig. 7**, a small amount of PIB additives decrease completely film boiling during quenching due to creation of an insulating layer [13, 14]. This is a new approach in controlling cooling intensity of liquid quenchants.

4. Discussion

In last decade, numerous experiments were fulfilled to show that intensive and uniform quenching doesn't decrease distortion. In contrary, it decreases distortion (**Fig. 8**) [6].

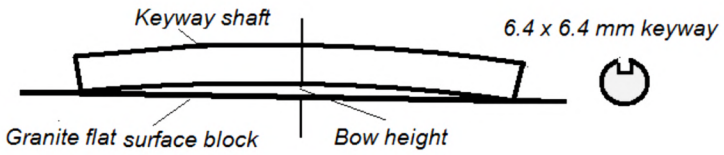

Fig. 8. Keyway shaft distortions [6]

Many others experiments were made connected with the measuring distortion of cylindrical steel parts after quenching in water flow up to 12 m/s where distortion was minimal (**Fig. 8, Table 5**). It means that film boiling can be eliminated completely without resulting in increasing distortion.

Thus, critical heat flux densities are very important values responsible for eliminating film boiling processes and they should be in DATABASE as a characteristic of any liquid quenchant.

Also, special additives to liquid quenchant should be investigated which create insulating layers on the surface of steel parts and contemporary methods for their testing should be developed. Some information concerning this issue is provided in [16–21].

Table 5
Keyway distortion measurements [6]

Batch oil	Single oil	Single IQ
0.25–0.51 mm	0.20–0.36 mm	0.08–0.12 mm

5. Conclusions

1. Liquid quenchant database should contain critical heat flux densities as the main parameters for any liquid used as a quenchant.

2. There is an optimal temperature of liquid where critical heat flux densities are maximal and distortion after quenching steel parts in optimal condition is minimal.

3. Any film boiling, especially local film boiling, during quenching is undesirable since it is a reason for big distortion and non-uniform surface hardness.

4. To eliminate any film boiling during quenching, one should increase critical heat flux densities and decrease initial heat flux during immersion of steel parts into cold liquid.

5. Up to present time, the main attention was paid to changing surface tension in order to control cooling intensity of liquid quenchants. Authors proposed to use insulating layers to decrease initial heat flux density and by this way eliminate film boiling.

6. New additives to liquid quenchants, which create insulating layers, should be further investigated and widely introduced to practice.

Acknowledgement

Authors are very grateful to FUCHS and IFHTSE for providing and delivering Thermisol GH 120, Thermisol GH 10 and Thermisol GB 46 oils for laboratory investigations in the frame of liquid quenchant DATABASE development.

References

[1] Mayinger, F. (1992). Thermo- and Fluiddynamic Principles of Heat Transfer During Cooling. Theory and Technology of Quenching, 41–72. doi: 10.1007/978-3-662-01596-4_3

[2] Liscic, B. (2016). Measurement and Recording of Quenching Intensity in Workshop Conditions Based on Temperature Gradients. Materials Performance and Characterization, 5 (1), MPC20160007. doi: 10.1520/mpc20160007

[3] Kobasko, N. I. (1980). Steel Quenching in Liquid Media Under Pressure. Kyiv: Naukova Dumka, 206.

[4] ISO 9950. Industrial Quenching Oils–Determination of Cooling Characteristics- Nickel-Alloy Probe Test Method, 1995(E) (1995). International Organization for Standardization, Geneva, Switzerland.

[5] ASTM D6200-01. Standard Test Method for Determination of Cooling Characteristics of Quench Oils by Cooling Curve Analysis (2012). ASTM International, West Conshohocken, PA. Available at: https://www.astm.org/cis/ru/index.html

[6] Kobasko, N. I., Aronov, M. A., Powell, J. A., Totten, G. E. (2010). Intensive Quenching Systems: Engineering and Design. ASTM International, West Conshohocken, USA, 234. doi: 10.1520/mnl64-eb

[7] Kobasko, N. I., Batista, A. A., Canale, L. C. F., Totten, G. E., Dobryvechir, V. V. (2013). Cooling Capacity of Coconut Oil, Palm Oil, and a Commercial Petroleum Oil by Solving the Heat Conductivity Inverse Problem. Materials Performance and Characterization, 2 (1), 20120047. doi: 10.1520/mpc20120047

[8] Kobasko, N. I., Marques, A., Canale, L. C. F., Totten, G. E., Dobryvechir, V. V. (2013). Cooling Capacity of Petroleum Oil Quenchants as a Function of Bath Temperature. Materials Performance and Characterization, 2 (1), 20130004. doi: 10.1520/mpc20130004

[9] Felde, I. (2015). Liquid Quenchant Database – Determination of Heat Transfer Coefficient during Quenching. IDE 2015, Bremen, Germany, 265–274.

[10] Kondratiev, G. M. (1957). Teplovye izmereniya [Thermal Measurements]. Moscow: Mashgiz, 244.

[11] Kobasko, N. I. (2011). Why Database for Cooling Capacity of Various Quenchants Should be Developed? Vol. V. COMPUTERS and SIMULATION in MODERN SCIENCE, 142–147.

[12] FUCHS. Available at: http://mactexoil.ie/index.php?route=product/product&path=86&product_id=317

[13] Lohvynenko, P. N., Moskalenko, A. A., Kobasko, N. I., Karsim, L. O., Riabov, S. V. (2016). Experimental Investigation of the Effect of Polyisobutilene Additives to Mineral Oil on Cooling Characteristics. Materials Performance and Characterization, 5 (1), MPC20150072. doi: 10.1520/mpc20150072

[14] Kobasko, N., Moskalenko, A., Lohvynenko, P., Karsim, L., Riabov, S. (2016). An effect of pib additives to mineral oil resulting in elimination of film boiling during steel parts quenching. EUREKA: Physics and Engineering, 3, 17–24. doi: 10.21303/2461-4262.2016.00076

[15] Liscic, B., Filetin, T. (2011). Global Database of Cooling Intensities of Liquid Quenchants. Proceedings of the European Conference on Heat Treatment. Quality in Heat Treatment, 40–49.

[16] Tensi, H. M., Totten, G. E., Kunzel, T. (2000). Physics and Technology of Quenching in Fluids – Part I. The 12th IFHTSE Congress Proceedings, 1–4.

[17] Totten, G. E., Bates, C. E., Clinton, M. A. (1993). Handbook of Quenchants and Quenching Technology. Materials Park, Ohio: ASM International, 507.

[18] UCON™ Fluids and Lubricants – Quenchants. The Dow Chemical Company. Available at: http://www.dow.com/ucon/formulated/fluids/quench.htm

[19] The Dow Chemical Company (2015). UCON™ ULTRAQUENCH™. A Plus Quenchant. Available at: http://chemtool.com/wp-content/uploads/2015/07/UCON-Ultraquench-A-Plus.pdf

[20] ASTM Standard D6482-99. Standard Test Method for Determination of Cooling Characteristics of Aqueous Polymer Quenchants with Agitation (Tensi Method) (2000). Annual Book of ASTM Standards. West Conshohocken, PA: ASTM International. doi: 10.1520/d6482-99

[21] ASTM Standard D6549-00. Standard Test Method for Determination of Cooling Characteristics of Quenchants by Cooling Curve Analysis with Agitation (Drayton Unit) (2000). Annual Book of ASTM Standards. West Conshohocken, PA: ASTM International. doi: 10.1520/d6549-00

SOLUTION OF THE SYNTHESIS PROBLEM OF BOUNDARY OPTIMAL CONTROL OF A ROD COOLING PROCESS WITH A HEAT CONDUCTIVE VISCOSITY

Mammadov Rashad Sirac
Department of General and Applied Mathematics & quot
Azerbaijan State University of Oil and Industry
20 Azadlig ave., Baku, Azerbaijan, AZ1010
Rasadmammadov@mail.ru

Qasimov Sardar Yusub
Department of General and Applied Mathematics & quot
Azerbaijan State University of Oil and Industry
20 Azadlig ave., Baku, Azerbaijan, AZ1010
sardarkasumov1955@mail.ru

Abstract

The problem of synthesis of the boundary optimal control of the cooling process of media with heat conductive viscosity is investigated. In addition to the distributed parameters, the concentrated parameters act on the system. This is due to the fact that the temperature of the external environment is unknown and varies according to a given law. As a result, the process is described by a system of partial differential equations and ordinary differential equations. In this case, heat transfer occurs at the right end of the rod. This complicates the obtaining of a solution of this boundary-value problem in an explicit form. But it is possible to establish the existence and uniqueness of the solution of the corresponding boundary-value problem for concrete admissible controls.

The criterion of quality is a quadratic functional and it is required to build control in the form of feedback. First by the Fourier method, the problem under consideration is formulated in an infinite-dimensional phase space. As a result, the problem of synthesis of optimal control in a functional space is obtained. To solve this problem, the dynamic programming method is used. To do this, let's introduce the Bellman functional and obtain the Bellman equation, which this functional satisfies. The solution of this equation allows to find the control parameter in the form of a functional defined on the set of the state function. Further, by introducing the corresponding functions, feedback control is constructed for the original problem. Unlike program control, this allows to influence the behavior of the system at any time, that is, to ensure the self-regulation of the process. However, let's note that the difficulties in solving this problem are connected with the justification of the proposed method. This is established by the investigation of a closed system.

Keywords: controlled object, feedback, Fourier series, dynamic programming method, Bellman functional, functional gradient, admissible control, Bellman equation.

DOI: 10.21303/2461-4262.2017.00391

1. Introduction

If the material does not have a conductive viscosity, the process of heat or cooling transfer is described by a parabolic equation. The problem of synthesis of optimal control of such systems has been studied sufficiently [1–6]. Since in a material with a heat-conducting viscosity the temperature gradient changes along the direction of heat transfer, the cooling process is described by a partial differential equation of higher order [7, 8].

In [7], the solvability of the boundary value problem corresponding to this type of process is investigated. And in [8] the problem of synthesizing the optimal control of this process is solved, when the control parameter is distributed.

But if there are external control parameters in the process of heat conduction, then the process is described by a set of equations in partial and ordinary derivatives [9–11]. The difficulty in solving the synthesis problem of optimal control in this case is due to the fact that it is not possible to find an explicit solution of the corresponding boundary-value problem. In addition, the closed system is solvable and ensures the self-regulation of the corresponding process.

The obtained results relate to the problems of optimal control with systems containing elements with distributed parameters, and they can be applied to the process of heating and cooling the material with the minimum energy expenditure.

2. Problem statement

Let the state of the controlled object be described by a vector function $\bar{u}(x,t)=(y(t),u(x,t))$ and $u(x,t)$ within the range $\overline{Q}=[0,T]\times[0,1]$ satisfies equation

$$\frac{\partial u}{\partial t}=a^2\frac{\partial^2 u}{\partial x^2}+\xi\frac{\partial^3 u}{\partial t\partial x^2}+p(x,t) \tag{1}$$

with initial and boundary conditions

$$u(x,0)=u^0(x), \tag{2}$$

$$\frac{\partial u(0,t)}{\partial x}=0,\ \frac{\partial u(1,t)}{\partial x}+\alpha u(1,t)=y(t), \tag{3}$$

where a, $\alpha>0$ – the real constant, $\xi=\text{const}>0$ – the coefficient of heat conductive viscosity, $u^0(x)$ – the given function of $W_2^1(0,1)$ and $p(x,t)$ – distributed control function.

An unknown function $y(t)$ occurring in condition (3) is assumed to satisfy equation

$$\frac{dy}{dt}=a_0u(1,t)+by+p_0(t) \tag{4}$$

with the initial condition

$$y(0)=y^0, \tag{5}$$

where $a_0\neq0$, b and y^0 – given real numbers, and $p_0(t)$ – concentrated control function.

A vector-valued function $\bar{p}(x,t)=(p_0(t),p(x,t))$ will be called an admissible control if $p_0(t)\in L_2(0,T)$, $p(x,t)\in L_2(Q)$.

The optimal control problem under consideration consists in finding an admissible control in the form of feedback $\bar{p}[x,t,\bar{u}]$, such that the functional

$$I[\bar{p}]=\beta_0y^2(T)+\beta\int_0^1[u(x,T)-\psi(x)]^2dx+$$
$$+\gamma_0\int_0^T p_0^2(t)dt+\gamma\int_0^T\int_0^1 p^2(x,t)dxdt \tag{6}$$

take the smallest possible value. Here $\beta_0,\beta=\text{const}\geq0$, $\beta_0+\beta\neq0$; γ_0, γ=const>0; T – a fixed time and $\psi(x)\in W_2^1(0,1)$ – a given function.

It can be established that for each particular admissible control $\bar{p}(x,t)=(p_0,(t),p(x,t))$ there exists a unique generalized solution $\bar{u}(x,t)=(y(t),u(x,t))$ of the boundary value problem (1)–(5) having the following properties:

1) $y(t)\in H^1(0,T)$, $u(x,t)\in V_2^{1,0}(Q)$;

2) for any function $\Phi(x,t)\in W_2^{1,1}(Q)$ that equal to zero for t=T, there is an integral identity

$$\int_0^T\int_0^1[-u(x,t)\Phi_t+a^2u_x\Phi_x]dxdt+\alpha a^2\int_0^T u(1,t)\Phi(1,t)dt+$$
$$+a^2\int_0^T y(t)\Phi(1,t)dt=\int_0^1 u^0(x)\Phi(x,0)dx+\int_0^1\Phi_x(x,0)u_x^0(x)dx-[y^0-\alpha u^0(1)]\Phi(1,0)+$$
$$+\int_0^T\int_0^1 p(x,t)dxdt; \tag{7}$$

3) the functions $y(t)$ and $u(x,t)$ satisfy the integral equation

$$y(t) = y^0 + \int_0^t [a_0 u(1,\tau) + by(\tau) + p_0(\tau)]d\tau. \quad (8)$$

For all $t \in [0,T]$.

3. Problem statement in an infinite-dimensional phase space

Let's consider in $L_2(0,1)$ an orthonormal system of functions

$$X_n(x) = \frac{\cos \lambda_n x}{\sqrt{\omega_n}}, \ n = 1,2,...,$$

where λ_n – eigenvalues of the boundary value problem

$$X''(x) + \lambda^2 X(x) = 0, \quad 0 < x < 1; \quad X'(0) = 0, \quad X'(1) + \alpha X(1) = 0; \quad (9)$$

which are positive roots of the equation $\lambda tg\lambda = \alpha$, and $\omega_n = \frac{\alpha + \alpha^2 + \lambda_n^2}{2(\alpha^2 + \lambda_n^2)}$ – normalizing factor.

The solution of problem (1)–(3) will be sought in the form of a Fourier series

$$u(x,t) = \sum_{k=1}^{\infty} u_k(t) X_k(x), \quad u_k(t) = \int_0^1 u(x,t) X_k(x) dx. \quad (10)$$

Let's multiply both sides of equation (1) by $X_k(x)$ and integrate along x from 0 to 1.

Taking into account (2)–(5) and (9), let's obtain an infinite system of ordinary differential equations for determining the function and the coefficients $y_k(t)$, $k = 1,2,...$:

$$\begin{cases} \frac{dy(t)}{dt} = by(t) + a_0 \sum_{k=1}^{\infty} X_k(1) u_k(t) + p_0(t), \\ \frac{du_k(t)}{dt} = -a^2 X_k(1) y(t) - \frac{a^2 \lambda_k^2}{1 + \xi \lambda_k^2} u_k(t) + p_k(t), \end{cases} \quad (11)$$

with initial conditions

$$y(0) = y^0, \quad u_k(0) = u_k^0, \quad k = 1,2,..., \quad (12)$$

where $p_k(t)$ and u_k^0 – Fourier coefficients of the functions $p(x,t)$ and $u^0(x)$.

Taking into account the orthonormality of the system of functions $\{X_k(x)\}$, the functional (6) can be represented in the form

$$I_\infty[p_0, p_1, ...] = \beta_0 y^2(T) + \beta \sum_{k=1}^{\infty} [y_k(T) - \psi_k]^2 +$$
$$+ \gamma_0 \int_0^T p_0^2(t) dt + \gamma \int_0^T \sum_{k=1}^{\infty} p_k^2(t) dt, \quad (13)$$

where ψ_k – the Fourier coefficients of the function.

Thus, the optimal control problem reduces to finding in the class of admissible controls such control $(p_0[t, y(t), y_1(t),...], p_1[t, y(t),...],...)$ and the corresponding solutions $(y(t), u_1(t), u_2(t),...)$ of the problem (11)–(12) in the form of feedback so that the functional (13) takes the smallest possible value.

For the obtained optimal control problem, the class of admissible controls consists of infinite-dimensional vector-valued functions $(p_0(t), p_1(t), p_2(t),...)$ satisfying condition

$$\int_0^T \sum_{k=0}^{\infty} p_k^2(t)dt < \infty. \tag{14}$$

Let's introduce the following infinite-dimensional vectors and matrices:

$$\bar{y}(t) = \{y(t), u_1(t), u_2(t),...\}, \quad \overline{y^0} = \{y^0, u_1^0, u_2^0,...\},$$

$$\bar{p}(t) = \left\{\sqrt{\frac{\gamma_0}{\gamma}}p_0(t), p_1(t), p_2(t),...\right\}, \quad \bar{\psi} = \{0, \psi_1, \psi_2,...\},$$

$$Q = \text{diaq}[\beta_0, \beta, \beta,...], \quad B = \text{diaq}\left[\sqrt{\frac{\gamma}{\gamma_0}}, 1, 1,...\right], \tag{15}$$

$$A = \begin{bmatrix} b & a_0X_1(1) & a_0X_2(1) & \cdots \\ -a^2X_1(1) & -\upsilon_1 & 0 & \cdots \\ -a^2X_2(1) & 0 & -\upsilon_2 & \cdots \\ \cdots & \cdots & \cdots & \cdots \end{bmatrix}, \quad \upsilon_k = \frac{a^2\lambda_k^2}{1+\xi\lambda_k^2}.$$

Using this notation, the problem (11), (12) with the quality criterion (13) can be represented in the following matrix form:

$$\frac{dy}{dt} = A\bar{y} + B\bar{p}, \quad 0 < t \le T, \tag{16}$$

$$\bar{y}(0) = \bar{y}^0; \tag{17}$$

$$I_\infty[\bar{p}] = [\bar{y}(T) - \bar{\psi}]^* Q[\bar{y}(T) - \bar{\psi}] + \gamma\int_0^T \bar{p}^{-2}(t)dt. \tag{18}$$

4. Application of the dynamic programming method

To solve the optimal control problem formulated above, under the constraints (16), (17) with the quality criterion (18), let's use the dynamic programming method. Following [3], let's introduce the Bellman functional

$$S[t, \bar{y}] = \min_{\substack{\bar{p}\{\tau\} \\ t\le\tau\le T}} ([\bar{y}(T) - \bar{\psi}]^* Q[\bar{y}(T) - \bar{\psi}] + \gamma\int_t^T \bar{p}^{-2}(\tau)d\tau. \tag{19}$$

Carrying out the well-known procedure of the dynamic programming method [3], let's obtain the Bellman equation:

$$-\frac{\partial S}{\partial t}=\min_{p(t)}\left\{\gamma\bar{p}^{2}(t)+\frac{S^{*}}{\partial\bar{y}}[A\bar{y}(t)+B\bar{p}(t)]\right\}. \tag{20}$$

It follows directly from the definition of the functional S by formula (19) that $S\geq 0$ and

$$S[T,\bar{y}(T)]=[\bar{y}(T)-\bar{\psi}]^{*}Q[\bar{y}(T)-\bar{\psi}]. \tag{21}$$

Thus, the solution of the optimal control problem is reduced to the definition of $\bar{p}(t)$ and nonnegative $S[t,\bar{y}]$ from equation (20) with the additional condition (21).

Let's suppose that admissible controls are arbitrary vector-valued functions satisfying condition (14). Then from the expression on the right-hand side of the Bellman equation, let's find that

$$\bar{p}(t)=-\frac{1}{2\gamma}B^{*}\frac{\partial S}{\partial t}. \tag{22}$$

Eliminating $\bar{p}(t)$ from equation (20), let's obtain

$$-\frac{\partial S}{\partial t}=-\frac{1}{4\gamma}\frac{\partial S^{*}}{\partial\bar{y}}BB^{*}\frac{\partial S}{\partial\bar{y}}+\frac{\partial S^{*}}{\partial\bar{y}}\cdot A\bar{y}. \tag{23}$$

The solution of this functional equation will be sought in the quadratic form

$$S[t,\bar{y}]=[\bar{y}(t)-\bar{\psi}]^{*}K(t)[\bar{y}(t)-\bar{\psi}]+2\phi^{*}(t)[\bar{y}(T)-\psi]+\eta(t), \tag{24}$$

where $K(t)=\{K_{ij}(t)\}_{i,j=0}^{\infty}$ – an infinite-dimensional symmetric matrix-function, $\bar{\phi}(t)=\{\phi_{i}(t)\}_{i=0}^{\infty}$ – an infinite-dimensional vector-valued function, $\eta(t)$ – a scalar function that are to be determined. They are found from the condition that the functional S defined by (24) satisfies equation (23).

Let's note that $K(t)$ must be a non-negative definite matrix for any $t\in[0,T]$.

Calculating the gradient of the functional (24), let's find that

$$\frac{\partial S}{\partial\bar{y}}=2K(t)[\bar{y}(t)-\bar{\psi}]+2\bar{\phi}(t). \tag{25}$$

Substituting this value in (23) and taking into account that the resulting equality must be satisfied for any vector function $\bar{y}(t)$, let's obtain:

$$\frac{d}{dt}K(t)=-A^{*}K(t)-K(t)A+\frac{1}{\gamma}K(t)BB^{*}K(t), \tag{26}$$

$$\frac{d}{dt}\phi(t)=-\left[-A^{*}+\frac{1}{\gamma}B^{*}K(t)\right]\phi(t)-K(t)A\psi, \tag{27}$$

$$\frac{d}{dt}\eta(t)=-\frac{1}{\gamma}\phi^{2}(t)-2\phi^{*}(t)A\bar{\psi}. \tag{28}$$

From condition (21) and formula (24):

$$K(T)=Q,\quad \phi(T)=0,\quad \eta(T)=0. \tag{29}$$

Thus, if the matrix $K(T)$ is determined from (26), then the vector $\phi(t)$ is determined from (27). After these functions can be determined, $\eta(t)$ is found from (28). This makes it possible to find the Fourier coefficients for the control function.

5. Construction of control in the form of feedback

Since the gradient of the functional (21) is calculated by the formula (22), then from (19) let's determine the optimal control in the form

$$\bar{p}(t) = -\frac{1}{\gamma}B^*K(t)\bar{y}(t) - \frac{1}{\gamma}B^*[\phi(t) - K(t)\bar{\psi}] \tag{30}$$

or passing to coordinate notations

$$\begin{cases} p_0(t) = -\dfrac{1}{\sqrt{\gamma_0\gamma}}K_{00}(t)y(t) - \dfrac{1}{\sqrt{\gamma_0\gamma}}\sum\limits_{j=1}^{\infty}K_{0j}(t)u_j(t) + \dfrac{1}{\sqrt{\gamma_0\gamma}}\left(-\phi_0(t) + \sum\limits_{j=1}^{\infty}K_{0j}(t)\psi_j\right), \\ p_i(t) = -\dfrac{1}{\gamma}K_{i0}(t)y(t) - \dfrac{1}{\gamma}\sum\limits_{j=1}^{\infty}K_{ij}(t)u_j(t) + \dfrac{1}{\gamma}\left(-\phi_i(t) + \sum\limits_{j=1}^{\infty}K_{ij}(t)\psi_j\right), \quad i = 1,2,... \end{cases}$$

Hence, introducing functions

$$K_0(t) = -\frac{1}{\sqrt{\gamma_0\gamma}}K_{00}(t), \quad K(x,s,t) = -\frac{1}{\gamma}\sum_{i,j=1}^{\infty}K_{ij}(t)X_i(x)X_j(s),$$

$$K_1(x,t) = -\frac{1}{\sqrt{\gamma_0\gamma}}\sum_{j=1}^{\infty}K_{0j}(t)X_j(x), \qquad K_2(x,t) = \sqrt{\frac{\gamma_0}{\gamma}}K_1(x,t),$$

$$q_0(t) = \frac{1}{\sqrt{\gamma_0\gamma}}\left(-\phi_0(t) + \sum_{j=1}^{\infty}K_{0j}(t)\psi_j\right),$$

$$q(x,t) = \frac{1}{\sqrt{\gamma_0\gamma}}\sum_{i=1}^{\infty}\left(-\phi_i(t) + \sum_{j=1}^{\infty}K_{ij}(t)\psi_j\right)X_i(x);$$

let's obtain a synthesized control for the initial problem in the following form:

$$\begin{cases} p_0(t) = K_0(t)y(t) + \int\limits_0^1 K_1(x,t)u(x,t)dx + q_0(t), \\ p(x,t) = K_2(x,t)y(t) + \int\limits_0^1 K(x,s,t)u(s,t)ds + q(x,t). \end{cases} \tag{31}$$

As can be seen, $\bar{p}(x,t) = (p_0(t), p(x,t))$ control is a functional defined on the set of the state function $\bar{u}(x,t) = (y(t), u(x,t))$.

Strictly speaking, the control (31), which is obtained by the formal solution of the Bellman equation, can't be considered as optimal. Therefore, it is necessary to justify the obtained result and first of all show that it belongs to the class of admissible controls.

The boundary-value problem corresponding to the control (31) or the closed system takes the form:

$$\frac{\partial u}{\partial t} = a^2\frac{\partial^2 u}{\partial x^2} + \xi\frac{\partial^3 u}{\partial t\partial x^2} + \int_0^1 K(x,\ s,\ t)ds + K_2(x,\ t)y(t) + q(x,\ t), \tag{32}$$

$$u(x, 0) = u^0(x),$$

$$\frac{\partial u(0,t)}{\partial x} = 0, \quad \frac{\partial u(1, t)}{\partial x} + \alpha u, \tag{33}$$

$$\frac{dy}{dt} = a_0 u(1, t) + (b + K_0(t))y(t) + \int_0^1 K_1(x, t)dx + q_0(t), \tag{34}$$

$$y(0) = y^0.$$

As a result, the process becomes self-regulating.

6. Conclusions

1. In a material with a heat conductive viscosity, the process of heat transfer is described by a third-order partial differential equation.

2. For each concrete admissible control from the class of quadratically summable functions, the considered boundary value problem has a unique generalized solution.

3. The Bellman equation solution is in the quadratic form.

4. The control parameter is found as a functional defined on the set of state functions.

5. The obtained results give an algorithm for solving the problem of synthesizing optimal control or constructing a controlling parameter in the form of feedback for various systems containing elements with distributed parameters.

6. In the future, various approximate methods for solving these problems can be considered.

References

[1] Bachoy, G. S. (1980). Ob odnoy zadache sinteza optimal'nogo upravleniya teplovym processom. Izvestiya Akademii nauk Moldavskoy SSR. Seriya: Fiziko-tekhnicheskih i matematicheskih nauk, 3, 29–36.

[2] Egorov, A. I. (2004). Osnovy teorii upravleniya. Moscow: FIZ MATLIT, 504.

[3] Mamedov, R. S. (2005). Optimal Control synthesis of distributed parameter system. The 1st International Conference on control and Optimization with Industrial Applications. Baku, 67–68.

[4] Mamedov, R. S., Karimov, V. A. (2010). Optimal stabilization problem for the oscillation proses an elastic rod. Continuous optimization and information – based technologies in the financial sector. Izmir, 130–133.

[5] Aida-zade, K. R., Abdullaev, V. M. (2012). On an approach to designing control of the distributed-parameter processes. Automation and Remote Control, 73 (9), 1443–1455. doi: 10.1134/s0005117912090019

[6] Ivanova, A. P. (2003). Upravlenie s obratnoy svyaz'yu dlya stohasticheskogo uravneniya teploprovodnosti. Izvestiya Akademii nauk. Teoriya i sistemy upravleniya, 5, 26–34.

[7] Ting, T. W. (1974). A cooling process according to two-temperature theory of heat conduction. Journal of Mathematical Analysis and Applications, 45 (1), 23–31. doi: 10.1016/0022-247x(74)90116-4

[8] Bachoy, G. S. (1988). Zadacha sinteza optimal'nogo upravleniya processom ohlazhdeniya slozhnyh sred. Matematicheskie issledovaniya, 101, 19–23.

[9] Mamedov, R. S. (2003). Sintez optimal'nogo upravleniya s minimal'noy energiey dlya sistem, soderzhashchih elementy s raspredelennymi parametrami. Problemy ispol'zovaniya ekonomicheskogo potenciala predpriyatiy v perekhodnom periode. Baku, 65–72.

[10] Egorov, A. I. (2006). Upravlenie sistemami s raspredelennymi i sosredotochennymi parametrami. Teoriya upravleniya i teoriya obobshchennyh resheniy uravneniy Gamil'tona-Yakobi. Ekaterinburg: Izd-vo Ural'skogo universiteta, 2.

[11] Egorov, A. I., Znamenskaya, L. N. (2005). Upravlenie kolebaniyami svyaznyh ob"ektov s raspredelennymi i sosredotochennymi parametrami. ZHVM i MF, 45 (10), 1766–1784.

DEVELOPMENT OF INFORMATION SUPPORT OF QUALITY MANAGEMENT OF UNDERGROUND PIPELINES

Larysa Yuzevych
Department of Metrology, Standardization and Certification
Lviv Polytechnic National University
12 Stepana Bandery str., Lviv, Ukraine, 79013
larysa.yuzevych@gmail.com

Ruslan Skrynkovskyy
Department of Business Economy and Information Technology
Lviv University of Business and Law
99 Kulparkivska str., Lviv, Ukraine, 79021
uan_lviv@ukr.net

Bohdan Koman
Department of System Design
Ivan Franko National University of Lviv
1 Universytetska str., Lviv, Ukraine, 79000
sonce_28@ukr.net

Abstract

Recommendations are worked out in relation to the evaluation of longevity and quality of underground metallic pipelines in the conditions of corrosion fatigue. The features of early exposure of crisis (before accident) situations are set. A complex qualimetric criterion is offered for determination of level of quality of pipeline by the account of his technological specific. The elements of investment project and methodology of estimation of resource are worked out and also influences of factors of different nature on risks and possibility of accident of gas pipelines.

The model of corrosion fatigue of metal is based on strength criterion of fracture mechanics according to which there is an act of destruction in an arbitrary elemental volume of a material if the total irreversibly scattered energy of plastic deformation for all load cycles will reach a critical value equal to the energy of destruction.

In order to control the corrosion process taking the polarization potential into account, a criterion relation is used to determine the rate of residual corrosion of a metal in the defect of the insulation coating, in particular, at the top of the crack, which is an anode region.

The adhesive strength criteria of biocorrosive aggressive soil, mechanical criteria for the stress intensity factor, the criterion of corrosion resistance defect, criterion correlation for estimating the speed of residual corrosion in defect of insulation coating with imposed diagnostic weight characteristics and diagnostic value of tests, that complement, clarify and improve the corrosion monitoring system of pipelines, helpful for controlling and optimizing of the corrosion process, and Development of recommendations for anti-corrosion protection of metal are used in areas with non-stationary plastic deformation.

Keywords: steel pipeline, normative and technical documentation, resource, low-cycle fatigue, corrosion, quality, risks, mechanical loading, investment project.

DOI: 10.21303/2461-4262.2017.00392

1. Introduction

One of the main problems in the field of industrial safety of facilities and enterprises of the oil and gas complex (OGC) is the shortcomings in the quality of regulatory and technical documentation and the issues of ensuring reliable operation of structural elements. In this area, it is necessary to ensure the improvement of the system of normative and technical documents [1–4]. Let's consider metal underground pipelines (MUPs), in particular, gas pipelines, through which gaseous hydrocarbons are transported. The MUPs destruction is accompanied by economic losses, and also threatens the personnel of the relevant enterprises and the environment.

Ensuring the MUPs project resource is an important task in the operation of modern OGC enterprises. The solution of this problem allows to clarify the choice of materials and design and

technological solutions, as well as to provide economically efficient operating conditions for OGS. The risks associated with the MUPs operation are associated with defects in metal (steel), which arise as a result of corrosion and cyclic loads. Among the main causes of damage (defects) are called nucleation and propagation of cracks from vibrations, high static and cyclic loads, stress concentrators, corrosion fatigue, cavitation-erosion wear, etc. [4, 5].

Calculations of parameters characterizing the corrosion fatigue and fatigue life of structural elements are labor-intensive processes, since during their implementation the researcher must operate with a large amount of data due to a combination of loading cycles and the search for critical locations. The necessity of their automation and integration with traditional complexes is obvious and is confirmed by the availability of commercial software products, as well as normative documents [1–3].

2. Literature reviews and problem statement

The presence of fatigue cracks on the surface of structural elements (MUPs) aggravates the problem of the calculated values of strength characteristics under the influence of corrosive media, which has not found its full solution to date [4]. In this connection, it is necessary to correct a number of shortcomings related to the lack of relevance of the relevant normative and technical documents (NTDs).

In [5] the methodology of improving the regulatory provision of operational safety of pipeline systems with vibration accounting is given. Mathematical model and algorithm for predicting the life of pipeline systems is proposed. The mathematical model makes it possible to develop normative recommendations on the assessment of the vibrational state of pipelines [5]. The effect of operational factors on the corrosion-fatigue failure of the steels of the main oil and gas pipelines is fully reflected in [1, 3]. These methods are advisable to use for the problem of improving regulatory documents related to the corrosion protection and strength of MUPs [1–3, 5].

The object of research is metal underground pipelines in conditions of corrosion-fatigue failure.

The subject of research is normative documents, which should be specified and improved on the basis of information obtained from the monitoring of the MUPs operation.

3. The aim and objectives of research

The aim of research is selection of information on the improvement of regulatory and technical support for monitoring the quality of metal underground pipelines in conditions of fatigue and the influence of aggressive corrosive environment, which will improve the quality of their non-destructive testing.

To achieve this aim, it is necessary to build a conceptual model of processes and develop recommendations on its rational functioning, taking into account the accumulation of defects and their distribution in the pipeline metal.

4. Research results on information support of quality control of underground pipelines

Normative documents [1–3] for technical diagnostics of underground metal pipelines in a corrosive (soil) environment must take into account the following elements (stages) [5], the interpretation of which is advisable to be improved taking into account more modern regulatory and methodological support:

– quantitative criteria for assessing the reliability of the investment project (improving the technology of corrosion protection of metal UPs);

– normative documents on corrosion and strength of structural elements;

– the calculated or experimental determination of the zones of location of the largest cyclic voltage and their corresponding values, depending on the number of cycles according to [1];

– in cases of corrosion-fatigue damage, calculation for fatigue should be carried out taking into account the requirements regarding the choice of permissible parameters for cyclic stresses and the actual number of cycles, accumulation of damage [4, 6, 7];

– checking the actual thickness of the walls of the stretched and neutral zones.

In the case of a decrease in strength characteristics of the metal below the requirements of NDs, but maintaining satisfactory characteristics of ductility and toughness, continued operation with design parameters is allowed with satisfactory results of the verification test for strength from internal pressure (safety margin relative to the actual yield strength of at least 1.5) and compliance with requirements of NDs [1]. It should be noted that existing normative documents are based on methods for assessing the maximum permissible strength characteristics of a metal, not including a sufficient amount of data to diagnose changes in the operation process.

Criteria characterizing the technical condition and residual life of the pipeline are the following parameters: pressure, temperature, working medium, mechanical load, vibration loads, fatigue strength, wear during operation [5].

When compiling the lists of pipeline systems, the defining characteristic is the functional affiliation of the pipeline [5]. For this, the pipelines are systematized and the criteria for their strength and reliability are established, taking into account the belonging of the software to a certain type [5]. An example can be trunk gas pipelines and oil pipelines, underground steel pipelines of cold and hot water supply system, etc.

Let's confine ourselves to the consideration of underground gas pipelines located in the soil electrolyte under conditions of low cycle fatigue. For MUPs, high-frequency fatigue is not observed [6]. To improve the NDs [1–3], it is advisable to build a complex mathematical model that will combine the physicochemical model of fatigue-corrosion processes of the type [7], the method of damage accumulation [8] and elements of the risk theory [9].

To estimate the rate of growth of the fatigue crack in the metal at the mean rectilinear section of the kinetic curve, let's use the Paris equation [10]:

$$V_a = da / dN = C_t (\Delta K)^n, \quad \Delta K_{th} < \Delta K < K_{IC}, \tag{1}$$

where $2a = L_T$ – crack length, N – the number of load cycles, K – stress intensity factor (SIF) (used in linear fracture mechanics to describe stress fields near the crack tip), ΔK – SIF range, C_t and n – the so-called Paris constants, ΔK_{th} – fatigue threshold, K_{IC} – fracture toughness of the material.

The relation (1) is improved [11, 12]:

$$da / dN = F(C_i, P_j(\sigma), A_n(\tau), B_m(S)), \tag{2}$$

where F – the symbol of the functional dependence, C_i – the constants characterizing the material-environment system, $P_j(\sigma)$ – the parameters characterizing the stress-strain state of the material and are functions of the external forces applied to the body, $A_n(\tau)$ – the parameters that determine physicochemical processes occurring between the deformed metal and the corrosive medium in time τ, $B_m(S)$ – parameters characterizing the state of the surfaces of the material S, which are formed upon destruction.

The rate of growth of the corrosion crack is characterized by three main parameters K_{max}, pH_{tC}, E_{tC} and the corresponding equation takes the form [12, 13]:

$$V_{ae} = \left(da / dN\right)_e = F(C_i, K_{max}, pH_{tC}, E_{tC}), \tag{3}$$

where K_{max} – the maximum SIF value in the cycle for normal breakaway cracks, pH_{tC} – the hydrogen index of the medium, E_{tC} – the electrode potential of the metal.

Let's generalize the Paris equations for determining the crack propagation velocity V_a, taking into account the information of [10–12, 14]:

$$V_{aep} = da / dN = C_a \times (\Delta K(a, \Delta a, \Delta\sigma), K_{max}, pH_{tC}, E_{tC})^n, \quad \Delta K_{th} < \Delta K < K_{IC}, \tag{4}$$

where Δa – the fracture quantum, $\Delta\sigma$ – stress range, n, C_a – the constants characterizing the "material (steel) – medium" system.

The durability (resource) of a structural element with a crack, that is, the period N_P is calculated by a formula similar to [11, 14]:

$$N_P = C_a \int_{ai}^{ac} \frac{da}{(\Delta K(a, \Delta a, \Delta\sigma), K_{max}, pH_{tC}, E_{tC})^n}, \quad k_N = N_P / N_{P*}, \tag{5}$$

where ai – the initial size of the macrocrack in the material, ac – the critical size of the fatigue macrocrack, N_{P*} – the number of load cycles of the base sample, and k_N – the relative number of load cycles. The parameter ai=d_*, where d_* is the size of the pre-destruction zone [13, 14].

pH_{tC}, E_{tC} parameters can be used for local anodic dissolution (LAD) and hydrogen cracking (HC) mechanism [12].

The method of quantitative estimation of LAD and the mechanism of HC is based on the assumption [12, 13]:

$$\Delta(da/dN)_e = (da/dN)_e - (da/dN)_a = \Delta(da/dN)_{eA} + \Delta(da/dN)_{eH}, \tag{6}$$

where $(da/dN)_e$ and $(da/dN)_a$ – the components of the propagation velocity of the crack, $\Delta(da/dN)_e$, $\Delta(da/dN)_{eA}$ and $\Delta(da/dN)_{eH}$ – the change in the components of the propagation velocity of the crack caused by LAD and HC.

The expression in the first approximation, based on the Faraday law, can be obtained as follows [12, 15]:

$$\Delta(da/dN)_{eA} = \beta_A \times \Delta E_A, \quad \Delta(da/dN)_{eH} = \beta_H \times \Delta E_H, \tag{7}$$

where β_A – the coefficient characterizing the "material (steel)-medium" system under investigation and depends on the density and atomic mass of the metal, the charge of cations that penetrate into solutions, the Faraday constant, the conductivity of electrolytes, the shape of the crack and the stress-strain state in the vicinity of the crack, ΔE_A – takes into account the synergetic effects (influence of voltage, hydrogen electrolytes present) on LAD, β_H – the coefficient characterizing the "material (steel) – medium" system and depends on the exposure time of the medium, the quantities of hydrogen and the fullness of the crack, the diffusion rate, the critical concentration of hydrogen in the stress section with the maximum tension, the stress-strain state in the vicinity of the crack, and other parameters that can' yet be determined accurately, ΔE_H – takes into account synergistic effects (stress effect, processes LAD, etc.) and provides these changes in hydrogen depolarization in the fracture as a result of corrosion fatigue.

The energy criterion for fracture mechanics is also based on the energy criterion of fracture mechanics, according to which an act of destruction occurs in an arbitrary elementary volume of material if the total irreversibly dispersed energy of plastic deformation W of all load cycles reaches a critical value W_Z equal to the material destruction energy [16, 17]:

$$W = \alpha \times W_Z \Rightarrow W_Z = W_0 + W_S + \Delta N \times W_C = \alpha \times \gamma_T \times \Delta a = \alpha \times \sigma_{0f} \times \delta_{fC} \times \Delta a, \tag{8}$$

where W_Z – the material destruction energy for a single static load, α – the Morrow coefficient [16], $W_0=\gamma_{T0}\times\Delta a$, W_0 and γ_{T0} – the energy and specific dissipation energy of plastic deformations under the previous load, respectively, $\sigma_{0f} \approx (\sigma_T + \sigma_B)/2$, σ_T, σ – the yield strength and strength of the material, respectively, δ_{fC} – critical crack opening, $\gamma_T = \sigma_{0f}\times\delta$ – specific fracture energy needed to form a unit of crack length.

For the component W_S related to the averaged stresses $W_0 = \gamma_{T0}\times\Delta a$, W_0 and the cyclic strain energy WC, the following expressions are given [17, 18]:

$$W_S = \sigma_{0f} \times \delta_{max} \times \Delta a, \quad W_C = \int_0^{l_{pf}} \sigma_{0f} \left[\delta_{f\,max}(s) - \delta_0\right] ds, \tag{9}$$

where δ_{max} – the maximum crack opening, $\delta_{fmax}(s_t)=(1–R)\times\delta_{max}(s_t)/2$ – the opening of the sides of the additional cut ($0\le s_t\le l_{pf}$), which is implied with the opening under static load, l_{pf} – length of the plastic zone, $R=P_{min}/P_{max}$ – load cycle asymmetry coefficient, P_{min}, P_{max} – minimum and maximum loads in the sample with a crack.

The values of W, W_Z (8) are determined through the parameters of the stress-strained state (SSS) in the zone of the fracture advance as the area of the corresponding sections under the model tension diagram for the reinforcement material, approximated by the power law for the voltage σ [16, 18]:

$$\sigma=\sigma_T+\zeta\times\varepsilon^m, \tag{10}$$

where ζ – coefficient of strain hardening of the material, σ_T, ζ, m – experimentally established constants for this material.

The critical expansion of the crack tip, taking into account the strengthening ζ, is calculated by the formula [19]:

$$\delta_{fC}=C_0\frac{K^2}{\sigma_{0f}E};\ \ C_0=0,6(1-\nu^2)\left(\frac{2(1+\nu)(1+\zeta)\sigma_0}{3\sqrt{\zeta}E}\right)^{\zeta}, \tag{11}$$

where ν – Poisson ratio, E – Young's modulus.

The critical opening δ_{fC} of the crack tip enters into the CCO criterion of strength (critical crack opening), which determines the ultimate equilibrium state of an elastic body with a crack at the time of reaching the opening crack δ_{fC} [20]:

$$\delta_1(L_t,\sigma_T)=\delta_{fC}. \tag{12}$$

With crack opening δ_{fC} in a simplified version connected SIF K and overpotential η of metal dissolution reaction on the basis of the known relationships [20, 21]:

$$K=\sqrt{\frac{E}{1-\nu^2}\cdot\left(WPL-Z_{si}F\rho\delta\frac{\eta}{M}\right)},$$

$$K=K_{1SCC}=\sqrt{E\cdot\sigma_T\cdot\delta_{fC}}, \tag{13}$$

where Z_{si} – the formal charge of the solvated (hydrated) ions, F=96500 Kl/mol – the Faraday constant, δ=2r – the width of the front of the impending microcrack, m, M is the molecular weight of the metal, Kg/mol (M=0,0558 kg/mol – for steel), K_{1SCC} – the threshold value of the SIF, that is, the minimum value of the corresponding to the beginning of the crack propagation under the influence of the mechanical load and the corrosive medium, WPL – the surface energy of plastic deformation, η – electrochemical overpotential (B), that is, the deviation of the electrode potential from its equilibrium (with respect to the electrode composition of the solution) thermodynamic value when the electrode under the current is polarized. It should be noted that the second relation (12) for K_{1SCC} follows from the CCO of the strength criterion (critical crack opening) (11).

The WPL parameter is included in the known formula (strength criterion) of Griffiths-Irvine-Orowan [20, 22]:

$$\sigma_*=\sqrt{\frac{4E\cdot WPL}{\pi\cdot L_T(1-\nu^2)}},\quad \sigma_*=\sqrt{\frac{4E\cdot WPL}{\pi\cdot L_T}}, \tag{14}$$

where the first formula is written for plane deformation, the second for a plane stress state, σ_* – the critical stress, WPL = J/2, J – the Rice's integral [23].

According to the results of contact deformation of various steel (17ГС, 17ГС-У, 06Г2НАБ, 10Г2ФБ, 10Г2ФБ-У, 10ЧГНМАЮ) used in MUPs [6], an empirical relationship is established that links SIF K to WPL [21]:

$$K = a_1 \cdot \sqrt{WPL} - a_2; \quad a_1 = 226 \cdot 10^6 \ \frac{\sqrt{H}}{M}; \quad a_2 = 6{,}98 \text{ MPa}\sqrt{m}. \tag{15}$$

In the ratio (15), it is necessary to set a_1=226, a_2=6,98, then the dimension of K will be given in MPA $\text{MPa} \cdot \sqrt{m}$, and WPL will be obtained in $(MJ^2)/m^2$.

To determine the density of the anode current I_A at the crack tip, taking into account the energy characteristics of the surface WPL layer, let's use the generalized Kaeshe-type relationship [15, 21]:

$$I_A = \frac{\alpha \cdot \chi \cdot \Delta\psi_{ak}}{\delta \cdot \ln\left((h + c + r)/\delta\right)} \cdot \left(1 + \beta_W \cdot \left(\frac{WPL - WPL0}{WPL0}\right)^S\right), \tag{16}$$

where α – the angle at the crack tip, χ –the electroconductivity of the electrolyte, $\Delta\psi_{ak}$ – the ohmic change in the electric potential between the anodic and cathodic parts, h, c – the depth of the cavity and the crack, respectively, r – the radius of the projection curvature of the juvenile surface. The relation (16) is written for the crack tip, which is the anode, β_W, S, WPL0 are experimentally determined constants.

The empirical initial formula for calculating the boundary of corrosion fatigue of metals has the form [7]:

$$\sigma_{ve} = \sigma_{vp}\left[1{,}128 - 2{,}849 \lg(Q_{dr} / Q_{cor})\right], \tag{17}$$

where σ_{vp}, σ_{ve} – fatigue limit (mechanical stress) in air and in the environment, respectively, Q_{dr}, Q_{cor} – the amount of electricity going for additional dissolution of the deformed metal at σ_{vp} and its corrosion in the absence of deformation. For stainless steels used in pipelines, the uncertainty of estimating σ_{vp}, σ_{ve} does not exceed 8 %.

For the basic model of accumulation of damages for metals under conditions of automotive deformation (fatigue), the Manson-Halford model based on the damage curve [24, 25] was adopted:

$$D_s = \left(N_s / N_{fs}\right)^q, \quad q = \left(N_{f(s-1)} / N_{fis}\right)^\beta, \quad \beta = m + a \cdot \text{sign}\left(N_{f2} / N_{f1} - 1\right), \tag{18}$$

where D_s – the material damageability at the s-th degree (area) of deformation (s =1, 2, 3,…, ns), N_s – the number of deformation cycles on the s-th power, N_{fs} – the number of cycles before the sample is destroyed under the deformation mode, which corresponds to the s-th power, q, β, m, a – empirical constants, for a number of materials (metals) $\beta \approx 0.4$.

The fatigue damage model is simply described by the ratio of the damage denoted as D_m to the number of cycles N.

Let's confine ourselves to a consideration of the low-cycle fatigue of metals. The evolution equation for describing the process of low-cycle fatigue of metals is [26, 27]:

$$D_z = \sum \Delta D_s = \sum_{s=1}^{ns} \Delta D_s,$$

$$\Delta D_s = f_s(\beta_u)\left(z_s\right)^{\alpha_s}\left(1 - D_s\right)^{-r_s} \Delta z_s \left(\alpha_s + 1\right)/\left(r_s + 1\right), \quad D_z \Rightarrow D_f,$$

$$\beta_u = \sigma / \sigma_u; \quad \sigma = \sigma_{kk} / 3; \quad f_s(\beta_u) = \exp(-k_s \beta_u), \tag{19}$$

where $z_s = (W_s - W_a)/(W_{fp} - W_a)$; $\Delta z_s = \Delta W_s/(W_{fp} - W_a)$; $\Delta W_s = \rho_{ij}\Delta e_{sij}$, D_z, D_f – the integral volume damageability of the material and its critical value, W_a – the specific energy value W_s at the end of the first stage of the process of fatigue damage accumulation at low cycle fatigue (LCF), W_{fp} – the local value of the specific fatigue damage accumulation energy corresponding to the creation of the macroscopic crack for LCF, ρ_{ij}, e_{ij} – the components of the residual microstress tensors and the deviator of elastic deformations, respectively, σ_{ii}, σ – the principal components and the first invariant of the macroscopic stress tensor, α_s, r_s, k_s – parameters (physical characteristics) of the material (determined experimentally).

The law of damage can be summarized as follows (including the period of energy accumulation) [28]:

$$\frac{dD_z}{dt} = \left(\frac{Ee^2}{2Z_S}\right)^{\lambda} e^{\lambda}\left(\frac{de}{dt}\right), \tag{20}$$

where $e=e_{kk}/3$ – the first invariant of the strain tensor, (20) introduces 2 damage parameters: the impact force Z_S and the damage index λ.

As a criterion for completing the stage of development of scattered microdamages and creating a microcrack, the criterion for achieving a critical value D_f (19) can be adopted.

Relation (1)–(20) is useful for describing the LCF of the material both in zones with developed non-stationary plastic deformations and in elastic zones of the material (metal) under cyclic loading.

Let's add the system (1)–(20) with information on the parameters characterizing a particular underground pipeline under operating conditions. For this, it is necessary to take into account the influence on the reliability Y_N of MUP of the internal working pressure p_S, the stresses σ_y from the temperature differences ΔT, the unevenness of laying the pipeline in the trench, in particular [29]:

$$\rho_K = \frac{8(H+\Delta H)}{L_x^2 + 4(H+\Delta H)^2}; \quad Y_N = Y(\sigma_y, p_S, \Delta T, \rho_K); \quad \beta_Y = \frac{Y_N}{Y_S}, \tag{21}$$

where, ρ_K – the pipe curvature in the pipeline section, H – the design change in the pipeline location mark, ΔH – the depth error of the pipeline laying (depth), L_x – the pipeline length with the same curvature ρ_K, Y_N – the reliability function of the pipeline section (mathematical expectation of the safety reserve), Y_S – standard (normative) value of the reserve strength, β_Y – safety characteristic.

For a pipe weakened on the outer surface by a cavern-like defect of depth h with a crack at the tip of depth c, we can write the ratio for the stress concentration coefficient K_t and the internal critical pressure $p=p_S$, similar to those presented in [21]:

$$K_t = (2{,}021 - 1{,}301\cdot\beta_K + 0{,}727\cdot\beta_K^2 - 0{,}147\cdot\beta_K^3)\cdot\frac{d}{d_1 - c};$$

$$p_S = \frac{2\sqrt{2}\cdot d\cdot\sigma_T}{3K_t\cdot D}\cdot\frac{(1{,}5+K_z)\cdot(r_0+c)^4}{(r_0+c)^4 + 0{,}5\cdot r_0^2(r_0+c)^2 + r_0^4}, \tag{22}$$

where

$$K_z = \left(\frac{d_1 - c}{2}\cdot\frac{2(d_1-c)+3r_0}{d_1 - c + r_0} - \frac{3d}{2K_t}\right)\Big/\left(\frac{d}{K_t} + \frac{r_0}{3}\cdot\left(\frac{r_0^3}{(d_1 - c + r_0)^3} - 1\right)\right); \quad \beta_K = \frac{r_0}{d_1 - c};$$

D – diameter of the pipe, d – the thickness of the pipe wall, the critical pressure p_S corresponds to the condition for reaching the limiting (plastic) state at the crack peak, according to the Huber-Mises-Hencky yield criterion [30].

This is a solution of scientific and applied problems of improving regulatory documents for operational safety and lifetime of the terminal of reactor nuclear power plants by developing a scientific and reasonable mathematical model and diagnostic algorithm [31]. Based on the research, normative acts were developed to assess the technical condition of the pipeline metal and to determine its resources for reassignment of operation and safe operation during the project period [31].

Three UPs modes are considered: NO – normal operation, VNO – violation of normal operating conditions, HT – hydraulic tests. Then the accumulated fatigue damage of equipment and pipelines from operating cycles of loading is determined by the coefficient a_{ex} [31]:

$$a_{ex} = \frac{N_{NE}}{[N_0]_{NE}} + \frac{N_{VNO}}{[N_0]_{VNO}} + \frac{N_{HT}}{[N_0]_{HT}}, \quad (23)$$

where $[N0]_{NO}$, $[N0]_{VNO}$, $[N0]_{HT}$ – number of cycles of the pipeline in the load modes of NO, VNO, HT accordingly, N_{NO}, N_{VNO}, N_{HT} – the actual number of cycles in the load modes NO, VNO, HT.

To check the corrosion process taking into account the polarization potential (PP) U_P, a criterial relationship is used to determine the rate of residual corrosion of the metal in the defect of the insulation coating, in particular at the crack tip, which is the anode region [32]:

$$I_A = I_{AY} \cdot 10^{V_{pt}}; \quad V_{pt} = \frac{\overline{E}_c - U_P}{b_{at}}, \quad (24)$$

where $\overline{E}_c$ – the average corrosion potential, I_{AY} – the density of the corrosion (anode) current (metal corrosion rate) at $\overline{E}_c = \overline{E}_P$, b_{at} – Tafel slope of the anodic polarization curve.

To control the corrosion process in the type of stress concentrator, let's use the results of experimental studies [11] for steel 20 and the relation (24).

Let's consider the situation when the relative tensile stress σ/σ_T varies from 0 to 1 [11]. At the same time $\overline{E}_c$=–0.092 V, while the corrosion current for steel 20 in a 3 % solution of NaCl increases linearly from 0.1 A/m^2 to 0.4 A/m^2. Taking these experimental data into account, let's generalize (24) and, as a result, obtain:

$$I_A = I_{AY}\left(1+\beta_S \times \sigma / \sigma_T\right) \cdot 10^{V_{pt}}; \quad \beta_S = 3, \quad (25)$$

where β_S – a dimensionless empirical parameter for steel 20 in a 3 % solution of NaCl.

The polarization potential (PP) U_P is considered the main criterion for corrosion protection of metal structures in an electrically conductive medium [32, 33]. It is empirically established and confirmed by many studies that the protective PP for steel underground pipelines should be in the range from –0.85 to –1.15 V relative to the mid-sulfate reference electrode (RE) [33].

In real conditions, the relationship between the constant and alternating current components i_A flowing between the metal and the medium can significantly differ through different characteristics of rectifiers and reactances. These shortcomings of known methods were eliminated using the proposed method for determining the PP with the ohmic component removed from the measurements of constant and variable electric voltages [33]. To get rid of the ohmic component from the measurement of the potential difference U_{MG}, the value of the alternating voltage was set in accordance with the constant using the harmonic coefficient determined from the measurements of the constant U_{GG} and the variable voltage V_{GG} at the same resistance between the reference electrode (RE) and the auxiliary electrode (AE). PP is determined by the formula [33]:

$$U_P = U_{MG} - V_{MG} \times U_{GG}/V_{GG}, \quad (26)$$

where U_{MG} – the potential difference between the pipeline metal and the electrode installed on the soil surface, $k_G=V_{GG}/U_{GG}$ – the measured harmonic coefficient.

The destruction of the pipe is possible when the defect depth h+c reaches the critical size h_{cr}, and the crack length L_T will exceed the critical value L_{cr}.

To estimate h_{cr}, let's use the relation [1, 34]:

$$h_{cr} = h + c_{cr} = d - L_T\sqrt{0{,}1785\frac{p_S}{\sigma_в}},$$

$$h_{cr} = d\sqrt{\frac{L_T}{D}}\left(1 - \frac{p_S(D-2d)}{2K_K K_S \sigma_в d}\right),$$

$$L_T \Rightarrow L_{cr} == \frac{1}{\pi}\left(\frac{8d}{p_S D}\right)^2 K_{fC}^2, \quad K_S = 1 + \frac{h+c}{d}\sqrt{\frac{L_T}{D}}, \tag{27}$$

where, K_K – the coefficient of crack sensitivity, c_{cr} – the critical value of the crack depth, K_S – the coefficient that takes into account the change in pipe thickness in the defective section of the pipeline, K_C the crack resistance parameter, which is determined experimentally by known mechanical testing methods. To determine K_K, laboratory mechanical tests are also carried out, in which the ratio of the strength limits of the defective and solid samples is taken into account [34]. It should be noted that the first formula (27) for h_{cr} is empirical.

The term of accident-free operation of the T_S facility (MUP) can be estimated from the formula [34]:

$$T_S = \left(h_{cr} - h_{max}\right)/I_A, \tag{28}$$

where h_{max} – the geometric size of the defect of the maximum permissible depth, the dimension of the anode current I_A – 1 mm/year.

Just as in [35] let's use the product $k_p=k_1\times k_2\times k_3$, k_1 – the coefficient of commercial gain, k, k_2 – the coefficient of MUP competitiveness, k_3 – MUP reliability factor ($k_3=Y_N$).

Taking into account these indices ($k_P=k_1\times k_2\times k_3$), just as in [35] the qualitative criterion (quality criterion) of the generalized MUP level takes the multiplicative form:

$$Z_1 = \prod_{i=1}^{m} k_i = k_1 \cdot k_2 \cdot k_3 \cdot k_4 \cdot k_5 \cdot k_6 \cdot k_7 \cdot k_8 \Rightarrow \max, \tag{29}$$

where k_4,(D_f), k_5(p_S), k_6(σ_{ve}), k_7(Y_N), k_8(T_S) – coefficients characterizing defectiveness D_f, strength p_S, corrosion fatigue limit $\sigma_{ve}(N_p)$, reliability Y_N, term of accident-free operation T_S (resource) of the structure.

Let's introduce the quality criterion Z_2in the additive form:

$$Z_2 = a_1 \cdot k_1 + a_2 \cdot k_2 + a_3 \cdot k_3 + a_4 \cdot k_4 + a_5 \cdot k_5 + a_6 \cdot k_6 + a_7 \cdot k_7 + a_8 \cdot k_8 \Rightarrow \max, \tag{30}$$

where a_j (j=1, 2, …, 8) – the weight coefficients.

Taking into account the information in [36–40], let's formulate the basic quantitative criteria for assessing the reliability of the investment project (improving the technology of corrosion protection of metal PTs) as in [39, 40], taking into account: DROI – the discounted rate of return on investment in the project, DPP – the payback period of the project, taking into account the discounting, the sensitivity of the project SR – safety margin of the project by its key parameters:

$$N_{DROI} = NVP / DCF_{INV} = PI - 1; \quad N_{DPP} = 1 - DPP / T_p, \tag{31}$$

where DCF_{INV} – the discounted cash flow from investment activity, NPV – the net present value of the project, PI – the project profitability index, T_P – the performance indicator horizon, N_{DROI}, N_{DPP} – the reliability indicators of the project according to the DROI and DPP criteria.

The overall index of reliability of investment project N_Z, taking into account the risk, is determined in the same way as in [36, 38] by the criterion:

$$N_Z = N_{DROI} \times N_{DPP} \times SR(R), \tag{32}$$

where SR – integral evaluation of project sensitivity using the key parameters of (1)–(28) and the risk R.

In areas with unsteady plastic deformation is expedient to use the criteria for adhesive strength biocorrosive aggressiveness of soil, mechanical criterion for the stress intensity factor (accounts for overstress of corrosion process), the criterion of defect corrosion resistance, criterion correlation to estimate the residual metal corrosion rate in the defect of the insulating coating together with introduced diagnostic weight characteristics and diagnostic value surveys that complement refines and improves the system of corrosion pipeline monitoring and can be used to control and optimize the corrosion process, and the development of corrosion protection guidelines [39, 40]. Optimization of the conditions for the protection of structural elements of oil and gas industry, that are described and regulated by the state standard [2], can be conducted with their help.

The joint use of relations (1)–(32) and criteria for corrosion monitoring of pipelines [39] allows to study, in detail, from the standpoint of corrosion fatigue, electrochemistry, physics of surface processes, fracture mechanics and risk theory, the mechanisms of propagation of corrosion fatigue cracks in underground metal pipelines located in aggressive environments, in particular, in sea water and soil electrolyte.

An estimation of uncertainty regarding the term of accident-free operation of the pipeline δT_S (MUP) (i. e. pipeline resource) according to formula (28) and data on pipe parameters, corrosion cracks and other [21]:

$$T_{S1}=12{,}9 \text{ years}, \ T_{S2}=18{,}7 \text{ years}, \ \delta T_S=2(T_{S2}-T_{S1})/(T_{S2}+T_{S1})\approx 0{,}37. \tag{33}$$

Taking into account information on the uncertainties of the density of the corrosion current I_A (16), additional information about I_A (25) and a number of parameters of the type p_S, c_{cr}, h_{cr} are decreased the uncertaintyδT_S in the ratios (1)–(27) from 37 % (33) to 9 %.

Based on the obtained results, it is possible to improve the normative and technical documents [1, 2] for metal pipelines in conditions of low-cycle corrosion fatigue.

5. Conclusions

1. A new complex mathematical model is proposed for estimating the resource and improving the quality of corrosion protection of metallic underground pipelines from the standpoint of corrosion fatigue, electrochemistry, surface physics, fracture mechanics and risk theory. The simulation takes into account the accumulation of damage in metals and allows to study the mechanisms of the propagation of corrosion fatigue cracks in underground metal pipelines located in corrosive environments, in particular, in sea water and soil electrolyte. These relationships are the basis for developing techniques for improving regulatory and technical documents for metal pipelines, which are in conditions of low-cycle corrosion fatigue.

2. The joint use of the criteria of corrosion fatigue and criteria for corrosion monitoring of pipelines proposed in this paper [39] will allow to study in detail the mechanisms of propagation of corrosion fatigue cracks in underground metal pipelines in the area of corrosion fatigue, electrochemistry, surface physics, fracture mechanics and risk theory in aggressive environments.

3. The presented research results make it possible to predict the change in the corrosion state of the pipeline metal with time and to calculate the service life of local sections and the entire pipeline as a whole.

4. A mathematical model has been developed and the research results can be used by the organizations of Ukrtransgaz (structural subdivisions with the right of branches whose production facilities

are located in all regions of Ukraine) [41] to solve problems related to the improvement of regulatory documentation for the protection of steel pipelines against corrosion and their technical diagnosis.

References

[1] DSTU-N B V.2.3-21:2008. Mahistral'ni truboprovody. Nastanova. Vyznachennya zalyshkovoyi mitsnosti mahistral'nykh truboprovodiv z defektamy (2008). Kyiv: Minrehionbud Ukrayiny.

[2] DSTU 4219-2003. Truboprovody stalevi mahistral'ni. Zahal'ni vymohy do zakhystu vid koroziyi (2003). Kyiv: Minrehionbud Ukrayiny, 72.

[3] DSTU B V.2.5-30:2006. Truboprovody stalevi pidzemni system kholodnoho i haryachoho vodopostachannya. Zahal'ni vymohy do zakhystu vid koroziyi (2006). Kyiv: Minbud Ukrayiny, 112.

[4] Petryna, Yu. D., Petryna, D. Yu., Kozak, O. L. (2012). Vplyv ekspluatatsiynykh chynnykiv na koroziyno-vtomne ruynuvannya staley mahistral'nykh naftohazoprovodiv. Rozvidka ta rozrobka naftovykh i hazovykh rodovyshch, 3 (44), 1–11. Available at: http://nbuv.gov.ua/UJRN/rrngr_2012_3_14

[5] Kiporenko, A. S. (2011). Sovershenstvovanie normativnogo obespecheniya ekspluatacionnoy bezopasnosti truboprovodnyh sistem atomnih elektrostanciy. Kharkiv: Ukrainskaya inzhenerno-pedagogicheskaya akademiya, 139.

[6] Anuchkin, M. P., Gorickiyb, V. N., Miroshnichenko, B. I. (1986). Truby dlya magistral'nyh truboprovodov. Moscow: Nedra, 232.

[7] Pohmurs'kiy, V. I,. Homa, M. S. (2008). Koroziyna vtoma metaliv ta splaviv. Lviv: Spolom, 152.

[8] Sangid, M. D. (2013). The physics of fatigue crack initiation. International Journal of Fatigue, 57, 58–72. doi: 10.1016/j.ijfatigue.2012.10.009

[9] Ray, A. (1999). Stochastic Modeling of Fatigue Crack Damage for Risk Analysis and Remaining Life Prediction. Journal of Dynamic Systems, Measurement, and Control, 121 (3), 386–393. doi: 10.1115/1.2802486

[10] Pugno, N., Ciavarella, M., Cornetti, P., Carpinteri, A. (2006). A generalized Paris' law for fatigue crack growth. Journal of the Mechanics and Physics of Solids, 54 (7), 1333–1349. doi: 10.1016/j.jmps.2006.01.007

[11] Dmytrakh, I. M., Panasyuk, V. V. (1999). Vplyv koroziynykh seredovyshch na lokal'ne ruynuvannya metaliv bilya kontsentratoriv napruzhen. Lviv: Redaktsiya zhurnalu "Fizyko-khimichna mekhanika materialiv", 340.

[12] Ratych, L. V. (1999). Anodic dissolution and hydrogen embrittlement contribution into corrosion-fatigue crack growth. Materials Science, 35 (3), 15–27.

[13] Ostash, O. P.; Panasuyk, V. V. (Ed.) (2015). Fracture mechanics and strength of materials. Vol. 15. Structure of materials and fatique life time of structural components. Lviv: Publishing House "SPOLOM", 312.

[14] Li, D. M., Nam, W. J., Lee, C. S. (1998). An Improvement on Prediction of Fatigue Crack Growth from Low Cycle Fatigue Properties. Engineering Fracture Mechanics, 60 (4), 397–406. doi: 10.1016/s0013-7944(98)00029-0

[15] Kaeshe, H. (1979). Die Korrosion der Metalle. Physikalisch-chemische Prinzipien und aktuelle Probleme. Berlin: Springer-Verlag, 400. doi: 10.1007/978-3-662-11502-2

[16] Morrow, J. (1950). Investigation of plastic strain energy as a criterion for finite fatigue life. The garret corporation report. Phaeniz, 105–108.

[17] Andreikiv, O. E., Lishchyns'ka, M. V. (1999). Equations of growth of fatigue cracks in inhomogeneous plates. Materials Science, 35 (3), 355–362. doi: 10.1007/bf02355479

[18] Li, Y. C., Huang, N. C. (1991). Fatigue crack speed of materials with linear hardening. International Journal of Solids and Structures, 27 (7), 865–883. doi: 10.1016/0020-7683(91)90021-7

[19] McMeeking, R. M. (1977). Finite deformation analysis of crack-tip opening in elastic-plastic materials and implications for fracture. Journal of the Mechanics and Physics of Solids, 25 (5), 357–381. doi: 10.1016/0022-5096(77)90003-5

[20] Panasyuk, V. V., Andreykiv, A. E., Parton, V. Z. (1988). Osnovy mekhaniki razrusheniya. Kyiv: Naukova dumka, 488.

[21] Valyashek, V. B., Kaplun, A. V., Yuzevych, V. M. (2015). Matematychne ta komp»yuterne modelyuvannya fizychnykh kharakterystyk materialu u vershyni trishchyny z urakhuvannyam efektu zmitsnen-

nya. Kompyuterno-intehrovani tekhnolohiyi: osvita, nauka, vyrobnytstvo, 18, 97–104. Available at: http://nbuv.gov.ua/UJRN/Kitonv_2015_18_18

[22] Chen, X., Mai, Y.-W. (2012). Fracture mechanics of electromagnetic mate-rials: nonlinear field theory and applications. New Jersey: Imperial College Press, 328. Available at: http://www.beck-shop.de/fachbuch/leseprobe/9781848166639_Excerpt_001.pdf doi: 10.1142/p760

[23] Rice, J. R. (1968). A Path Independent Integral and the Approximate Analysis of Strain Concentration by Notches and Cracks. Journal of Applied Mechanics, 35 (2), 379–386. doi: 10.1115/1.3601206

[24] Manson, S. S., Halford, G. R. (1981). Practical implementation of the double linear damage rule and damage curve approach for treating cumulative fatigue damage. International Journal of Fracture, 17 (2), 169–192. doi: 10.1007/bf00053519

[25] Manson, S. S., Halford, G. R. (1986). Re-examination of cumulative fatigue damage analysis-an engineering perspective. Engineering Fracture Mechanics, 25 (5-6), 539–571. doi: 10.1016/0013-7944(86)90022-6

[26] Ellyin, F., Kujawski, D. (1986). An energy-based fatigue failure criterion. Microstructure and Mechanical Behaviour of Materials, 11, 591−601.

[27] Bol'shuhin, M. A., Zverev, D. L., Kaydalov, V. B., Korotkih, Yu. G. (2010). Ocenka dolgovechnosti konstrukcionnyh materialov pri sovmestnyh processah malociklovoy i mnogociklovoy ustalosti. Problemy prochnosti i plastichnosti, 72, 28–35.

[28] Desmorat, R. (2006). Damage and fatigue. Continuum damage mechanics modeling for fatigue of materials and structures. REGC. Geomechanics in energy production. Cachan, 10, 849–877. Available at: w3.lmt.ens-cachan.fr/PDFs/DESMORAT.2006.7.pdf

[29] Pichuhin, S. F., Zyma, O. Ye., Vynnykov, P. Yu. (2015). Nadiynist' liniynoyi chastyny pidzemnykh mahistral'nykh truboprovodiv. Zbirnyk naukovykh prats'. Seriya: haluzeve mashynobuduvannya, budivnytstvo. Poltava: PoltNTU, 1 (43), 17–28.

[30] Banabic, D. (2010). Plastic Behaviour of Sheet Metal. Sheet Metal Forming Processes. Berlin: Springer, 27–140. doi: 10.1007/978-3-540-88113-1_2

[31] Pakhalovych, M. (2017). Improving normative documents on the safe operation of the elements of pipeline systems of nuclear power plants beyond design term. Kharkiv, 24.

[32] Polyakov, S. H., Klymenko, A. V., Kovalenko, S. Yu. (2010). Systema koroziynoho monitorynhu truboprovodiv. Nauka ta innovatsiyi, 6 (5), 25–28.

[33] Dzhala, R. M., Verbenets, B. Y., Melnyk, M. I. (2016). Measuring of Electric Potentials for the Diagnostics of Corrosion Protection of the Metal Structures. Materials Science, 52 (1), 140–145. doi: 10.1007/s11003-016-9936-y

[34] Akbashev, R. M., Zhulyaev, S. I., Kurdyumov, N. I. (2016). Prognozirovanie ostatochnogo sroka bezavariynoy sluzhby polyh metallicheskih obektov pod vliyaniem obshchey korrozii ih naruzhnoy poverhnosti pri provedenii ekspertizy promyshlennoy bezopasnosti. Nauka, tekhnika i obrazovanie, 3 (21), 124–126.

[35] Panchenko, S., Lavrukhin, O., Shapatina, O. (2017). Creating a qualimetric criterion for the generalized level of vehicle. Eastern-European Journal of Enterprise Technologies, 1 (3 (85)), 39–45. doi: 10.15587/1729-4061.2017.92203

[36] Gorbunov, D. V. (2014). Riski innovatsionnyih proektov i metodyi ih otsenki. Vektor nauki TGU, 3 (29), 123–126.

[37] Florescu, M. S. (2012). Analysis of economic risk in european investment projects. Revista Romana de Economie, 34 (1), 47–67. Available at: http://revecon.ro/articles/2012-1/2012-1-3.pdf

[38] Yuzevych, V. M., Klyuvak, O. V. (2015). Ekonomichnyy analiz rivniv efektyvnosti ta yakosti internet-platizhnykh system pidpryyemstva. Biznes Inform, 1, 160–164.

[39] Chaban, O. P., Yuzevych, L. M. (2015). Modelyuvannya ta yakist' monitorynhu diahnostychnykh system. Vymiryuval'na tekhnika ta metrolohiya, 76, 92–98.

[40] Chaban, O. P., Yuzevych, V. M. (2015). Matematychne modelyuvannya diahnostychnykh oznak dlya zabezpechennya systemy funktsionuvannya medychnykh posluh. Systemy obrobky informatsiyi, 2 (127), 108–113.

[41] Ofitsiynyi sayt PAT "UKRTRANS HAZ". Available at: http://utg.ua/utg/about-company/affiliates/

MATHEMATICAL MODEL'S CHOICE REASONING AND ITS IMPLEMENTATION FOR THE EVALUATION OF THE STRENGTH OF TECHNOLOGICAL VESSELS

Andrii Karpash
Zond, Research and Production Firm
Str. Mykytynetska 5a, Ivano-Frankivsk, Ukraine, 76000
ankarpash@gmail.com

Andrii Oliinyk
Department of Mathematical Methods of Engineering
Ivano-Frankivsk National Technical University of Oil and Gas
Str. Karpatska 15, Ivano-Frankivsk, Ukraine, 76000
andrij-olijnyk@rambler.ru

Abstract

In connection with the global increase in the intensity of use of working equipment related to high-risk facilities and the expiry of the service life limit, the question arises of determining the actual technical condition and forecasting the residual resource. From the analysis of the approaches to determining the technical state and on the analysis of regulatory documents, it becomes clear that the regulated methods of assessing the technical state are obsolete, such that they do not ensure the reliability of the obtained control results.

A new technique for determining the actual technical state through monitoring the level of stresses in the body of high-risk objects is proposed. The new technique takes into account additional physical and mechanical parameters that affect the stress-strain state, and have not yet been used. In other words, the technique of multivariable control of stress determination was proposed.

Mathematical models of the process of deformation and stress for cylindrical vessels with a spherical and conic dome operating under the action of high pressure are proposed.

Keywords: high pressure vessels, mathematical model of stress state of vessels, method of associative analysis.

DOI: 10.21303/2461-4262.2017.00396

1. Introduction

The objects of increased danger are operated practically in each sector of industry, which are different in their structure and principle of operation. This is a wide range of mechanisms and process equipment, which, as a rule, operate under various operating conditions and under conditions of long-term operation.

Determination of the actual technical condition and the service life limit is an interesting and actual direction for operating organizations. This list is evidenced by many reasons:

− intensification of production processes is increasing at enterprises;
− the level of operational loads is increasing;
− there are new requirements for technological equipment;
− the remaining resource is spent or is on the verge of its end;
− the level of rearmament and reconstruction of equipment is quite low.

Having enough information about the technical condition of the facility, the operator can characterize and establish safe operation parameters at a specific time of operation. Greater informativity will allow to predict the behavior of the technical state of the working object in the process of changing operating parameters. The condition for predicting the technical condition is the uninterrupted and reliable operation of the facility.

The main objective and mandatory requirement for the operator is the reliability of the results obtained to determine the actual technical condition of the process equipment. Therefore, new methods and approaches in this direction are necessary and relevant.

To ensure the conditions given above, a new technique for determining the actual technical state through monitoring the stress level in the metal of high-risk objects is proposed. The new

technique represents mathematical models of the deformation and stress state of vessels operating under pressure, taking into account additional physical and mechanical parameters.

2. Literature review and problem statement

From the analysis of known methods of controlling the physical and mechanical properties of the material [1–5] and from the practice of specialized organizations that conduct technical diagnosis of long-term operation objects, it follows that the evaluation of the actual technical condition is carried out by one or two informative parameters. In most cases, this is the thickness of the wall and the hardness of the metal, which is not enough to fully characterize the state of the object. Based on the results of other control methods, existing defects are identified that require elimination, that is, a situation arises that results in stopping, operating and repairing equipment. The method of acoustic emission is described in [6]. The essence of the method consists in the analysis of acoustic signals, directly depend on the elastic and plastic deformation, as well as on the applied load.

The disadvantage of the method is the impossibility of monitoring without the applied load. Work [7] presents the results of research in the development of methods and technical means for monitoring the physical and mechanical characteristics of metal structures. In particular, the problems of determining the yield strength, ultimate strength and toughness for a complex of informative parameters (magnetic parameters, hardness, thermal conductivity, etc.) are considered. In [8], the disadvantages of the methods of monitoring the technical state by separate parameters are presented. Advantages of using multivariable control are given. An overview of three magnetic methods for nondestructive testing, in particular magnetic flux, Barkhausen noise and magnetic memory of metal, is presented in [9]. The first two are active methods, and the last is passive. The physical mechanisms of the methods and experimental studies are analyzed. In work [10], an evaluation of the method for determining the stress in a sample of steel subjected to a static load (tensile test) is described. Measurements of deformation are presented using traditional extensometers and optical systems. 3D model of material deformation and displacement fields in the axial and radial directions is also calculated.

Analysis of methods for controlling the physical and mechanical properties of metals shows the absence of a comprehensive approach to determining the stress state of metal structures. Known approaches to determine the actual technical state do not take into account a set of informative parameters that represent individual factors of influence.

It should be noted that one of the main parameters of the technical state is its stress-strain state (SSS), which occurs even at the stage of manufacturing and installation of the facility and is constantly changing in the process of operating technological equipment [11, 12]. In other words, SSS depends on a certain number of factors that affect the exploited facility. If a number of necessary factors of influence to identify and develop an approach to measuring the informative parameters that these factors will represent, we will obtain a methodology for multivariable control. And this will allow obtaining a multifaceted characteristic of the stressed state of the exploited object. Understanding the behavior and the cause of the change in the stress state and premature correction of operating conditions, help prevent the occurrence of stress concentrators and subsequent formations of defects and failures.

The main disadvantage of the methods of SSS control at operation sites is the complexity of its conduct in the field and expensive equipment.

From the analysis of the normative and technical base [13–16], which regulates the definition and monitoring of the actual technical condition, some of the factors of influence shown in **Fig. 1** are not taken into account, resulting in distortion of actual data directly obtained during the process of the control itself.

From the practice of monitoring the technical condition of equipment, there are many cases when operating organizations, in addition to standard, regulated programs, require additional methods for diagnosing technological equipment. The task of the additional survey is obtaining information and analyzes the physical and mechanical characteristics of the metal, taking into account the factors of influence that are not taken into account in the regulated program.

The expected result is an increase in the accuracy of determining the actual technical condition and predicting the residual life of the equipment.

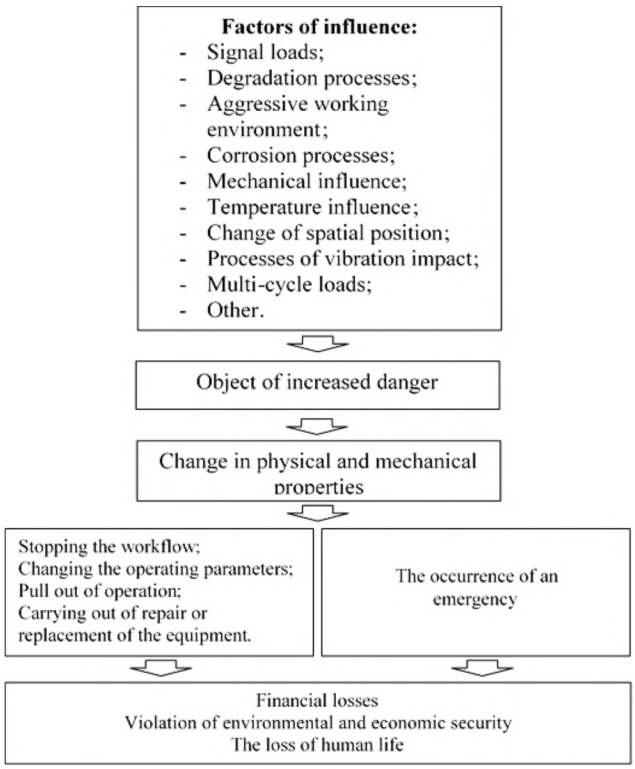

Fig. 1. Factors affecting the operation object

Therefore, in order to obtain the most accurate information when determining and monitoring the SSS of long-term operation facilities, it is effective:

– the use of multivariable control (the advantage is a comprehensive assessment, taking into account many factors and factors affecting the behavior of the change in the stress state);

– construction and implementation of mathematical models of SSS on the obtained control parameters.

3. The aim and objectives of research

The aim of research is development of a new approach to monitoring and assessing the actual technical condition of high-risk facilities that will simplify and reduce the cost of monitoring the actual technical condition, save time and human resources, obtain reliable data on the state of the facility through the use of a set of informative parameters that characterize the real factors of impact on the object.

To achieve this aim, the following tasks are set:

1. Set the type of the mathematical model for determining the parameters of the stress state after changing the spatial configuration of the object.

2. Develop a new technique for determining stresses, taking into account a set of informative parameters that depend on the change in force factors.

3. Develop a methodology for identifying factors on which an asymmetric change in the stress-strain state depends on the method of associative analysis.

4. Materials and methods for research of the stress-strain state of vessels operating under pressure and factors of force action

The efficiency of the operation of vessels operating under the influence of high pressure depends on current information about the parameters of the technical condition, and in particular

SSS [11]. In the process of functioning of systems, they are exposed to a complex of force factors. The material of these objects are deteriorated, its physical and mechanical characteristics change. This can lead to the appearance of gradual and sudden failures due to material defects and, as a consequence, to the disruption of the construction continuity. An important factor in the force impact is also a violation of the symmetry of the structure due to subsidence of the ground, landslides, earthquakes, the intensity of vibration effects, temperature gradients, and the like. Considering industrial systems as modeling objects (**Fig. 2**), it is possible to offer a formal approach to the description of functioning. The input and output characteristics of the systems determining the deformation of the object of investigation are determined:

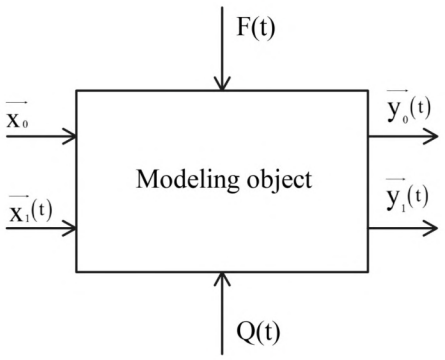

Fig. 2. The main characteristics of high pressure vessels as a simulation object

In the operation process of the modeling object (MO), which is characterized by some initial characteristics $\vec{x}_0$, which are of a permanent nature (geometric dimensions, general constructive scheme), and $\vec{x}_1(t)$, which are time variables (operating conditions, seasonal weather factors, force factors, material properties), actions of perturbing factors on MO occur. The disturbing factors are non-stationary in nature and can either permanently act on MO Q(t) (own weight, the reaction forces of soils and foundations, the consequences of possible defects committed during the MO construction), or have a temporary character F(t) (the action of non-design power factors, aerodynamic loads, changes in physical-mechanical, electrical characteristics due to long-term operation of objects).

In the process of MO operation, the initial characteristics change, which leads to the fact that the real MO position is characterized by new values $\vec{y}_0$ and $\vec{y}_1(t)$, which differ from the original characteristics $\vec{x}_0$ and $\vec{x}_1(t)$.

The main parameters that characterize the ability of these industrial objects to perform the tasks are strength, stability and stress, as well as the possibility of permissible displacement of structures that does not lead to violations of stable functioning. All these characteristics can be combined into a single indicator that can be considered a priority for assessing the technical condition and residual life of MO: vessels that are under the influence of high pressure and SSS.

Such generalization is quite motivated, since practically all factors of negative influence, which cause the appearance of defects and failures of MO, act on the SSS parameters, on the emergence of critical stress values in the material. Thus, the general functional equation describing the modeling object (vessel, operated under the action of high pressure) can be written in the following form:

$$\begin{Bmatrix} \vec{y}_0 \\ \vec{y}_1(t) \end{Bmatrix} = A\left(Q(t), F(t), \vec{x}_0, \vec{x}_1(t)\right) \begin{Bmatrix} \vec{x}_0 \\ \vec{x}_1(t) \end{Bmatrix}, \quad (1)$$

where $A(Q(t),F(t), \vec{x}_0, \vec{x}_1(t))$ – some operator that takes into account the effect on the object of the initial and perturbing factors described above. Depending on (1), the unknowns are the quantities $\vec{y}_0, \vec{y}_1$ (t), although in many cases the information about Q (t) and F (t), their quantitative characteristics, the topology of the action, etc. are not enough or completely absent.

In this case, problem (1) can be put in the form of a functional equation of the form:

$$\begin{Bmatrix} \overrightarrow{y_0} \\ \overrightarrow{y_1}(t) \end{Bmatrix} = A\left(\overrightarrow{x_0}, \overrightarrow{x_1}(t)\right) \begin{Bmatrix} \overrightarrow{x_0} \\ \overrightarrow{x_1}(t) \end{Bmatrix}. \quad (2)$$

In addition, in many cases equation (2) can be written in the following form:

$$\begin{Bmatrix} \overrightarrow{y_0} \\ \overrightarrow{y_1}(t) \end{Bmatrix} = A_н \begin{Bmatrix} \overrightarrow{x_0} \\ \overrightarrow{x_1}(t) \end{Bmatrix}, \quad (3)$$

where $A_н$ – some operator, usually with an unknown structure that takes the MO of state ($\overrightarrow{x_0}, \overrightarrow{x_1}$ (t)) to the state ($\overrightarrow{y_0}, \overrightarrow{y_1}$ (t)) and plays the role of a kind of "black box" when only the initial and final state of the system is known. The situation (3) is the most characteristic for the modeling of objects, which, on the one hand, are under the influence of known, but those that are difficult formalized force factors, and on the other hand, the parameters ($\overrightarrow{x_0}, \overrightarrow{x_1}$ (t)) and ($\overrightarrow{y_0}, \overrightarrow{y_1}$ (t)). As a rule, problems (2), (3) belong to the class of ill-posed regularization problems (transformation into the correct problem) for which it is necessary to develop special algorithms. As for problem (1), it is, as a rule, well posed and the complexity of the solution is determined only by the structure of the operator A(Q(t),F(t), $\overrightarrow{x_0}, \overrightarrow{x_1}$ (t)).

The problem of evaluation of the change in the stress-strain state of vessels under high pressure is referred to and solved in the form (3). The problem of reconstructing the nature and structure $A_н$ is solved on the basis of experimentally known sets of parameters ($\overrightarrow{x_0}, \overrightarrow{x_1}$ (t)) and ($\overrightarrow{y_0}, \overrightarrow{y_1}$ (t)).

When studying the stress state of vessels working under pressure, the approach modeled and justified in [11] is used. According to this approach, the technique for determining the component of the stress tensor and deformations using known coordinates of a certain set of points on the surface of the object is used to evaluate the change in the SSS. For this object, a parametric representation of it as a three-dimensional deformed body is known at the initial and control time. In this case, the components of the stress tensor and strains are calculated without using, as a rule, unknown information about the forces and load, which cause such change in the spatial configuration. Two types of pressure vessels are considered: with spherical and conical upper parts. Vessel with a spherical dome is shown in **Fig. 3**. The following parametric representation in the spherical and cylindrical (for the upper part) coordinate systems is valid in the initial (not deformed) moment of time for the coordinates of the points of the vessel surface:

$$\begin{cases} x = r\cos\varphi, & 0 \le \varphi \le r_{пр}; \\ y = r\sin\varphi, & R_{ID} \le r \le R_{OD}; \\ z = S, & 0 \le S \le L; \end{cases}$$

$$\begin{cases} x = r\sin\theta\cos\varphi, & \dfrac{\pi}{2} \le \theta \le \theta_0; \\ y = r\sin\theta\sin\varphi, & R'_{OD} \le r \le R'_{ID}; \\ z = r\cos\theta, & 0 \le \varphi \le 2\pi. \end{cases} \quad (4)$$

It should be noted that before the end of the cylindrical part of the representation is carried out in a cylindrical coordinate system, and for a spherical part in a spherical part, the angle θ_0 specifies the angle of conjugation of these two parts (**Fig. 3**). The coordinates r for these two parts will satisfy the conjugation conditions $R_{ID}=R'_{ID}\cos\theta$ and $R_{OD}=R'_{OD}\cos\theta$.

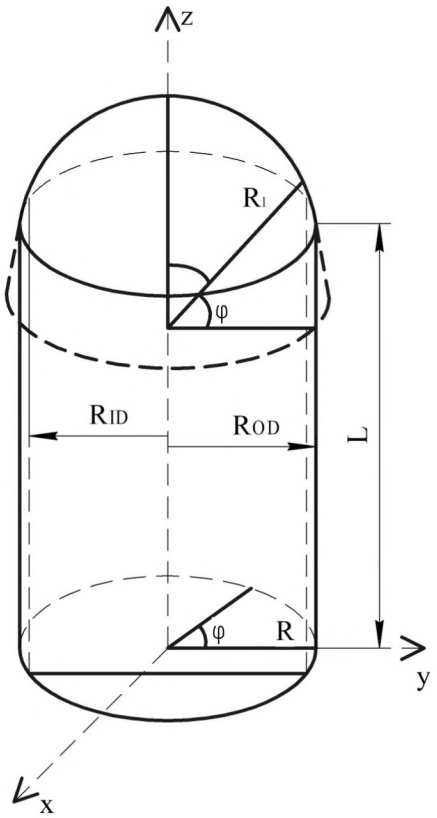

Fig. 3. Vessel with spherical configuration of the upper part

At the control point in time, the representation (4) acquires a different kind.

$$\begin{cases} x = X_L - Rn_x + \rho(S,\varphi,r,t)\cos\omega(S,\varphi,r,t)b_x + \rho(S,\varphi,r,t)\sin\omega(S,\varphi,r,t)n_x + \psi(S,\varphi,r,t)\tau_x; \\ y = Y_L - Rn_y + \rho(S,\varphi,r,t)\cos\omega(S,\varphi,r,t)b_y + \rho(S,\varphi,r,t)\sin\omega(S,\varphi,r,t)n_y + \psi(S,\varphi,r,t)\tau_y; \\ z = Z_L - Rn_z + \rho(S,\varphi,r,t)\cos\omega(S,\varphi,r,t)b_z + \rho(S,\varphi,r,t)\sin\omega(S,\varphi,r,t)n_z + \psi(S,\varphi,r,t)\tau_z, \end{cases} \quad (5)$$

where ρ(S,φ,r,t); ω(S,φ,r,t); Ψ(S,φ,r,t) – the functions that find the displacements of points in the radial, tangential and longitudinal directions; $\vec{r_L}$ $(X_L Y_L Z_L)$ – coordinates of points on the axis of the pipe; $\vec{n}$ $(n_x n_y n_z)$; $\vec{b}$ $(b_x b_y b_z)$; $\vec{\tau}$ $(\tau_x \tau_y \tau_z)$ – the components of the normal vectors, the binormal and the tangent to the tube axis.

In practical calculations, the functions ρ(S,φ,r,t); ω(S,φ,r,t); Ψ(S,φ,r,t) satisfy the following conditions:

$$\begin{aligned} \rho(S,\varphi,r,t) &\approx r + r_1(S,\varphi,r,t), \\ \omega(S,\varphi,r,t) &\approx \varphi + \varphi_1(S,\varphi,r,t), \\ \psi(S,\varphi,r,t) &\approx \psi + \psi_1(S,\varphi,r,t), \end{aligned} \quad (6)$$

where $|r_1(S,\varphi,r,t)| \ll 1$; $|\varphi_1(S,\varphi,r,t)| \ll 1$; $|\psi_1(S,\varphi,r,t)| \ll 1$ that is, the pipe generally retains a cylindrical configuration. To describe the spherical part, either the second representation is taken in (1) or the radii of curvature of the spherical part are listed from the results of experimental measurements of the coordinates of the upper part. Let's suppose that the coordinates of the points $(x_i y_i z_i)$ are organized on the upper part, then minimizing the function:

$$S(x_0;y_0;z_0;R) = \sum_{i=1}^{N}\left[(x_i - x_0)^2 + (y_i - y_0)^2 + (z_i - z_0)^2 - R^2\right]^2, \quad (7)$$

find the new coordinates of the center of the spherical part (x_0; y_0; z_0) and the radius of the deformed sphere. Optimization (7) is carried out by finding the expression for R^2: differentiates (7) with respect to R, resulting in:

$$R^2 = \frac{1}{N}\sum\left[\left(x_i - x_0\right)^2 + \left(y_i - y_0\right)^2 - \left(z_i - z_0\right)^2 - R^2\right], \tag{8}$$

after which the given expression is substituted in (7) and we obtain the problem of finding the coordinates (x_0, y_0, z_0), which obviously has a unique solution, because with this substitution the problem of minimizing a positive definite quadratic form is obtained. This allows to uniquely calculate the center (x_0, y_0, z_0) and the radius R of the deformed dome of the vessel.

According to the data for the conical upper part, which is shown in **Fig. 4**, similarly to (4) for the second system describing the conical part, the following representation holds:

$$\begin{cases} x = r\cos\varphi, & 0 \le \varphi \le r_{np}; \\ y = r\sin\varphi, & L \le S \le L_1; \\ z = S, & 0 \le r(S) \le R_{OD}, \end{cases} \tag{9}$$

where L_1 determines the angle at the base of the conic section:

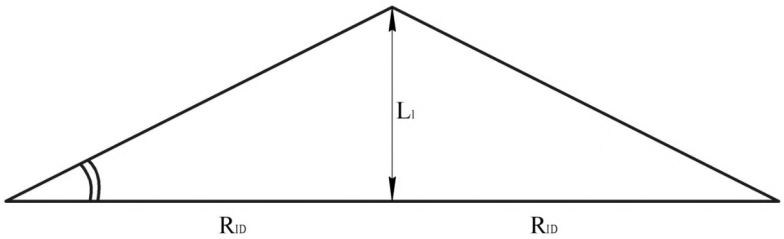

Fig. 4. Formalization of the conical part

At the control time, the coordinates of the cylindrical part are described with (5), the description of the conical part or remains the same as in (9), or can be refined from the results of measurements of a certain set of coordinates of the points of the conical part. If denote $\overrightarrow{R_0}(S,\varphi,r,t))$ radius vector of each point of the not deformed vessel under pressure, and $\vec{r}$ (S,φ,r,t) is the radius vector at the control moment, where the representations (4)–(9) allow to determine the following values:

– components of the vectors of local bases [17]:

$$\overline{E_0^i} = \frac{\overline{R_0}}{x_i} \quad x_1 = S;\ x_2 = \varphi;\ x_3 = r;$$
$$\overline{E^i} = \frac{\partial \bar{r}}{\partial x_i} \quad x_1 = S;\ x_2 = \varphi;\ x_3 = r; \tag{10}$$

– components of the metric tensor at two points in time:

$$g_{ij}^0 = \overline{E_0^i E_0^j}, \quad j,i = 1,2,3,$$
$$g_{ij} = \overline{E^i E^j}; \tag{11}$$

– components of the strain tensor:

$$\mathring{a}_{ij} = \frac{1}{2}(g_{ij} - g_{ij}^0); \tag{12}$$

– components of the stress tensor in the framework of the model of elastic deformations:

$$\sigma_{ij} = \lambda I_1(\varepsilon) g_{ij}^0 + 2\mu\varepsilon_{ij}, \tag{13}$$

where λ and μ – the Lame parameters of the material, and $I_1(\varepsilon)$ – the first invariant of the deformation tensor:

$$I_1(\varepsilon) = \sum_{i,j=1}^{3} \varepsilon_{ij} g^{ij}, \tag{14}$$

where $\overset{o}{g}^{ij}$ – matrix components are inversed to $\overset{o}{g}_{ij}$.

When reproducing the coordinates of points on the surface at the control time, interpolation (cubic spline, cubic spline with smoothing [11]) and least-squares approximation procedures are widely used [18]. These algorithms are implemented using standard software packages [19].

The values of mechanical stresses obtained according to the procedure (4)–(14) characterize the real stresses – in the case when it can be assumed that at the initial moment of time the stress in the vessel working under pressure is zero. If, at the initial time, the stresses are unknown, the obtained values will characterize the change in the stressed state of the vessel operating under pressure.

The obtained values of stresses (or characteristics of their changes) are obtained without using mathematically formalized values of forces, loads of different nature that act on the object. The found components can be written:

$$\sigma_{ij} = \sigma_{ij}^t + \sigma_{ij}^{uf}, \tag{15}$$

where σ_{ij} – stresses found by (14); σ_{ij}^t – the value of the stresses that can be determined theoretically (ring stresses from the action of internal pressure, temperature differences, etc.). As a rule, the stresses are indicated at the same point at each point of the body or as functions of spatial coordinates; σ_{ij}^{uf} – residual, unformalized stress, the nature of which often remains unknown. In particular, for a cylindrical part of a vessel, the stresses are determined from known formulas.

For a pipe subjected to an internal pressure Pa:

$$\begin{aligned}
\sigma_{rr} &= \frac{R_{ID}^2 \cdot P}{R_{OD}^2 - R_{ID}^2} \cdot \left(1 - \frac{R_{OD}^2}{r^2}\right), \\
\sigma_{\theta\theta} &= \frac{R_{ID}^2 \cdot P}{R_{OD}^2 - R_{ID}^2} \cdot \left(1 + \frac{R_{OD}^2}{r^2}\right), \\
\sigma_{zz} &= \frac{\lambda}{\lambda + \mu} \cdot \frac{R_{ID}^2 \cdot P}{R_{OD}^2 - R_{ID}^2}.
\end{aligned} \tag{16}$$

For a spherical part, as shown in **Fig. 5**, where α – the angle defining the part of the sphere that is the upper dome of the vessel, φ – the angle value for the given point; H – the wall thickness, R – the radius of curvature. All the components of the stress tensor are defined by the formulas:

Meridional stresses under the action of its own weight:

$$\sigma_m = -\frac{\gamma_m \cdot R}{1 + \cos\varphi}, \tag{17}$$

where γ_m – density of material.

Ring stresses:

$$\sigma_{\theta\theta} = \gamma_m \cdot R \cdot \frac{1-\cos\varphi-\cos^2\varphi}{1+\cos\varphi}. \quad (18)$$

Under the action of pressure P[12]:

$$\sigma_m = \sigma_{\theta\theta} = \frac{PR}{2h}. \quad (19)$$

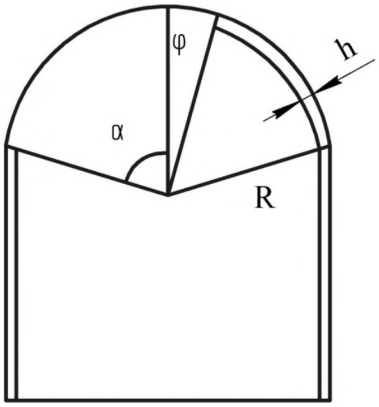

Fig. 5. Scheme of the spherical part

For the conical part, as shown in **Fig. 6**, under the influence of internal pressure, stresses arise (where h – the wall thickness, ω – the displacement in the direction of the normal, 2α – the angle at the conic vertex):

$$\sigma_m = \frac{pxtg\alpha}{2h}; \quad (20)$$

$$\sigma_{\theta\theta} = \frac{pxtg\alpha}{h}; \quad (21)$$

$$\omega = \frac{3px^2tg^2\alpha}{4hE}, \quad (22)$$

where E – Young's modulus of material.

The above formulas concern only the basic, most easily formalized stresses.

The subject of further research is the stress σ_{ij}^H, calculation by (4)−(15) with allowance for (16)−(22). The nature of these stresses is unknown, therefore it is necessary to put forward a hypothesis on what parameters these stresses depend on, what is the reason for their occurrence. The stress can depend on the physical and mechanical properties of the material, electrical parameters, etc. Let x_i…..x_N – N − factors affecting on σ_{ij}^H. If measurements σ_{ij}^H, are made for different values of the parameters x_i, then to determine the degree of interrelation between σ_{ij} and x_i the method of associative analysis is used. For σ_{ij}^H, and x_i, the values of σ and X^i are determined, which determine the median of the distribution of these quantities for their range changes, while the **Table 1** is completed, which contains the results of N experiments by the criterion of their hit in the corresponding interval. This yields [19].

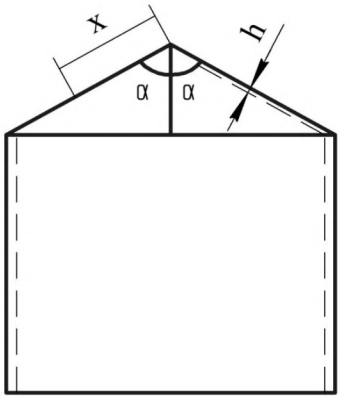

Fig. 6. Diagram of a conic vertex

Table 1
The results of N experiments on the criterion of their entry into the corresponding interval

	$\sigma_{ij}^{H}>\sigma$	$\sigma_{ij}^{H}>\sigma$		
$x_i < X^i$	a	b	a+b	
$x_i > X^i$	c	d	c+d	a+b+c+d=N
	a+c	b+d	N	

where a, b, c, d – the number of experiments with the corresponding values (x_i; σ_{ij}^{H}). Then the coefficients are determined:

$$\psi_T = \frac{3}{\sqrt{N-1}}, \tag{23}$$

$$\psi_E = \frac{ad - bc}{\sqrt{(a+b)(c+d)(a+c)(b+d)}}. \tag{24}$$

If $\Psi_E>\Psi_T$, then the relationship between x_i and $\sigma_{ij}^{H}$is significant, it requires further investigation; if $\Psi_E<\Psi_T$, then the relationship between the quantities is not significant, it can be neglected. With a significant relationship between the values σ_{ij}^{H} and x_i, k=1, 2, 3 the least square method can be used to construct an incomplete cubic model of the form:

$$\sigma_{ij}^{H} = \eta(x_1x_2x_2) = \theta_0 + \theta_1x_1 + \theta_2x_2 + \theta_3x_3 + \theta_{12}x_1x_2 + \theta_{13}x_1x_3 + \\ + \theta_{23}x_2x_3 + \theta_{123}x_1x_2x_3, \tag{25}$$

which under certain conditions [19] can be adequately replaced by a linear model:

$$\sigma_{ij}^{H} = \eta(x_1x_2x_2) = \theta_0 + \theta_1x_1 + \theta_2x_2 + \theta_3x_3. \tag{26}$$

The choice of representation (25) or (26) makes it possible to obtain relationships convenient for practical analysis between stresses and identified factors of influence on SSS, and also to analyze these dependencies to assess the relative influence of each of the identified factors.

5. Research results of the stress-strain state of vessels working under pressure and factors of force influence

In the process of researching ways to determine the actual technical condition of high-risk facilities, namely vessels operating under the pressure, through SSS determination, the following results are achieved:

1. The type of the mathematical model is established. An algorithm for regularizing the incorrect problem of SSS recovery from incomplete information on the displacement of the surface points is proposed.

2. A methodology for calculating the components of strain tensors has been developed, namely, a technique for determining the SSS of objects using a metric tensor for undeformed and deformed vessels is proposed.

3. Identification of the force factors. It is proposed to use the method of associative analysis to identify significant factors of influence.

Also, an important achievement is the determination of the direction of further research, namely the experimental work on the models of pressure vessels, in order to obtain a set of informative parameters. Industrial testing is carried out.

6. Discussion of research results of the stress-strain state of vessels and the choice of factors of force action

The advantages of the proposed method for SSS evaluation of vessels operating under pressure include the moment that information about deformation is obtained without using data on all forces and loads that last for a long time on the object. In fact, this information is some integral characteristic of the object.

The proposed technique for determining and evaluating the stress state is carried out by means of multivariable control. It allows to take into account several additional factors of influence that have not been taken into account and on which the behavior of the change in the stress state depends. The technique of multivariable control is convenient for use in the field conditions. The main disadvantage is the multiple measurements of a set of informative parameters and the use of several means of measurement.

The conducted studies use the approaches and mathematical models developed for SSS research of the main pipelines. These models are improved taking into account the more complex spatial configuration of the object. For the first time, a technique is proposed for identifying the factors of force action, which cause the appearance of asymmetric deformations of the object.

7. Conclusions

1. The mathematical formulation of the problem of SSS evaluation on the basis of experimental data is formulated as an incorrect problem of reconstructing the displacement field for vessels with different types of domes from data on the displacement of a certain set of points of the object.

2. A mathematical model of the vessel's SSS has been developed, as an algorithm for regularizing an ill-posed problem.

3. The relationship between real SSS and standard loads for structures with different types of domes is established in order to identify zones of asymmetric stresses.

4. The technique of determining the factors of force actions is proposed, most of all they affect the SSS of designs using the methods of associative analysis.

5. Advantages of this method is a comprehensive assessment of the actual technical condition for many informative parameters, depend on the force factors of influence, and the evaluation of SSS parameters is made without using information about the forces and loads acting on the object.

6. The disadvantages include the process of multiple measurements of informative parameters using a large number of technical means of control. Also, to obtain the results of the SSS level, further processing of the measurement results is necessary.

7. To consolidate the proposed technique, it is necessary to conduct experimental studies on model samples of pressure vessels and to conduct industrial approbation. It is suggested to use the above approaches for evaluation of SSS parameters for objects where only measuring the movement of points on the surface is possible without carrying out more complicated hardware studies.

References

[1] Kliuev, V., Fursov, A., Fylynov, M. (2007). Podkhody k postroeniyu system otsenki ostatochnoho resursa tekhnicheskikh obektov. Kontrol. Diahnostika, 3, 18–23.

[2] Karpash, A., Tatsakovych, N., Dotsenko, Ye. (2016). Features of the modern control techniques application to determine metal constructions deflected mode. Scientific proceedings «NDT Day 2016», 1 (187), 319–324.

[3] Karpash, O., Karpash, M., Dotsenko, Ye. (2008). Doslidzhennia vzaiemozviazku mizh strukturnym stanom stalei ta fizyko-mekhanichnymy kharakterystykamy stalei. Fizyko-khimichna mekhanika materialiv, 2 (7), 724–729.

[4] Karpash, A. (2012). Analiz vidomykh metodiv kontroliu fizyko-mekhanichnykh kharakterystyk metalu. Naftohazova enerhetyka, 1 (17), 70–82.

[5] Vashchyshak, S., Karpash, A. (2012). Current approaches to the determination of physic-mechanical properties of metals oil and gas facilities. Scientific proceedings «NDT Day 2012», 1 (133), 260–264.

[6] Skalsky, V., Hirnyj, S., Basarab, R. (2013). Nondestructive evaluation of pipelines: magneto-acoustic diagnostics of deformation. Oil and Gas Business, 5, 301–313.

[7] Karpash, M., Dotsenko, Ye., Tatsakovych, N. (2011). New non-destructive methods for physical and mechanical properties evaluation of metalworks materials. Edition of Scientific Machine Union, 19, 32–36.

[8] Piotrowski, L., Augustyniak, B., Chmielewski, M., Kowalewski, Z. (2010). Multiparameter analysis of the Barkhausen noise signal and its application for the assessment of plastic deformation level in 13HMF grade steel. Measurement Science and Technology, 21 (11), 115702. doi: 10.1088/0957-0233/21/11/115702

[9] Wang, Z. D., Gu, Y., Wang, Y. S. (2012). A review of three magnetic NDT technologies. Journal of Magnetism and Magnetic Materials, 324 (4), 382–388. doi: 10.1016/j.jmmm.2011.08.048

[10] Bogusz, P., Poplawski, A., Morka, A., Niezgoda, T. (2015). Evaluation of true stress in engineering materials using optical deformation measurement methods. Journal of KONES. Powertrain and Transport, 19 (4), 53–64. doi: 10.5604/12314005.1138307

[11] Oliinyk, A. (2010). Matematychni modeli protsesu kvazistatsionarnoho deformuvannia truboprovidnykh ta promyslovykh system pry zmini yikh prostorovoi konfihuratsii. Ivano-Frankivsk: IFNTUNH, 320.

[12] Pisarenko, G., Yakovlev, A., Matveev, V. (1988). Spravochnyk po soprotyvlenyiu materyalov. Kyiv: Naukova dumka, 736.

[13] Pravyla bezpeky i bezpechnoi ekspluatatsii posudyn, shcho pratsiuiut pid tyskom: NPAOP 0.00-1.59-87 (1987). Derzhhirpromnahliad.

[14] Posudyny, shcho pratsiuiut pid tyskom na promyslovykh pidpryiemstvakh: Instruktsiia z ekspertnoho obstezhennia (Tekhnichnoho diahnostuvannia) (2006). Ministerstvo promyslovoi polityky Ukrainy.

[15] Obladnannia tekhnolohichne naftopererobnykh, naftokhimichnykh ta khimichnykh vyrobnytstv. Tekhnichne diahnostuvannia. Zahalni tekhnichni vymohy: DSTU 4046-2001 (2001). Derzhstandart Ukrainy.

[16] Sosudi y apparati. Normi y metodi rascheta na prochnost: HOST-14249-89 (1989). Mynysterstvo khymycheskoho y neftianoho mashynostroenyia.

[17] Sedov, L. (1970). Mekhanyka sploshnikh sred. Vol. 2. Moscow: Nauka, 572.

[18] Samarskyi, A., Hulyn, A. (1989). Chyslennie metody. Moscow: Nauka, 432.

[19] Doroshenko, V. (1993). Osnovy naukovykh doslidzhen. Kyiv: ISDO, 128.